PROCEEDINGS

OF THE PAKISTAN ACADEMY OF SCIENCES:

A. Physical and Computational Sciences

PAKISTAN ACADEMY OF SCIENCES
ISLAMABAD, PAKISTAN

HEC Recognized, Category Y

PROCEEDINGS
OF THE PAKISTAN ACADEMY OF SCIENCES:
A. Physical and Computational Sciences

C O N T E N T S

Volume 59, No. 1, March 2022 — **Page**

Research Articles

Pakistan Academy of Sciences

Research Article

Extent and Evaluation of Flash Flood Resilience in Mountainous Communities of Daral and Chail Valleys, District Swat, Pakistan

Muhammad Barkat Ali Khan[1*], and Atta-ur-Rahman[2]

[1]Department of Geography, Government College Madyan, Swat, Pakistan
[2]Department of Geography, University of Peshawar, Pakistan.

Abstract: This study aimed to explore the extent and evaluation of flash flood resilience in mountainous communities of Daral and Chail valleys of Swat. After collecting data from primary and secondary sources, the parameters of Disaster Resilience Capacity (DRC) model was applied for data analysis. The analysis reveals that stream discharge increases during summer mainly because of the rapid melting of snow, ice, glaciers and monsoonal rains, which results in flash floods. The communities living in the mountainous areas of Daral and Chail valleys face problems of multitudes of socio-economic and infrastructural flash flood damages almost every year. However, limited communities have adopted indigenous resilience strategies to bounce back from the recurrent adverse impacts of flash floods. It was found from the analysis that due to indigenous resilience practices by the local communities and the location of most mountainous communities, Daral valley is more resilient to flash floods as compared to Chail valley. Contrary to this, the extent and level of flash flood resilience in Chail valley are low as most of the mountainous communities are more vulnerable to seasonal flash floods. Some wise practices can enhance resilience to flash floods, especially land use planning, community preparedness, afforestation, and improved accessibility and communications.

Keywords: Flash Flood, Mountain community, Flood Resilience,

1. INTRODUCTION

In the world, natural calamities are associated with the possibilities of bringing adversaries to human beings and their environment [17]. The phenomenon that carries the potentials of being a threat to human lives and their properties is called hazard. [1]. Among the hazards, flash flood is a type of flood hazard that happens abruptly suddenly with very little time for early warnings and emergency response. Flash floods occur rapidly and is also characterised with associated hazards including mudflow, landslides and causes death toll, casualties and infrastructural damages [2]. Landslide is a broader term including a wide variety of mass movements associated with slope failure, movement of debris and rocks due to the influence of gravity. [3].

The term resilience is widely used to "to avoid" in the field of disaster risk management. However, the common uses including description of jumping,

leaping and rebounding [4]. In the framework of disaster resilience it is defined as the capabilities related to preparedness, response and recovery before, during and after the disaster. Disaster resilience enhances the capacities to mitigate the adverse impacts of natural hazard, it deals with prevention, adaptation and mitigation. The ability of an actor or a system to bear shocks and return to its state of origin is also known as disaster resilience. Resilience is also considered as the capability to handle with the unanticipated dangers and to bounce back in an effective way [5]. Resilience is differently defined in different disciplines, therefore there is a long list of definitions, but one thing is common in all these definitions to focus on the ability to resist and absorb shocks of unforeseen events and to recover [6]. The concept of resilience is being used by researchers both as process and as an outcome [7]. The concept of resilience refers to the capacity of a community to adapt, cope with, and recover through changing impacts and sustaining a suitable

structure and function during and after a hazard [8]. The indigenous factors related to a specific locality may have positive or negative impacts on level of resilience [1].

The main features of resilience are repelling the impacts of disasters and recovering from and acclimatising with the new settings to manage any unforeseen hazard [18]. Community resilience is explained at various inter-related levels, such as the community's capacity to "bounce back" and use of their own resources to recover. The objectives of resilience are to contribute to protecting human lives, the built environment, and livelihoods and to safeguard administrative and economic stability [9]. Mountainous communities are considered to be at greater risk to natural disasters due to low level of resilience, the factors including, steep slopes, rugged topography, geology, heavy precipitation, and surface lithology. [10]. Though the inhabitants of mountainous communities live there for centuries, they handle the dangers posed by natural calamities, including earthquakes, landslides, extreme temperature, storms, and flash floods [11]. Regardless of all the dangers posed by mountainous areas, a large number of people reside there. Due to sharp population increase and high land value in the plain areas, the settlements are sprawling towards mountains. Due to continuous anthropogenic activities over the fragile slopes and

social and economic systems changes, the degree of people's proneness to various hazards has been increasing [12].

The mountains are; naturally active landforms therefore, the mountainous communities are vulnerable to natural calamities. Generally, the rural settlements are associated with mountains, but it is not only rural, according to current estimates, more than 50 % of world population lives in urban areas and there are urban localities within the mountains. In urban areas with nearby mountains the settlements sprawl into the slopes because the poor people are pushed to the mountains for housing due to comparatively low land value. It makes them more vulnerable to natural hazards including flash floods [13].

There are three associated aspects related to natural hazards in mountainous areas. The mountains are hydrologically and geo-physically more active and are also biologically diverse due to multiplicity in altitude, humidity and temperature. The second point is that mountainous regions have different social makeup, including isolated small settlements dependent upon agriculture, livestock, and forest wood to larger diversified urban settlements with complex transportation and communication networks. The urban settlements in the mountainous areas also attract migrants for jobs,
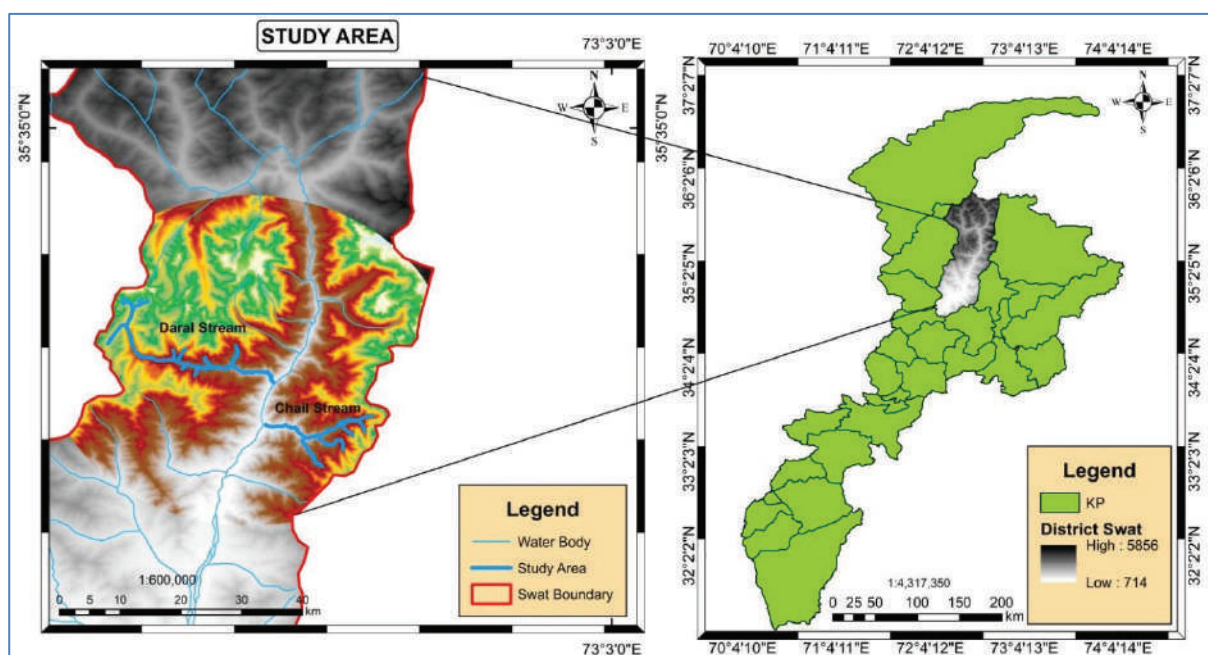
Fig. 1. Location of the study area

tourism and other economic activities. The third point is that the mountains are communicated with other areas through water, air, people, information, economy, goods and services etc. With time, the linkages between highlands and lowlands have sharply increased in number and importance [1].

1.1 The Study Area

Swat valley is situated in the northern part of Pakistan bordering with Chitral and Gilgit Baltistan which are in the northern extremes of the country. Swat valley is mountainous with natural beauty and is a famous tourist destination. In Swat Valley, river flooding dominates downstream Madyan while flash floods dominate in the valley's upper reaches [20]. The research work was conducted in the sub valleys of Daral and Chail. Daral valley is drained by Daral stream as an important tributary of river Swat which join the river at the town of Bahrain, the valley is situated in the north-western part of Swat valley. There are high up mountains in the valley with maximum altitude reaching up to 15,000 feet above mean sea level, while the altitude at lower reaches of the alley is 4600 feet above mean sea level. The valley settlements comprise medium and small villages, hamlets, and scattered settlements. There are ten medium and small villages in the valley and 12 hamlets with isolated settlements. High mountain peaks surround the valley therefore the monsoon influence is considered to be low. The precipitation is mostly received in the form of snow during winter and as rain during spring, the snow fall reaches up to five meter depth during winter [14].

Chail a sub valley is situated in the northeast of Swat valley, extended towards east at the town of Madyan. There are high up mountains with perennial streams, the valley is also rich in natural resources with diversified flora and fauna. The valley lies at 35° 3' 40" to 35°11' 40" north latitude and 72°32' 1" to 72°43' 3" east longitude (Figure 1). The valley is also prone to natural calamities, including flash floods, landsliding, snow avalanches, etc. In Chail valley, most of the settlements are situated along the main stream and its tributaries, making them more prone to flash floods [15]. The settlements in Chail valley are distributed in medium and small villages and hamlets with isolated houses. According to census 2017 the people are inhibited in 20 medium

and small villages grouped around three major localities, including Bashigram, Shanko and Chail. According to Census 2017 the total population of the valley is 20,091 consist of 2820 households [19].

2. MATERIAL AND METHODS

All possible efforts were being made during the research work to collect consummate information by applying different tools and models. Data collection was started initially by a pilot survey in which the valley was visited. The tools were made based on the compatibility with the local area and theme of research. The tools consist of structured interviews through questionnaires, semi structured interviews, focused group discussions and direct observations.The diversified tools were used for different respondents including households, civil society, key informants, government line departments and commercial points.There are medium and small size villages in the target valleys, including 20 in Chail valley and ten in Daral valley with surrounding hamlets and scattered isolated houses. During data collection ten localities were selected on the basis of proneness to the flash floods including five in Chail valley and five in Daral valley. During data collection the tools including household questionnaire, semi structured interviews with the key informants, focussed group discussion, and direct observations were used in these localities. In each of the ten selected localities 20 household questionnaires, at least one FGD and three semi structured interviews were conducted. During data collection the information was also triangulated by using different types of tools for same type of information.

The information was properly analysed after data collection by applying different latest software, including MS Excel, MS Access, and SPSS. The maps and related data was presented by using Arc GIS software. The Disaster Resilience Capacity (DRC) model was applied during data collection and analysis. In the DRC model there five levels, the first one describes the DRC of communities. As shown in (Figure 2) in the second level the DRC is divided into two including community preparedness (CPD) and community environmental conditions (CEC)

In the third level, the CPD criteria is further

divided and focussing on the disaster preparedness, early warning system, capabilities of emergency response and reporting system, the CEC at the third level further focus on assessment of hazards of landslide and flash floods. Then in the fourth and fifth levels the parameters of third level are further subdivided for having detailed information. According to the scale developed by Satty in 1980 from one to nine was used for measurement of every element, 1 is used for less significance while 9 is used for more significance [16].

(Figure 2) is showing the details of five hierarchies the multiple criteria decision-making technique was used. The system of hierarchies simplify complicated issues related to the research.

There is a hierarchic scheme of five levels for evaluating Disaster Resilience Capacity (DRC).

3. RESULTS AND DISCUSSION

3.1 Vulnerability to Flash Floods

3.1.1 Vulnerabilities to Flash Floods in Chail Valley

The seasonal flash floods are prominent in Chail valley; 2010 flood was extremely disastrous for the valley, in the five surveyed localities a total of 255 houses were washed away. The flood also destroyed agriculture lands along the streams, water mills, forest trees, and fish hatcheries. The detail
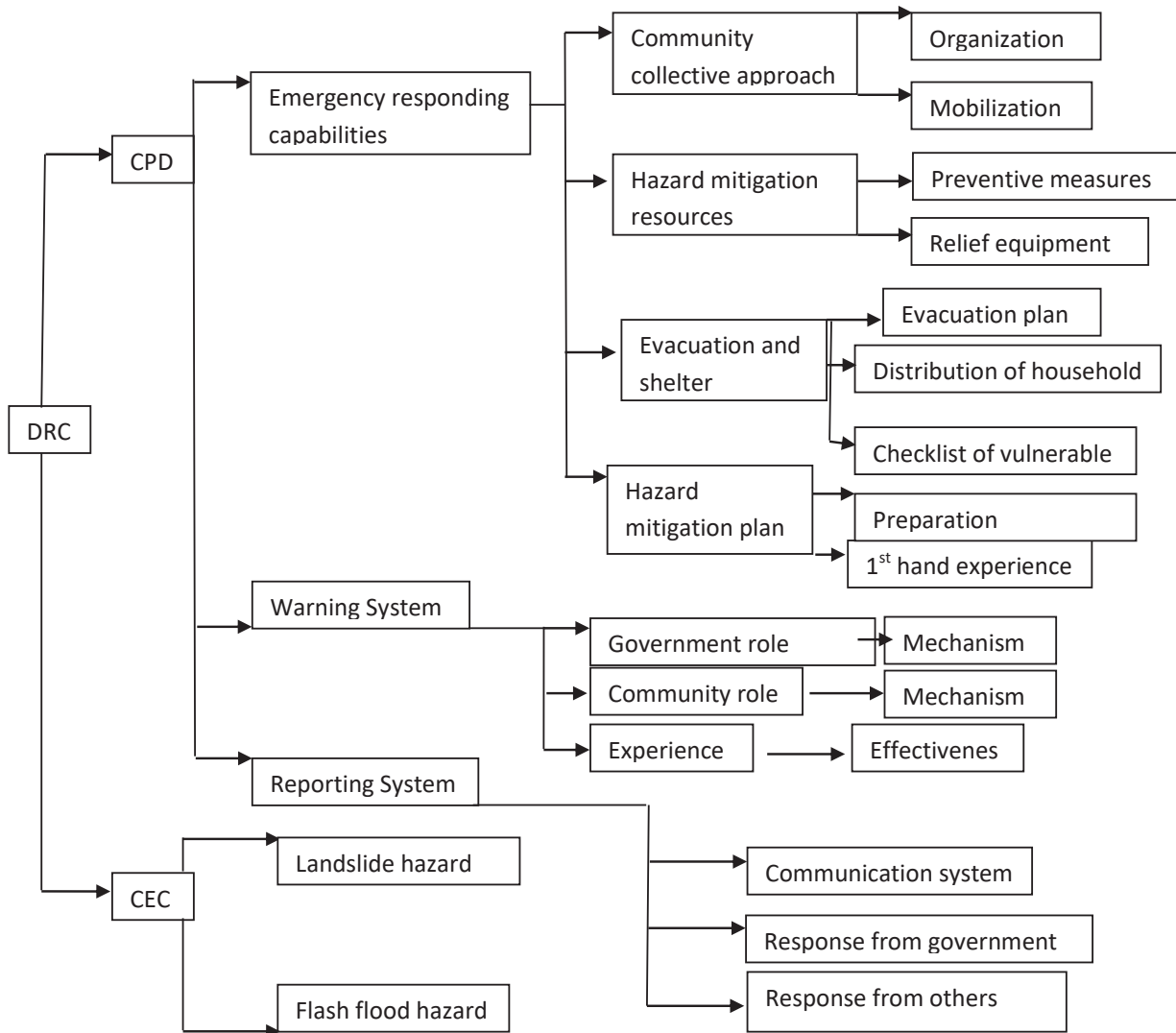
Fig. 2. Research process

of vulnerabilities is shown in (Table 1). In Chail valley, according to household survey in the five selected localities, 49 % of the respondents told that roads and bridges are most vulnerable, while 46 % responded that houses are most vulnerable, besides, 5 % told that agriculture lands are more vulnerable. (Table 1) shows that the most vulnerable to flash floods are roads/bridges, houses and water supply system and the least vulnerable are hotels/shops and irrigation channels.

In Chail valley, to cross the stream the people fixed wooden bridges at different points. In the bigger localities like Bashigram, Shanko and Chail the settlements are situated along both the sides. While some of the people live at one side of the stream while their agriculture lands are lying towards the other side. Therefore, for local people's routine mobility to cross the stream, the wooden bridges are very important.

3.1.2 Vulnerability to Flash Floods in Daral Valley

According to the household survey in Daral valley, 47 % of the respondents were of the opinion that roads and bridges are more vulnerable, after roads the agriculture lands were considered more vulnerable, 31 % responded about agriculture lands are more vulnerable, Furthermore houses were considered to be most vulnerable and 18% of the respondents responded about it, while 2 % told that hotels and shops are more vulnerable. (Table 2) is showing that the most vulnerable to flash floods are roads/bridges, houses and water supply and the least vulnerable are hotels/shops and irrigation channels. (Table 2) also shows that houses are considered the second most vulnerable to flash floods.

In Daral valley as shown in (Table 2) mobility of local people to cross stream is highly vulnerable to seasonal flash floods due to washing away of wooden bridges. These wooden bridges are also very important for evacuation, the people also face problems in evacuation. In Daral valley, roads and pathways are also found along both sides of the stream and damaged during flash floods. The patches of agriculture land along both the sides of stream are also being affected by the overflow of the stream during flash floods. In the valley however most of the settlements are situated a bit far from the stream but still some of the settlements

Table 1. Chail valley, Vulnerability to flash floods (Responses are in %age)

Vulnerability rank	Houses	Agriculture land	Roads/Bridges	Water Supply	Irrigation Channel	Shops/Hotel
Most vulnerable	46	5	49	–	–	–
2nd most vulnerable	41	10	37	12	–	–
3rd most vulnerable	5	41	14	38	2	–
4th most vulnerable	8	19	–	33	27	13
5th most vulnerable	–	15	–	12	57	7
6th most vulnerable	–	9	–	–	12	33
Not vulnerable	–	1	–	5	2	47
Total	**100**	**100**	**100**	**100**	**100**	**100**

Source: Field Survey, 2018

Table 2. Daral valley, Vulnerability to Flash floods (Responses are in %age)

Vulnerability ranking	Houses	Agriculture land	Roads/Bridges	Water Supply	Irrigation Channel	Shops/hotel
Most vulnerable	18	31	47	2	–	2
2nd most vulnerable	57	18	15	6	–	4
3rd most vulnerable	21	11	38	26	–	4
4th most vulnerable	4	–	–	32	–	27
5th most vulnerable	–	1	–	34	35	1
6th most vulnerable	–	10	–	–	50	10
Not vulnerable	–	29	–	–	15	52
Total	100	100	100	100	100	100

Source: Field Survey, 2018

are situated close to stream on vulnerable points and are vulnerable to flash floods.

3.2 Causes of Flash Floods

During data collection different causes of flash floods were explored after having inputs from key informants, existing literature and direct observations. Based on that the causes of flash floods were listed and the respondents were asked to rank causes according to their significance to cause flash flood.

3.2.1 Causes of Flash Floods in Chail Valley

Chail valley, due to the location of settlements and other resources, is considered more prone to flash floods than Daral valley. After the 2010 flood due to lateral erosion, the stream flows in a wide channel. The tributaries of Chail stream transport the weathered rock material in the shape of boulder or gravel and deposit it in the down valley areas.

During field survey the respondents recorded (Table 3) torrential rainfall as the most significant cause stated by 49% respondents, while 22% reported it as second most significant, 21% as 3rd most significant and 8% as fourth most significant cause. The second most significant cause of flash floods was reported as cloud bursts followed by high snow melt, deforestation and overgrazing.

3.2.2 Causes of Flash Floods in Daral Valley

As compared to Chail valley, Daral valley is narrow and the slopes are steeper with hard rock materials. In the lower part of the valley towards Bahrain town the settlements including Jheel and Niam are more prone to flash floods, while in the middle and upper reaches of the valley the settlements are situated a bit far from the main Daral stream therefore the roads and bridges are prone to flash floods while the settlements are prone to flash floods of the tributaries and gullies of Daral stream running along the settlements.

As mentioned in (Table 4) most of the respondents stated that torrential rainfall is the major cause of flash floods followed by high snow melt, clouds burst, deforestation and overgrazing. During summer the heavy rainfall in the catchment area causes overflow in the tributaries and gullies and exceed the flow of Daral stream, during summer due to increase in diurnal temperature also contribute to high snow melt and increase in stream flow.

3.3 Chail valley: Communities' Resilience against Flash floods

In Chail valley before flood 2010 the stream was flowing in a narrow deep channel, there were trees in large number towards both the sides of the stream and the seasonal floods were not disastrous

Table 3. Chail valley, Causes of flash floods (Responses are in %age)

Ranking of causes	Torrential rainfall	High snow melt	Clouds burst	Loose rocks	Deforestation	Over grazing
Most significant	49	12	12	_	18	9
2nd most significant	22	43	8	_	9	18
3rd most significant	21	18	60	_	_	1
4th most significant	8	8	12	12	58	2
5th most significant	_	19	8	1	12	57
6th most significant	_	_	_	78	_	9
Insignificant	_	_	_	9	3	4
Total	100	100	100	100	100	100

Source: Field Survey, 2018

during peak seasons, except lateral erosion at few points. There were also trout fish hatcheries along the stream. During the massive flood 2010 the trees and grassy point bars were washed away, the houses close to the stream were destroyed, the width of stream channel was increased by few times. After 2010 every year, the valley faces flash floods in June, July and August, it results in blockage of road access to some of the villages and sub valleys. Every year during flood season the small bridges are being washed away and the houses are more prone to seasonal flash floods.

3.4 Chail Valley: Communities' Preparedness against flash floods

In Chail valley the resilience was evaluated according to the elements mentioned in (Table 5), each of the elements was scored according to its significance in the sample localities, the average of sample localities for Chail valley is mentioned against each element. Score 9 is for maximum significance and 1 for least significance.

In Chail valley the communities are more proactive to help each other in emergency situation, therefore however without any formal body the communities are organized and mobilized to help each other and to cope with flash floods. The people also care about vulnerable people, however they are not having formal lists but they care about disable, elderly women and children during flash floods. The community got a good experience to respond to floods during and after flood 2010. The people are

also proactive in warning each other on time while the government's warning system is very poor. In the valley, most of the villages are lacking evacuation plan and some of the villages and sub valleys lack access to main roads. In some of the elements including relief equipment, preventive measures, distribution of households and preparation for flash floods the target villages got intermediate figures. The community is responding to rehabilitate their infrastructure after flash floods, the re keeping some of the equipment and after flood 2010 some of the organizations also provided them with basic skills and equipment.

3.5 Chail Valley: Communities' environmental conditions and flash floods

Some of the components of community environmental conditions differ before and after flood 2010. In Chail valley the slope gradient is comparatively gentle and the rocks are in loose form. Chail valley was experiencing flash floods each year during the months of June, July and August. During floods, the area was experiencing flash floods, which resulted in lateral erosion at few points. The settlements were safe from flash floods because open spaces were covered with big trees between stream and settlements.

In 2010 the area was hit by a devastating flood that brought huge damages and changed local environmental conditions. The stream channel was increased in size, the open spaces were washed away and the settlements along the stream are now

Table 4. Daral valley, Causes of flash flood (Responses are in %age)

Ranking of Causes	Torrential rainfall	High snow melt	Clouds burst	Loose rocks	Deforestation	Over grazing
Most significant	46	32	12	–	9	1
2nd most significant	34	36	18	–	3	9
3rd most significant	16	22	51	–	9	2
4th most significant	3	8	10	22	46	2
5th most significant	1	2	9	5	18	51
6th most significant	–	–	–	43	1	10
Not significant	–	–	–	30	14	25
Total	100	100	100	100	100	100

Source: Field Survey, 2018

Table 5. Chail valley, Communities' resilience score according to the model (1-9)

Elements	Average Score	Remarks
Community mobilization/organization	6.17	Collective approach of local people
Preventive measures	4.31	Site selection, alternate routes
Relief equipment	3.68	Some communities are having relief equipment
Evacuation plan	4.03	No access to hospital and markets during flash floods for most communities
Distribution of household	4.67	The big villages situated close Chail stream
Checklist of vulnerable	5.22	Having knowledge and value for vulnerable
Preparation	3.45	Collective approach towards emergencies
1st hand experience	6.59	Experience in flood 2010, and seasonal floods every year
Warning systems government	3.58	Less effective government warning system
Warning system community	6.35	Communities are proactive to communicate with each other
Response from government	4.15	Less effective response from government
Response from others	4.4	Response only for recovery after flood 2010

Source: Field Survey, 2018

Table 6. Chail valley, Houses destroyed in the sample villages during flash floods 2010

Village Name	No. of houses destroyed
Badalai	55
Depo	15
Kuz Chail	25
Shinko	65
Bashigram	95
Total	255

Fig. 3. Settlements in Chail valley exposed to flash floods and access of a sub valley to main road, they loss this access during flash floods

adjacent to the stream channel. In the selected five localities a total of 255 houses, adjacent agriculture lands and 04 fish hatcheries were washed away.

During flood 2010 the width of Chail valley was increased and now some of the sub valleys and villages are accessed through a road across stream channel and small bridges. After 2010 flood the flash floods became more disastrous in the valley. Every year the road across the stream channel and small bridges are washed and some of the sub valleys and villages are disconnected with the main road. These communities are not having access to main road in case of any emergency or food shortage, especially during evacuation. Some of the villages are now accessed by chair lefts and it will be difficult for a crowd to evacuate in case of unanticipated situation. There is also very weak response from government to rehabilitate bridges and access roads. Therefore after flood 2010 the communities in Chail valley are more vulnerable to flash floods.

3.6 Daral valley: Communities' Preparedness to flash floods

In Daral valley the resilience was evaluated according to the elements mentioned in Table 7, each of the elements was scored according to its significance in the sample localities, the average of sample localities for Daral valley is mentioned against each element.

In Daral valley, the communities are also more proactive to help each other in emergency situations; therefore, without any formal body, the communities are organized and mobilized to help each other and cope with the flash floods. They also work together to rehabilitate bridges or any side wall damaged during flash floods. The people also care about vulnerable people including disable, elderly, women and children during flash floods. Like Chail valley, the communities got a good experience responding to flash floods during and after flood 2010. The people are also proactive in warning each other on time while the government's warning system is very poor. In the valley most of the villages are situated on steep slopes and lacking evacuation plan and they are also not accessed by road. Mostly the communities are not keeping any relief equipment for any emergency situation. The community is responding on their own to

rehabilitate their infrastructure after flash floods.

3.7 Daral Valley: Communities' Environmental Conditions and flash floods

In Daral valley the slope is steep and the valley composed of hard rocks. Due to the local environmental conditions, most communities are a bit safe from direct damages, including washing away houses by flash floods. Before flood 2010 the peak flow was observed during the months of June, July and August. Daral stream was flowing in a very narrow channel almost a gorge with steep slopes towards both sides. During peak flow the stream was cutting its sides due to lateral erosion at few points especially in the down valley areas near Bahrain town.

During flood 2010 a very devastating flood hit the area, due to some local environmental conditions the damages were not that much as compared to the stream flow. Mostly the damages occurred in the down valley communities; it washed away hotels, bridges, roads and houses. In Daral valley the communities situated on upside are more resilient to the direct damages of flash floods. (Table 8) showing damages to houses in the five sample localities during flood 2010.

After flood 2010 flash floods are occurring in the months of June, July and August. Mostly it results into washing away temporary bridges, adjacent agriculture lands and side walls. In Daral valley the environmental conditions were not so much changed during the floods except few points and down valley areas, apart from that the stream is still flowing in a narrow channel with steep slopes towards both sides.

Following is the comparative analysis of Chail and Daral valleys

i.   In Chail valley the settlements are comparatively more vulnerable to flash floods than Daral valley due to the location of settlements close to the stream.

ii. In Chail valley, some sub valleys, especially Kwandai remain cut off from the main road every year due to seasonal floods, making it less resilient to flash floods.

iii. The slope is much steeper in Daral than
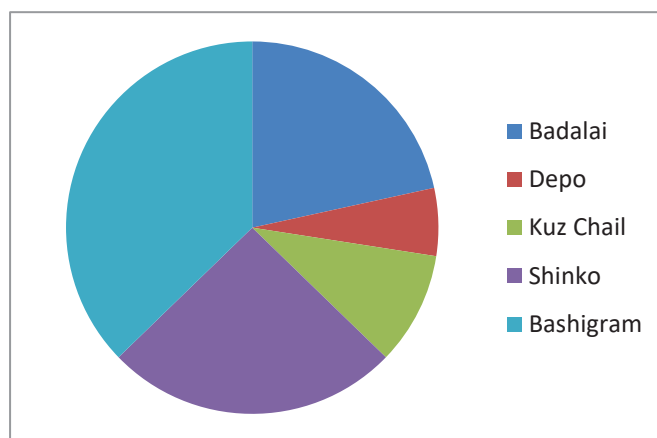
Source: Field Survey 2018

Fig. 4. Houses destroyed in the surveyed villages of Chail valley during flash floods 2010

Table 7. Daral Valley, Communities' Resilience score according to the model (1-9)

Elements	Average score	Remarks
Community mobilization/organization	7	Collective approach during natural hazards
Preventive measures	4	Most settlements on safe sites
Relief equipment	3	Not having special relief equipment
Evacuation plan	5	Having tough alternate routes to access Bahrain
Distribution of household	6	Houses on mountain slopes away from stream
Checklist of vulnerable	7	Knowledge of disable and vulnerable
Preparation	3	No collective approach for preparation
1st hand experience	5	The communities experiencing flash floods after and during 2010.
Warning systems government	2	Less effective early warning system by the government
Warning system community	5	The communities are proactive to inform each other
Response from government	2	The response is slow and very limited
Response from others	1	Different organizations worked only after 2010

Source: Field Survey 2018

Table 8. Houses destroyed in the surveyed villages of Chail valley during flash floods 2010

Village Name	No. of destroyed houses
Jheel	80
Niam	8
Lagan	11
Lagankar	4
Shaledar	2
Total	**105**
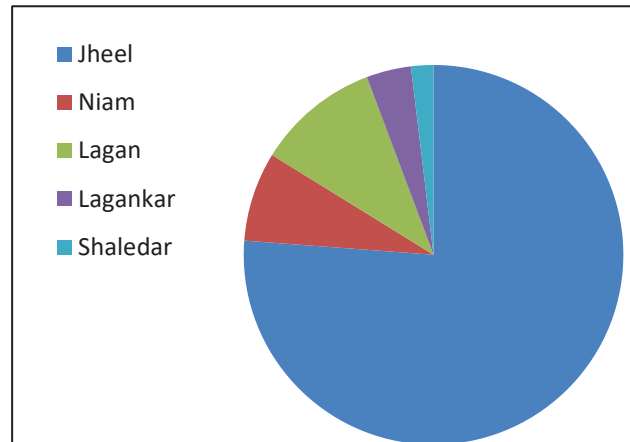
Fig. 5. Chail valley, Houses destroyed in the sample villages during flash floods 2010

Fig. 6. Daral valley is narrow and the settlements are situated on hillslopes above the stream.

Chail valley, but in Chail the rocks are in unconsolidated form while in Daral the rocks are in compact form so the flash floods in Chail valley also results into associated hazards especially land sliding and debris flow.

4. CONCLUSION

The resilience level differs due to differences in community preparedness and local environmental conditions in both the valleys. The Chail valley is resilient due to anthropogenic factors. The people are aware of flash floods. They keep some equipment for emergencies and quickly recover their access to main road and bridges after flash floods. Due to a comparatively wider valley, evacuation during unforeseen conditions will be comparatively easy. While Daral valley is resilient

due to natural factors, however the valley is narrow and hardly accessible but the rocks are mostly tough and the settlements are mostly situated on safe sites on mountain slopes. Due to the narrow valley and location of settlements on steep slopes, evacuation and access to basic health services during emergency situations are more challenging. The resilience level is considered low in both the valleys mainly due to evacuation and accessibility to emergency health services and safe places in case of flash floods. There is no any effective early warning system but the local people are proactive to inform each other in case of any unanticipated situation. In case of emergency related to flash floods, including casualties and damage to houses, rescue activities will be almost impossible to most of the communities in both the valleys due to hard access and rugged topography. The associated

hazards with flash floods further aggravate the situation especially to the far flung isolated settlements on the mountain slopes.

Due to diversity in local environmental conditions and community preparedness the resilience level differs from place to place within the target valleys. Generally it can be concluded that however some of the natural and anthropogenic factors contribute to the resilience level but in the target valleys due to rugged topography, lack of planning, lack of proper evacuation plan and emergency response, poor infrastructure, and unpaved houses on fragile slopes the resilience level to flash floods is considered low.

5. ACKNOWLEDGEMENTS

6. CONFLICT OF INTEREST

The authors declare no conflict of interest.

7. REFERENCES

1. Gardner, J. S. and Dekens, J. Mountain hazards and the resilience of social–ecological systems: lessons learned in India and Canada. Natural Hazards, 41, 317-336 (2007).
2. Collier, C.G. Flash flood forecasting: What are the limits of predictability ?. Quaterly journal of the royal meteorological society. Meteorol. Soc.133: 3-23 (2007).
3. Hemasinghe, H., Rangali, R.S.S., Deshapriya, N.L., & Samarakoon, L.. Landslide susceptibility mapping using logistic regression model (a case study in Badulla District, Sri Lanka). Procedia Engineering, 212: 1046–1053 (2018).
4. Alexander, D. E. Resilience and disaster risk reduction: an etymological journey. Natural Hazards and Earth System Sciences, 13, 2707–2716 (2013).
5. Dake K., Wildavsky A. Individual Differences in Risk Perception and Risk-Taking Preferences. In: Garrick B.J., Gekler W.C. (eds) The Analysis, Communication, and Perception of Risk. Advances in Risk Analysis, vol 9. Springer, Boston, MA (1991).
6. Baharmand, H. Boersma, K. Meesters, K. Mulder, F. Wolbers, J. A multidisciplinary perspective on supporting community disaster resilience in Nepal. Resilience: a multidisciplinary perspective, 1-11 (2016).
7. Manyena, S.B., The concept of resilience revisited. Disasters 30 (4), 433–450 (2006).
8. Pelling, M. The vulnerability of cities: Natural disasters and social resilience. Earthscan Publications Limited, p. 212 (2003).
9. Juhász, L. Podolcsak, A. Doleschall, J. Open Source Web Gis Solutions in Disaster Management – with Special Emphasis On Inland Excess Water Modeling. Journal of Environmental Geography, 9(1-2), 15-21(2016).
10. Chen, S.C. Fereng, J.W. Wang, Wu, T.Y. Wang. J.J. Assessment of disaster resilience capacity of hillslope communities with high risk for geological hazards. Engineering Geology, 98, 86-101(2008).
11. Hewitt, K. Regions of risk: a geographical introduction to disasters. Longman, London,2, 365-382 (1997).
12. Gardner, J.S. Natural hazards risk in the Kullu District, Himachal Pradesh, India. Geogr Rev, 92:282–306 (2002).
13. Korup, O. Mountain Hazards and Climamte Change. Mountains and Climate Change: A Global Concern: Sustainable Mountain Development Series published by Austrian Development This publication was supported by the Austrian Development Cooperation and Swiss Agency for Development and Cooperation, 61-75 (2014).
14. Sher, H. Ali, H. Rehman, S. Identification and Conservation of Important Plant Areas (IPAS) for the Distribution Of Medicinal, Aromatic And Economic Plants In The Hindukush-Himalaya Mountain Range. Pakistan Journal of Botany, 44, 187-194 (2012).
15. Zaman, L. et al. The Impact of Training Provided by Malteser International through Community Based Disaster Risk Management Committees (Cbdrmc) to Local People in Chail Valley District Swat. Journal of Applied Environmental and Biological Sciences, 6 48-55 (2016).
16. Saaty, T.L. The Analytic Hierarchy Process. John Wiley, New York, 287–288 (1980).
17. Rahman, A. Disaster risk management: flood

perspective. VDM Verlag Publishing Co, Saarbrücken, p. 192 (2010).

18. World Disaster Report (WDR), Focus on community resilience. International Federation of Red Cross and Red Crescent Societies, Geneva, p. 232 (2004).

19. Government of Pakistan (GoP) District census Report of Swat, Population Census Organization, Islamabad (2017).

20. Rahman, A. Farzana, Rahman, G. Shaw, R. Flood Disasters and Land Use Planning in Swat Valley, Eastern Hindu Kush. Chapter 10 in the book Land use management in Disaster Risk Reduction. Published by Springer Japan, 179-195 (2017).

Pakistan Academy of Sciences

Research Article

Unit Xgamma Distribution: Its Properties, Estimation and Application

Sharqa Hashmi[1], Muhammad Ahsan-ul-Haq[2*], Javeria Zafar[2], and Mundher Abdullah Khaleel[3]

[1]HED, Govt. of the Punjab, Lahore, Pakistan.
[2]College of Statistical & Actuarial Sciences, University of the Punjab, Lahore, Pakistan.
[3]College of Computer Science and Mathematics, Department of Mathematics,
Tikrit University, Iraq.

Abstract: A new one-parameter model for unit-interval datasets is introduced. The proposed distribution is termed "Unit Xgamma distribution." Some mathematical properties of the new distribution are derived. We also characterize it using truncated moments and a hazard function. Maximum likelihood, least-squares, weighted least-squares, Anderson-Darling, Cramer-von Mises, and maximum product spacing are among the five estimation methods used to estimate the parameter. A Monte Carlo simulation was used to test the efficacy of these developed estimators. The flexibility of the proposed distribution was assessed using water capacity data. The proposed unit Xgamma distribution can be used for bounded datasets as an alternative to the well-known competitive distributions available in the literature.

Keywords: Unit-Xgamma Moments Risk Measures Estimation Data Analysis.

1. INTRODUCTION

The bounded distributions, which are based on the unit interval, are useful for modeling the behavior of random variables with intervals (0,1). The Beta distribution [1] is considered a bounded distribution and is extensively used for modeling such data sets. There is always a need for other models for modeling bounded data sets. Some such important well-known distributions include Kumaraswamy distribution [2], Unit Burr-III [4], Unit Gompertz distribution [5], Unit Lindley distribution [6], Unit Gamma distribution [7], Unit Birnbaum-Saunders distribution [8], Unit-inverse Gaussian distribution [3], Unit Weibull distribution [9], Unit Logistic distribution [10], Unit modified Burr III distribution [11], unit Rayleigh distribution [12], Unit power-logarithmic distribution [13], odd Frechet power function distribution [14], Unit Burr XIII distribution [15], modified Kumaraswamy distribution [16], Unit Teissier distribution [17], inflated unit Birnbaum-Saunders distribution [18] and log-XLindley

distribution because (i) it can be considered as an appropriate distribution to model the skewed data where other competent models available in the literature may not be adequately fitted; (ii) it can also be applied to model various real data sets in the fields of survival and industrial reliability.

The Xgamma distribution was introduced [20] to model lifetime data sets. The Xgamma distribution was derived using a finite gamma and exponential distribution mixture. A random variable Y has Xgamma distribution, if its probability density function (pdf) $g(x)$ and cumulative distribution function (cdf) $G(x)$ are, respectively, given by:

$$g(y;\theta) = \frac{\theta^2}{(1+\theta)}\left(1 + \frac{\theta}{2}y^2\right)\exp(-\theta y), \quad y \geq 0. \quad (1)$$

$$G(y;\theta) = 1 - \left[\frac{1 + \theta + \theta y + \frac{\theta^2 y^2}{2}}{(1+\theta)}\right]\exp(-\theta y). \quad (2)$$

where θ is the scale parameter.

The inspiration of this work is to propose a new distribution from the Xgamma distribution by a transformation $X = Y/(1 + Y)$, where Y has the Xgamma distribution.

- The proposed distribution comprises the behavior of the Beta distribution and provides better fits than some well-known lifetime probability distributions, such as the Kumaraswamy distribution.
- The proposed distribution is capable of data analysis of increasing hazard rate function.
- It can be viewed as the most suitable probability model for fitting negatively skewed data sets.

The paper is structured as follows: In Section 2, we present the Unit-Xgamma distribution (UXG) along with graphical representations of its pdf, cdf, and reliability function. In Section 3, some mathematical properties, including moments and associated measures, actuarial measures, and order statistics. The new distribution is also characterized based on truncated moments and hazard function. The parameter is estimated using five different estimation methods in Section 4. Monte-Carlo simulations are performed in Section 5 to investigate the performance of these estimators. The analysis of a real data set has been presented in Section 6. In the last section, we conclude our study.

2. UNIT-XGAMMA DISTRIBUTION

The Unit-Xgamma distribution is derived using the transformation $X = Y/(1 + Y)$ with support on the unit interval. The cdf and pdf of the proposed distribution respectively are given by

$$F(x)$$
$$= 1 - \frac{1 + \theta + \theta\left(\frac{x}{1-x}\right) + \frac{\theta^2}{2}\left(\frac{x}{1-x}\right)^2}{(1 + \theta)}e^{-\theta\left(\frac{x}{1-x}\right)},$$
$$0 < x < 1, \theta > 0.$$
(3)

and

$$f(x) = \left(\frac{\theta^2}{1+\theta}\right)\left[\frac{1}{(1-x)^2}\right]\left[1 + \frac{\theta}{2}\left(\frac{x}{1-x}\right)^2\right]e^{-\theta\left(\frac{x}{1-x}\right)},$$

$$0 < x < 1 \qquad (4)$$

Figure 1 shows the shapes of the UXG distribution's pdf and cdf for various parameter values.
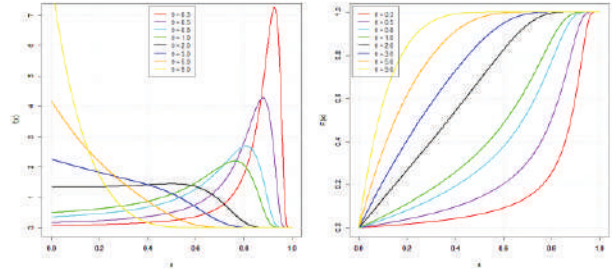
Fig. 1: Plots of pdf and cdf for UXG Distribution

$$S(x) = \frac{e^{\frac{-x\theta}{1-x}}\{2(1+\theta) - 2x(2+\theta) + x^2(2+\theta^2)\}}{2(1-x)^2(1+\theta)},$$
(5)

$$h(x) = \frac{\theta^2\left\{1 + \frac{x^2\theta}{2(1-x)^2}\right\}}{(1-x)^2\left[1 + \theta + \frac{x\theta}{1-x} + \frac{x^2\theta^2}{2(1-x)^2}\right]}.$$
(6)

Figure 2 shows the survival and hazard functions of the UXG distribution for various parameter values.
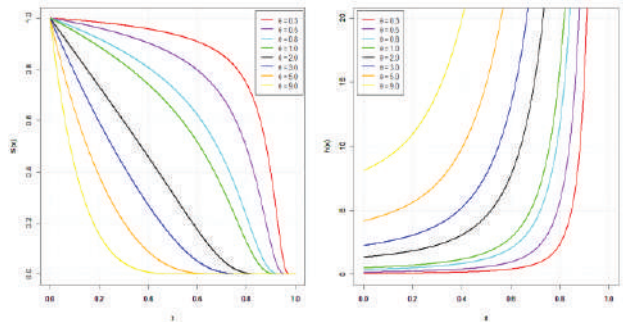
Fig. 2: Survival and hazard plots for UXG distribution

The shape of a pdf can be studied by limiting behavior at origin and one. The hazard function also showed the same results at the origin. That is

$$\lim_{x\to 0} h(x) = \lim_{x\to 0} f(x) = \frac{\theta^2}{1+\theta}$$

and shapes of pdf and hazard function at the upper limit are given by

$$\lim_{x\to\infty} f(x) = 0, \ \lim_{x\to\infty} h(x) = \infty$$

This shows that distribution begins from a point on the vertical axis. Now, it is needed to get more knowledge about its trend at origin by taking the limit of f'(x). f'(x) may be negative (positive), the pdf goes downward (upward) at the origin.

The first derivative of (4) is

$$\lim_{x \to 0} \frac{df(x)}{dx} = \frac{(2-\theta)\theta^2}{1+\theta}$$

For $\theta > 2$, the pdf goes down and upwards otherwise.

3. MATHEMATICAL PROPERTIES

3.1. Moments

If the random variable X is UXG distribution, then its rth moment about the origin can be given as

$$\mu_r' = \int_0^1 x^r f(x) \, dx$$

$$\mu_r' = \frac{\theta^2}{1+\theta} \int_0^1 \frac{x^r}{(1-x)^2} e^{-\theta\left(\frac{x}{1-x}\right)} dx$$

$$+ \frac{\theta^3}{2(1+\theta)} \int_0^1 \frac{x^{r+1}}{(1-x)^3} e^{-\theta\left(\frac{x}{1-x}\right)} dx \quad (7)$$

Considering first integral

$$I_1 = \left(\frac{\theta^2}{1+\theta}\right) \int_0^1 \frac{x^r}{(1-x)^2} e^{-\theta\left(\frac{x}{1-x}\right)} dx$$

Using transformation $z = \left(\frac{x}{1-x}\right)$, we get the expression

$$I_1 = \left(\frac{\theta^2}{1+\theta}\right) \int_0^\infty \left(\frac{z}{1+z}\right)^r e^{-\theta z} dz$$

Again taking $y = 1 + z$

$$I_1 = \left(\frac{\theta^2 e^\theta}{1+\theta}\right) \int_1^\infty \left(1 - \frac{1}{z}\right)^r e^{-\theta z} dz$$

Using expansion $(1-x)^p = \sum_{k=0}^\infty (-1)^k \binom{p}{k}(x)^k$

$$= \left(\frac{\theta^2 e^\theta}{1+\theta}\right) \sum_{k=0}^\infty (-1)^k \binom{r}{k} \int_1^\infty \left(\frac{1}{z}\right)^k e^{-\theta z} dz$$

$$= \left(\frac{\theta e^\theta}{1+\theta}\right) \sum_{k=0}^\infty (-1)^k \binom{r}{k} \theta^k \Gamma(1-k,\theta) \quad (8)$$

Now taking the second term of Eq. (7)

$$I_2 = \frac{\theta^3}{2(1+\theta)} \int_0^1 \frac{x^{r+2}}{(1-x)^4} e^{-\theta\left(\frac{x}{1-x}\right)} dx$$

Using transformation $z = \left(\frac{x}{1-x}\right)$, we get the following expression

$$I_2 = \frac{\theta^3 e^\theta}{2(1+\theta)} \int_1^\infty \left(1 - \frac{1}{z}\right)^{r+2} \left(\frac{1}{z}\right)^2 e^{-\theta z} dz$$

$$= \frac{\theta^3 e^\theta}{2(1+\theta)} \sum_{k=0}^\infty (-1)^k \binom{r+2}{k} \int_1^\infty \left(\frac{1}{z}\right)^{k+2} e^{-\theta z} dz$$

$$= \frac{\theta^3 e^\theta}{2(1+\theta)} \sum_{k=0}^\infty (-1)^k \binom{r+2}{k} \theta^{k+1} \Gamma(-k-1,\theta) \quad (9)$$

The final expression of ordinary moments is μ_r'

$$= \left(\frac{\theta e^\theta}{1+\theta}\right) \sum_{k=0}^\infty (-1)^k \binom{r}{k} \theta^k \Gamma(1-k,\theta)$$

$$+ \frac{\theta^3 e^\theta}{2(1+\theta)} \sum_{k=0}^\infty (-1)^k \binom{r+1}{k} \theta^k \Gamma(2-k,\theta). \quad (10)$$

The moment generating function of UXG distribution is obtained by using Eq. (10), given as

$$M_x(t) = E(e^{tX})$$

$$= \sum_{r=0}^\infty \frac{t^r}{r!} E(X^r). \quad (11)$$

The numerical values of mean, variance, dispersion index, skewness, and kurtosis for some selected values of parameters are presented in Table 1. The behavior of UXG distribution is negatively for lower values of $\theta \leq 1$ and positively skewed for $\theta > 1$. The UXG distribution is leptokurtic for $\theta \leq 0.5 \text{ or } \theta > 5$ and $\theta = 5$ model is mesokurtic. Also, for $0.5 < \theta < 5$, UXG model is platykurtic.

3.2. Actuarial Measures

In this subsection we derived two risk measures, value at risk (VaR) and tail value at risk (TVaR). For more information about actuarial measures, readers can consult the following studies [21] [22] [23].

The VaR of UXG is derived as $x_p = F^{-1}(t)$, where t is the solution of the equation

Hashmi et al

Table 1: Some descriptive measures for some specific values of θ.

θ	μ	σ^2	DI	Skewness	Kurtosis
0.3	0.82190	0.02792	0.03397	-2.40551	9.18987
0.5	0.72439	0.04266	0.05889	-1.53032	4.76441
0.8	0.61147	0.05271	0.08620	-0.90568	2.85768
1.0	0.55274	0.05452	0.09864	-0.64885	2.36971
2.0	0.36979	0.04554	0.12315	0.04662	1.91532
3.0	0.27578	0.03378	0.12249	0.40451	2.19210
4.0	0.21908	0.02527	0.11535	0.64096	2.57963
5.0	0.18134	0.01939	0.10693	0.81396	2.97398
7.0	0.13445	0.01228	0.09134	1.05525	3.69344
9.0	0.10660	0.00840	0.07880	1.21769	4.29919
12	0.08117	0.00526	0.06480	1.38233	5.02381
15	0.06547	0.00359	0.05483	1.49321	5.58091
20	0.04945	0.00215	0.04348	1.61401	6.25796

Table 2: The risk measures (VaR and TVaR) for the UXG distribution

θ	Significance level	VaR_p	$TVaR_p$
	0.70	0.85683	0.26838
	0.75	0.86887	0.22525
	0.80	0.88061	0.18149
0.50	0.85	0.89244	0.13719
	0.90	0.90506	0.09224
	0.95	0.92016	0.04664
	0.99	0.94051	0.00947
	0.70	0.72049	0.23814
	0.75	0.74382	0.20153
	0.80	0.76660	0.16378
1.0	0.85	0.78961	0.12487
	0.90	0.81414	0.08479
	0.95	0.84349	0.04339
	0.99	0.88306	0.00896
	0.70	0.51093	0.18823
	0.75	0.54572	0.16181
	0.80	0.58118	0.13364
2.0	0.85	0.61831	0.10366
	0.90	0.65914	0.07175
	0.95	0.70943	0.03760
	0.99	0.77929	0.00804
	0.70	0.24178	0.10797
	0.75	0.27041	0.09519
	0.80	0.30284	0.08087
5.0	0.85	0.34069	0.06482
	0.90	0.38733	0.04666
	0.95	0.45238	0.02579
	0.99	0.55669	0.00598

$$\left(\frac{x}{1-x}\right) + \frac{\theta}{2}\left(\frac{x}{1-x}\right)^2 e^{-\theta\left(\frac{x}{1-x}\right)} = -\frac{p(1+\theta)}{\theta}$$

TVaR of X is defined as

$$TVaR_p(x) = \frac{1}{1-p}\int_{VaR}^{\infty} xf(x)\,dx \qquad (12)$$

Using Eq. (4) in (12), we get

$$TVaR_p(x) = \frac{e^{\theta}\left(\frac{\theta^2}{1+\theta}\right)}{1-p}\left[\frac{e^{\left(\frac{1}{1-VaR}\right)}}{\theta} - \Gamma\left(0, \frac{1}{1-VaR}\right)\right.$$

$$\left. + \frac{\theta}{2}\sum_{k=0}^{\infty}(-1)^k\binom{3}{k}\theta^{k+1}\Gamma\left(-1\right.\right.$$

$$\left.\left. - k, \frac{1}{1-VaR}\right)\right]. \qquad (13)$$

Some numerical values of VaR and TVaR are presented in Table 2.

3.3. Order Statistics

Order statistics is commonly used and performed in the statistical literature. Let $X_1, X_2, \ldots, X_n$ represent r.v. with cdf $F(x)$. If $X_{1:n}, X_{2:n}, \ldots, X_{n:n}$ are the related ordered random samples of size n, then the pdf of rth order statistic is given as

$$f_{r:n} = W[F(x)]^{r-1}[1-F(x)]^{n-r}f(x)$$

where $W = \dfrac{n!}{(r-1)!\,(n-r)!}$

By using binomial expansion

$$= W\sum_{l=0}^{n-r}(-1)^l\binom{n-r}{l}[F(x)]^{r+l-1}f(x)$$

$$= W\sum_{l=0}^{n-r}(-1)^l\binom{n-r}{l}\times$$

$$\left[1 - \frac{1+\theta+\theta\left(\frac{x}{1-x}\right)+\frac{\theta}{2}\left(\frac{x}{(1-x)^2}\right)^2}{1+\theta}e^{-\theta\left(\frac{x}{1-x}\right)}\right]^{r+l-1}\times$$

$$\left(\frac{\theta^2}{1+\theta}\right)\left[\frac{1}{(1-x)^2}\right]\left[1+\frac{\theta}{2}\left(\frac{x}{(1-x)^2}\right)^2\right]e^{-\theta\left(\frac{x}{1-x}\right)}$$

$$= W\frac{\theta^2}{1+\theta}\sum_{l=0}^{n-r}(-1)^l\binom{n-r}{l}\frac{1}{(1-x)^2}$$

$$\times\left[1+\frac{\theta}{2}\left(\frac{x}{(1-x)^2}\right)^2\right]e^{-\theta\left(\frac{x}{1-x}\right)}$$

$$\times\sum_{s=0}^{r+l+1}(-1)^s\binom{r+l+1}{s}\left[\frac{1+\theta+\theta\left(\frac{x}{1-x}\right)+\frac{\theta}{2}\left(\frac{x}{(1-x)^2}\right)^2}{1+\theta}\right]^s e^{-\theta s\left(\frac{x}{1-x}\right)}$$

$$= W\frac{\theta^2}{1+\theta}\sum_{l=0}^{n-r}\sum_{s=0}^{r+l+1}(-1)^{l+s}\binom{n-r}{l}\binom{r+l+1}{s}\frac{1}{(1-x)^2}\left[1\right.$$

$$\left.+\frac{\theta}{2}\left(\frac{x}{(1-x)^2}\right)^2\right]\left[\frac{1+\theta+\theta\left(\frac{x}{1-x}\right)+\frac{\theta}{2}\left(\frac{x}{(1-x)^2}\right)^2}{1+\theta}\right]^s e^{-\theta(s+1)\left(\frac{x}{1-x}\right)}$$

By using exponential expansion

$$f_{r:n}$$

$$= W\frac{\theta^2}{1+\theta}\sum_{l=0}^{n-r}\sum_{s=0}^{r+l+1}\sum_{q=0}^{\infty}(-1)^{l+s+q}\frac{(\theta(s+1))^q}{q!}\binom{n-r}{l}\binom{r+l+1}{s}$$

$$\times\frac{x^q}{(1-x)^{q+2}}$$

$$\times\left[1+\frac{\theta}{2}\left(\frac{x}{(1-x)^2}\right)^2\right]\left[\frac{1+\theta+\theta\left(\frac{x}{1-x}\right)+\frac{\theta}{2}\left(\frac{x}{(1-x)^2}\right)^2}{1+\theta}\right]^s.$$

3.4. Characterizations

The presence of a new stochastic function must be validated against the underlying model's requirements. Glänzel [24] suggests that studying characterizations could be useful in this approach. The ratio of two truncated moments is used to characterize the UXG distribution. So we use the idea of Glänzel to characterize the UXG distribution.

Proposition 1: Let $X: \Omega \to (0,1)$ be distributed as Eq. (4) and

$$q_1(x) = \left\{1 + \frac{x^2\theta}{2(1-x)^2}\right\}^{-1}$$

$$q_2(x) = q_1(x)\ e^{\frac{x\theta}{x-1}}, \quad x > 0. \qquad (18)$$

The random variable X follows UXG if and only if the function η defined in Theorem [24] is of the form

$$\eta(x) = \frac{1}{2}e^{\frac{x\theta}{x-1}} \qquad (19)$$

Proof:

$$(1 - F(x))E[q_1(X)|X \geq x] = \int_x^1 \frac{e^{\frac{x\theta}{x-1}}\theta^2}{(x-1)^2(1+\theta)}dx$$

$$= \frac{e^{\frac{x\theta}{x-1}}\theta}{(1+\theta)}, 0 < x < 1$$

Similarly,

$$(1 - F(x))E[q_2(X)|X \geq x] = \frac{e^{\frac{2x\theta}{x-1}}\theta}{2(1+\theta)}, \quad 0 < x < 1$$

Now

$$\eta(x) = \frac{E[q_2(X)|X \geq x]}{E[q_1(X)|X \geq x]} = \frac{1}{2}e^{\frac{x\theta}{x-1}}$$

Completes the proof.

and $\eta(x)q_1(x) - q_2(x) = q_1(x)\left[\eta(x) - e^{\frac{x\theta}{x-1}}\right]$

$$= \frac{e^{\frac{x\theta}{-1+x}}(-1+x)^2}{2 + x(-4 + x(2+\theta))} < 0$$

$$\acute{s}(x) = \frac{\acute{\eta}(x)q_1(x)}{\eta(x)q_1(x) - q_2(x)} = \frac{\theta}{(x-1)^2}$$

and hence

$$s(x) = -\ln\left(e^{-\frac{x\theta}{1-x}}\right), \quad 0 < x < 1 \qquad (20)$$

Now by Proposition (1), X has density (4).

Corollary 1: Assume $X: \Omega \to (0,1)$ be a continuous random variable, then $q_1(x)$ is the same as in Proposition 1. The pdf of X is (4) if and only if the differential equation is satisfied by functions $q_2(x)$ and η(x) stated in Theorem [24].

$$\frac{\acute{\eta}(x)q_1(x)}{\eta(x)q_1(x) - q_2(x)} = \frac{\theta(2+x(-4+x(2+\theta)))}{2(-1+x)^4}, \quad 0 < x < 1$$

(21) The general solution of the differential Eq. (21) is

$$\eta(x) = \left[e^{\frac{x\theta}{-1+x}}\right]^{-1}$$

$$\times \left[\int_0^x \frac{-\theta}{(1-x)^2}[q_2(x)\{q_1(x)\}^{-1}]dx + D\right],$$

D is the constant in this equation. Note that in Proposition 1 with $D = 0$, $q_1(x)$, $q_2(x)$ and $\eta(x)$ are set of functions that satisfy the differential Eq.(21).

The hazard function-related characterization of the UXG distribution is now given. The hazard function h(x) is known to satisfy the following differential equation.

$$\frac{\acute{f}(x)}{f(x)} = \frac{\acute{h}(x)}{h(x)} - h(x)$$

Proposition 2: If $h(x)$ satisfies the differential equation, then X is a continuous random variable range between 0 and 1 with pdf Eq. (4).

$$\acute{h}(x) - 2(1-x)^{-1}h(x)$$

$$= \frac{2\left(-2 + x\left(6 + x(-4+\theta)\right)\right)\theta^3}{(x-1)^2\left(2(1+\theta) - 2x(2+\theta) + x^2(2+\theta^2)\right)^2}. \qquad (22)$$

under the boundary conditions h(0)≥0.

Proof: If r.v. X has the HR given in (6) then

$$\acute{h}(x)$$

$$= \frac{1}{(x-1)^3(2(1+\theta) - 2x(2+\theta) + x^2(2+\theta^2))^2)}$$

$$\times \left[\begin{array}{l}-((2\theta^2(4(x-1)^4 + 2(x-1)^2(1+x^2)\theta \\ +(x-1)x^2(2x-5)\theta^2 + x^4\theta^3))\end{array}\right]$$

and substitution of the above result in

$\acute{h}(x) - 2(1-x)^{-1}h(x)$ and the result follows.

Conversely, if Eq. (22) holds then

$$\frac{d}{dx}[(1-x)^2h(x)]$$

$$= \frac{d}{dx}\left(\frac{\theta^2(1 + \frac{x^2\theta}{2(1-x)^2})}{1+\theta + \frac{x\theta}{1-x} + \frac{x^2\theta^2}{2(1-x)^2}}\right)$$

$$h(x) = \frac{\theta^2(1 + \frac{x^2\theta}{2(1-x)^2})}{(1-x)^2(1+\theta + \frac{x\theta}{1-x} + \frac{x^2\theta^2}{2(1-x)^2})}$$

$$+ C$$

which implies C=0.

4. PARAMETER ESTIMATION

In this section, we investigate the estimation of unknown parameter θ of UXG distribution using different well-known estimation methods. The considered estimation methods are; maximum likelihood, Anderson Darling, Cramer Von Mises, ordinary least squares, weighted least square, and maximum product spacing. For more detail reader can consult following studies [25], [26] [27]. Now onwards, a random sample is denoted by $x_1, x_2, x_3, \dots, x_n$ from the $UXG(\theta)$ distribution of size n. The nonlinear equations of different estimation methods can be solved using statistical software (e.g., R, Mathematica). We used R in this study.

4.1. Maximum Likelihood Estimation

The most favorable parametric estimating method is the MLE method. The reason is described by theoretical acceptance of the estimators' limiting characteristics, such as consistency, efficiency, and asymptotic normality. The method of MLE of the UXG model is given below. The MLE of θ is obtained by maximizing the log-likelihood function for θ, the log-likelihood function $l(\theta)$ is equal to

$$l(\theta) = n \log\left(\frac{\theta^2}{1+\theta}\right) - 2\sum_{i=1}^{n} \log[1 - x_i]$$

$$+ \sum_{i=1}^{n} \log\left[1 + \frac{\theta}{2}\left(\frac{x_i}{1-x_i}\right)^2\right]$$

$$+ \theta \sum_{i=1}^{n} \left(\frac{x_i}{1-x_i}\right).$$

$U_\theta = \partial l(\theta)/\partial\theta$ is given below
U_θ

$$= \frac{n(1+\theta)\left[\frac{2\theta}{1+\theta} - \frac{\theta^2}{(1+\theta)^2}\right]}{\theta^2}$$

$$+ \sum_{i=1}^{n} \frac{x_i^2}{2(1-x_i)^2\left(1 + \frac{\theta x_i^2}{2(1-x_i)^2}\right)}$$

$$- \sum_{i=1}^{n} \left(\frac{x_i}{1-x_i}\right)$$

equating U_θ to zero and it can be solved using statistical software R.

4.2. Least Squares and Weighted Least Squares

We now take into account the methods of ordinary least squares (OLS) estimation and weighted least-squares (WLS) estimation. OLS estimation method was firstly presented by Swain (1988). It is a nonlinear method of estimation, especially when the MLEs cannot be obtained in an explicit form. The OLS of θ can be obtained by minimizing the least square function L(θ)

$$L(\theta) = \sum_{i=1}^{n} \left(F(x_{(i)}; \theta) - \frac{i}{n+1}\right)^2.$$

with respect to θ, where x(i), (i=1,2,3,…..,n) is the ith element of the ordered observations $x_1, x_2, x_3 \dots, x_n$ and $\hat{F}(.)$ is empirical CDF of ith observation. i.e., $\hat{F}(.) = \frac{i}{n+1}$.

By using Eq. (3) and $\hat{F}(.)$, we have

$$= \sum_{i=1}^{n} \left(1 - \frac{1+\theta+\theta\left(\frac{x_{(i)}}{1-x_{(i)}}\right)+\frac{\theta^2}{2}\left(\frac{x_{(i)}}{1-x_{(i)}}\right)^2}{(1+\theta)} e^{-\theta\left(\frac{x_{(i)}}{1-x_{(i)}}\right)} - \right.$$

$$\left. \frac{i}{n+1}\right)^2.$$

Thus, the LSE can be obtained by equating the equation to zero, i.e., $\partial L(\theta)/\partial\theta = 0$

$$\frac{\partial L(\theta)}{\partial\theta}$$

$$= 2\sum_{i=1}^{n} \eta_i \left(1 - \frac{i}{1+n}\right.$$

$$\left. - \frac{e^{-\frac{\theta x_{(i)}}{1-x_{(i)}}}\left(1 + \theta + \frac{\theta x_{(i)}}{1-x_{(i)}} + \frac{\theta^2 x_{(i)}^2}{2(1-x_{(i)})^2}\right)}{1+\theta}\right).$$

where

$$\eta_i$$
$$= \frac{-1}{2(x_{(i)} - 1)^3(1 + \theta)^2}$$
$$\times \left(x_i\theta e^{\frac{x_{(i)}\theta}{x_{(i)}-1}} \left\{ \begin{array}{l} 2(2 + \theta) - x_{(i)} \\ (8 + 3\theta) + x_{(i)}{}^2(4 + 2\theta + \theta^2) \end{array} \right\} \right)$$
$$\tag{23}$$

The weighted least square estimate (WLS) of θ, can be obtained by minimizing the weighted least square function with respect to θ, defined by

$$WLS(\theta) = \sum_{i=1}^{n} \frac{(n + 1)^2(n + 2)}{i(n - i + 1)} \left[F(x_{(i)}; \theta) - \frac{i}{n + 1} \right]^2$$

$$= \sum_{i=1}^{n} \frac{(n + 1)^2(n + 2)^2}{i(n - i + 1)} \times$$

$$\left[1 - \frac{1 + \theta + \theta\left(\frac{x_{(i)}}{1 - x_{(i)}}\right) + \frac{\theta^2}{2}\left(\frac{x_{(i)}}{1 - x_{(i)}}\right)^2}{(1 + \theta)} e^{-\theta\left(\frac{x_{(i)}}{1 - x_{(i)}}\right)} \right.$$
$$\left. - \frac{i}{n + 1} \right]$$

$\partial WLS(\theta)/\partial\theta = 0$ gives the WLSQE of θ.

$$\frac{\partial WLS(\theta)}{\partial \theta} = 2 \sum_{i=1}^{n} \eta_i \frac{(n + 1)^2(n + 2)}{i(n - i + 1)} \times$$

$$\left(1 - \frac{i}{1 + n} - \frac{e^{-\frac{\theta x_{(i)}}{1 - x_{(i)}}}(1 + \theta + \frac{\theta x_{(i)}}{1 - x_{(i)}} + \frac{\theta^2 x_{(i)}^2}{2(1 - x_{(i)})^2})}{1 + \theta} \right)$$

where η_i is given by Eq. (23).

4.3. Cramer-von Misses Estimation

Another method for obtaining estimates is the Cramer-von Mises (CVM) estimates by minimizing its function with respect to θ. It is defined by

$$C(\theta) = \frac{1}{12n} + \sum_{i=1}^{n} \left[F(x_{(i)}; \theta) - \frac{2i - 1}{2n} \right]^2$$

$$= \sum_{i=1}^{n} \left[1 \right.$$
$$- \frac{1 + \theta + \theta\left(\frac{x_{(i)}}{1 - x_{(i)}}\right) + \frac{\theta^2}{2}\left(\frac{x_{(i)}}{1 - x_{(i)}}\right)^2}{(1 + \theta)} e^{-\theta\left(\frac{x_{(i)}}{1 - x_{(i)}}\right)}$$
$$\left. - \frac{2i - 1}{2n} \right]^2 + \frac{1}{12n}$$

Thus, the CVM estimates are obtained by the given equation: $\partial C(\theta)/\partial\theta = 0$, where

$$\frac{\partial C(\theta)}{\partial \theta}$$

$$= 2 \sum_{i=1}^{n} \eta_i \left(1 \right.$$
$$- \frac{1 + \theta + \theta\left(\frac{x_{(i)}}{1 - x_{(i)}}\right) + \frac{\theta^2}{2}\left(\frac{x_{(i)}}{1 - x_{(i)}}\right)^2}{(1 + \theta)} e^{-\theta\left(\frac{x_{(i)}}{1 - x_{(i)}}\right)}$$
$$\left. - \frac{2i - 1}{2n} \right)$$

where η_i is given by Eq. (23).

The CVE shows that this estimator's bias (θ) is lower than those of other minimum distance estimators.

4.4. Anderson-Darling Estimation

The Anderson-Darling (AD) estimate of θ can be obtained by minimizing the following function, with respect to θ, which is given by

$$A(\theta) = -n - \frac{1}{n}\sum_{i=1}^{n}(2i - 1)$$

$$\times \left[\log F(x_{(i)}; \theta) + \log[1 - F(x_{(n+1-i)}; \theta)] \right]$$

Thus, the AD estimate can be determined by solving the following equation: $\partial A(\theta)/\partial\theta = 0$,

$$\frac{\partial A(\theta)}{\partial \theta} = -\frac{1}{n} \sum_{i=1}^{n} (2i - 1)$$

$$\times \left(\frac{\eta_i}{F(x_{(i)}; \theta)} \right.$$

$$\left. - \frac{\eta_{n+1-i}}{1 - F(x_{(n+1-i)}; \theta)} \right).$$

where η_i is given in Eq. (23).

Note that all estimation methods can be obtained by using numerical methods.

4.5. Maximum Product Spacing Estimation

For $u = 1,2,3, \dots, h + 1$, assume $D_u(\theta) = F(x_{(u)} | \theta) - F(x_{(u-1)} | \theta)$, be the uniform spacings of a random sample from the UXG model, where $F(x_{(0)} | \theta) = 0$, $F(x_{(h+1)} | \theta) = 1$ and $\sum_{r=1}^{h+1} D_u(\theta) = 1$. The MPSE of the parameter θ, say $\hat{\lambda}$, can be estimated by maximizing the geometric mean of the spacings

$$MPSE(\lambda) = \left[\prod_{u=1}^{h+1} D_u(\lambda) \right]^{\frac{1}{h+1}}$$

with respect to the parameter θ.

5. SIMULATION STUDY

In this section, some simulation studies are presented for the comparison of different estimation methods such as maximum likelihood estimation (MLE), least-squares estimation (OLS), weighted least square estimation (WLS), Cramer-von Mises estimation (CVM), Anderson-Darling estimation (AD) and maximum product spacing (MPS). In simulation studies, both small and large sample sizes are considered. We evaluate the performance of the estimators by bias, mean squared errors.

We consider the UXG model, and data are simulated using $N = 10,000$ with sample sizes n=20, 50, 80, 100, and 200 for some specific values of a parameter. Simulated bias and MSE are given in Tables 2-8.

Table 2: The simulated biases and MSEs of the UXG model for (θ=0.3)

n		ML	AD	CVM	OLS	WLS	MPS
20	Bias	0.00685	0.00467	0.00646	0.00508	0.00454	0.00499
	MSE	0.00185	0.00201	0.00231	0.00228	0.00214	0.00168
50	Bias	0.00259	0.00184	0.00259	0.00204	0.00189	0.00341
	MSE	0.00074	0.00081	0.00090	0.00089	0.00083	0.00071
80	Bias	0.00057	0.00019	0.00018	0.00017	0.00008	0.00354
	MSE	0.00044	0.00048	0.00052	0.00052	0.00049	0.00044
100	Bias	0.00191	0.00111	0.00137	0.00109	0.00120	0.00156
	MSE	0.00034	0.00038	0.00042	0.00042	0.00039	0.00033
200	Bias	0.00031	0.00027	0.00058	0.00044	0.00033	0.00167
	MSE	0.00017	0.00019	0.00021	0.00020	0.00019	0.00017

Table 3: The simulated biases and MSEs of the UXG model for (θ=0.5)

n		ML	AD	CVM	OLS	WLS	MPS
20	Bias	0.01231	0.00812	0.01221	0.00662	0.00618	0.00959
	MSE	0.00597	0.00662	0.00766	0.00737	0.00676	0.00534
50	Bias	0.00477	0.00264	0.00368	0.00269	0.00402	0.00658
	MSE	0.00217	0.00245	0.00274	0.00271	0.00246	0.00207
80	Bias	0.00260	0.00169	0.00260	0.00185	0.00164	0.00479
	MSE	0.00133	0.00150	0.00164	0.00163	0.00151	0.00128
100	Bias	0.00187	0.00155	0.00210	0.00144	0.00172	0.00448
	MSE	0.00106	0.00117	0.00131	0.00129	0.00120	0.00103
200	Bias	0.00122	0.00095	0.00091	0.00097	0.00093	0.00248
	MSE	0.00051	0.00059	0.00064	0.00063	0.00061	0.00052

Table 4: The simulated biases and MSEs of the UXG model for (θ=1.0)

n		ML	AD	CVM	OLS	WLS	MPS
20	Bias	0.03171	0.01993	0.02883	0.01879	0.01888	0.01950
	MSE	0.02842	0.03072	0.03716	0.03601	0.03413	0.02487
50	Bias	0.01168	0.00620	0.01049	0.00872	0.00720	0.01592
	MSE	0.00994	0.01135	0.01291	0.01339	0.01188	0.00970
80	Bias	0.00728	0.00368	0.00688	0.00514	0.00465	0.01012
	MSE	0.00632	0.00711	0.00806	0.00815	0.00733	0.00609
100	Bias	0.00595	0.00471	0.00545	0.00405	0.00392	0.00901
	MSE	0.00499	0.00564	0.00629	0.00628	0.00578	0.00474
200	Bias	0.00315	0.00121	0.00260	0.00178	0.00121	0.00518
	MSE	0.00239	0.00281	0.00311	0.00310	0.00281	0.00240

Table 5: The simulated biases and MSEs of the UXG model for (θ=1.5)

n		ML	AD	CVM	OLS	WLS	MPS
20	Bias	0.04783	0.03207	0.04273	0.03108	0.02652	0.02727
	MSE	0.07092	0.07885	0.09671	0.09256	0.08777	0.06315
50	Bias	0.01895	0.01320	0.01862	0.01269	0.01408	0.02325
	MSE	0.02547	0.02924	0.03307	0.03326	0.03040	0.02420
80	Bias	0.01113	0.00968	0.01201	0.01085	0.00763	0.01505
	MSE	0.01526	0.01808	0.02066	0.02026	0.01837	0.01502
100	Bias	0.00993	0.00671	0.00696	0.00737	0.00393	0.01496
	MSE	0.01205	0.01414	0.01619	0.01611	0.01413	0.01224
200	Bias	0.00378	0.00233	0.00380	0.00130	0.00371	0.00864
	MSE	0.00597	0.00697	0.00770	0.00768	0.00721	0.00600

Table 6: The simulated biases and MSEs of the UXG model for (θ=2.0)

n		ML	AD	CVM	OLS	WLS	MPS
20	Bias	0.07189	0.04638	0.07121	0.05729	0.05001	0.04358
	MSE	0.15423	0.17641	0.21967	0.21614	0.19800	0.13118
50	Bias	0.02671	0.01201	0.01794	0.01226	0.01291	0.03152
	MSE	0.04729	0.05204	0.05935	0.05893	0.05326	0.04445
80	Bias	0.02303	0.01623	0.02137	0.01776	0.01737	0.01769
	MSE	0.03029	0.03439	0.03949	0.03924	0.03534	0.02860
100	Bias	0.00860	0.00345	0.00749	0.00461	0.00434	0.02521
	MSE	0.02393	0.02754	0.03091	0.03080	0.02803	0.02352
200	Bias	0.00634	0.00722	0.01055	0.00910	0.00772	0.01312
	6MSE	0.01200	0.01412	0.01608	0.01603	0.01424	0.01186

Table 7: The simulated biases and MSEs of the UXG model for (θ=3.0)

n		ML	AD	CVM	OLS	WLS	MPS
20	Bias	0.12381	0.07841	0.04273	0.08121	0.08188	0.07461
	MSE	0.36624	0.39167	0.09671	0.47460	0.45088	0.30881
50	Bias	0.04934	0.03282	0.01862	0.03397	0.03251	0.04010
	MSE	0.12587	0.14534	0.03307	0.16815	0.15049	0.11975
80	Bias	0.02901	0.01785	0.01201	0.01465	0.01972	0.03396
	MSE	0.07490	0.08930	0.02066	0.09717	0.09358	0.07316
100	Bias	0.02240	0.01198	0.00696	0.01459	0.01432	0.03357
	MSE	0.05912	0.06956	0.01619	0.07882	0.07222	0.05711
200	Bias	0.02910	0.03448	0.00770	0.03867	0.03437	0.02904
	6MSE	0.01201	0.00852	0.00380	0.00968	0.00636	0.02065

Table 8: The simulated biases and MSEs of the UXG model for (θ=5.0)

n		ML	AD	CVM	OLS	WLS	MPS
20	Bias	0.21736	0.13968	0.20750	0.16371	0.13319	0.11997
	MSE	1.14258	1.28215	1.62899	1.57041	1.41972	0.99647
50	Bias	0.08943	0.06451	0.06921	0.06478	0.04772	0.08697
	MSE	0.39571	0.46983	0.52545	0.53176	0.47153	0.37371
80	Bias	0.05461	0.03895	0.04216	0.03479	0.03175	0.07200
	MSE	0.24553	0.28065	0.31496	0.31822	0.28564	0.23001
100	Bias	0.04117	0.02626	0.04053	0.03854	0.02625	0.05860
	MSE	0.19236	0.22304	0.26136	0.25799	0.22927	0.18659
200	Bias	0.09231	0.10894	0.12467	0.12419	0.10977	0.09221
	MSE	0.01840	0.01645	0.02161	0.01445	0.01007	0.02868

The following observations can be made from Table 2-8.

1. The estimators of θ show the characteristic of consistency i.e., the MSE decreases as the sample size (n) increases.
2. The bias of $\hat{\theta}$ drops with increasing n for all the methods of estimation.
3. The bias of $\hat{\theta}$ generally increases with increasing θ for any given θ and n.

6. MODELING REAL DATA

In this section, we present an analysis on a real data set to display the modeling behaviour of UXG distribution in comparison with the competitive distributions. The data set comprises water capacity month-wise from the Shasta reservoir in California in the month of February from 1991–2010. The observations are: 0.338936, 0.431915, 0.759932, 0.724626, 0.757583, 0.811556, 0.785339, 0.783660, 0.815627, 0.847413, 0.768007, 0.843485, 0.787408, 0.849868, 0.695970, 0.842316, 0.828689, 0.580194, 0.430681 and 0.742563.

To begin, we plot the total time test (TTT) plot and the box plot in Figure 3 to analyze the underlying distribution of the given data set. The TTT plot depicts the empirical hazard rate function as it increases. The data is negatively skewed, as seen by the box plot. To see if this data set follows the UXG and most popular lifespan distributions, we use the Anderson-Darling (AD),

Cramer von-Misses (CVM) and Kolmogorov-Smirnov (KS) test statistics.
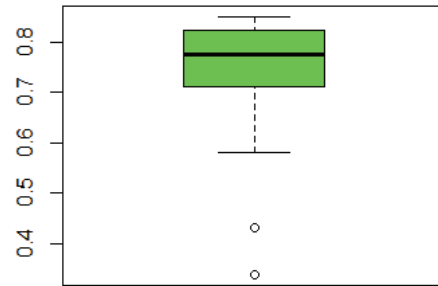
Fig. 3. Box plot for water capacity data
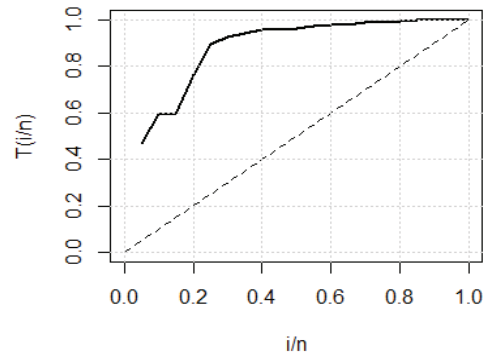
Fig. 4. TTT plot for water capacity data

Now, we apply UXG, Kumaraswamy, Beta Distribution, Unit Burr III, Unit Lindley, Topp Leon distributions as a model to the water capacity data set and Table 10 provides the ML estimates

Table 9: Some competitive models for the UXG distribution

Sr.	Distribution	Author(s)	References
1	Beta distribution (BD)	Gupta & NADarajah, (2004)	[1]
2	Kumaraswamy distribution (KwD)	Kumaraswamy, (1980)	[2]
3	Unit Burr III distribution (UBIII)	Modi & Gill, (2019)	[3]
4	Topp leon distribution (TLD)	Nadarajah & Kotz, (2003)	[24]
5	Unit Lindley distribution (ULin)	Mazucheli et al., (2019)	[5]

Table 10: ML estimates and Model selection measures

Model	MLEs	LogL	AIC	BIC	CVM	AD	KS
KwD(α,β)	6.3475 (1.5574) 4.4890 (2.0406)	13.475	-22.949	-20.958	0.2505	1.5325	0.2209
BD(α,β)	7.3157 (2.3181) 2.9099 (0.8755)	12.562	-21.124	-19.132	0.2861	1.6137	0.2359
UBIIID(α,β)	3.4965 (0.8154) 1.5291 (0.2243)	11.077	-18.154	-16.163	0.2999	1.6658	0.2379
TLD(λ)	8.6653 (1.9376)	11.588	-21.175	-20.179	0.3319	1.7858	0.2549
ULinD(θ)	0.4958 (0.0806)	13.827	-25.654	-24.659	6.0498	1.8333	0.7484
UXGD(θ)	**0.6810 (0.0985)**	**14.024**	**-26.048**	**-25.052**	**0.2452**	**1.4224**	**0.2066**

According to Table 10, the UXG distribution fits the water capacity data set better than the other competitive distributions since the accuracy measures for determining the ideal distribution for a given data set are smaller. The histogram of the water capacity data set and the fitted densities, estimated HR and PP plots are displayed in Figure 4. From Figure 4, it is observed that the fitted density of UXG distribution fits the data well and fitted (estimated) HR shows an increasing trend which is also confirmed by the TTT plot.
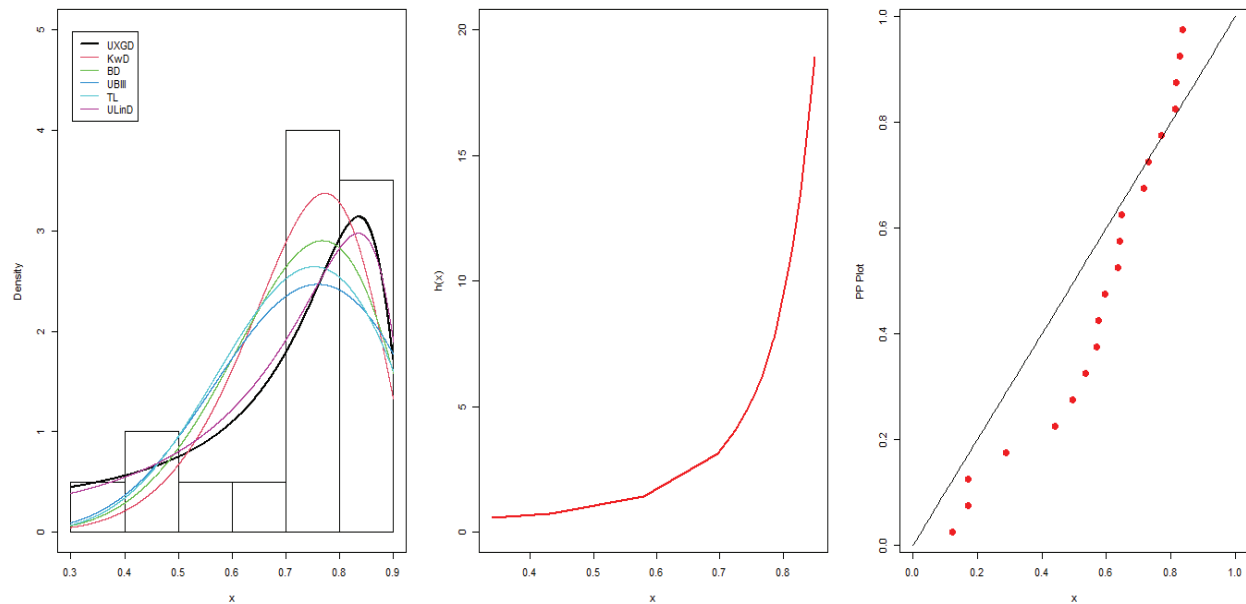

Fig. 4: (Left) Fitted densities, (middle) estimated HRF and (right) PP plot for the data set.

Figure 5 gives the value of the MLE of parameter θ. The maximum value of the LogL function is at θ = 0.6810 for UXG distribution. Conclusively, Table 10 and Figure 4 show that the UXG model has a very adequate fitting to the empirical data of the water capacity.
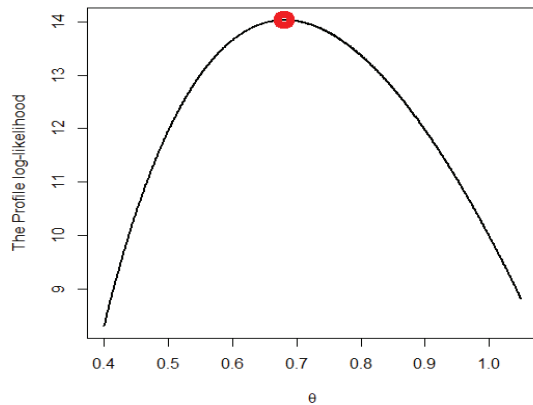

Fig. 5: Profile Log-Likelihood plot

7. CONCLUDING REMARKS

The UXG distribution is a new model introduced in this study. Some mathematical properties of the new distribution, such as its moments and associated measures, are derived. Two actuarial measures; VaR and TVaR are derived. For this model, we obtained a density of ordered statistics and two different characterizations. Comprehensive simulation studies on multiple sample sizes; small, moderate, and large sizes are used to compare the efficiency of the five methods of estimate stated above. The simulation results showed that the ML estimator is the best performing estimator for bias and MSE criteria for all sample sizes. UXG distribution presents a better fit to the water capacity data than other competent models. Thus we can say that the UXG distribution being a parsimonious model provides adequate and preferable modeling performance for water capacity data and is more flexible than some well-known probability distributions that are extensively famous for the application of lifetime data sets.

8. REFERENCES

1. A. K. Gupta and S. Nadarajah, *Handbook of beta distribution and its applications.* CRC press, 2004.
2. P. Kumaraswamy, "A generalized probability density function for double-bounded random processes," *J. Hydrol.*, vol. 46, no. 1–2, pp. 79–88, 1980.
3. M. E. Ghitany, J. Mazucheli, A. F. B. Menezes, and F. Alqallaf, "The unit-inverse Gaussian distribution: A new alternative to two-parameter distributions on the unit interval," *Commun. Stat. - Theory Methods,* vol. 48, no. 14, pp. 3423–3438, 2019.
4. K. Modi and V. Gill, "Unit Burr-III distribution with application," *J. Stat. Manag. Syst.*, vol. 0510, pp. 1–14, 2019.
5. J. Mazucheli, A. F. Menezes, and S. Dey, "Unit-Gompertz distribution with applications," Statistica, vol. 79, no. 1, pp. 25–43, 2019.
6. J. Mazucheli, A. F. B. Menezes, and S. Chakraborty, "On the one parameter unit-Lindley distribution and its associated regression model for proportion data," *J. Appl. Stat.,* vol. 46, no. 4, pp. 700–714, 2019.
7. J. Mazucheli, A. F. B. Menezes, and S. Dey, "Improved maximum-likelihood estimators for the parameters of the unit-gamma distribution," *Commun. Stat. - Theory Methods,* vol. 47, no. 15, pp. 3767–3778, 2018.
8. J. Mazucheli, A. F. B. Menezes, A. F. B. Menezes, S. Dey, A. F. B. Menezes, and S. Dey, "The unit-Birnbaum-Saunders distribution with applications," *Chil. J. Stat.*, vol. 9, no. 1, pp. 47–57, 2018.
9. J. Mazucheli, A. F. B. Menezes, and M. E. Ghitany, "The unit-Weibull distribution and associated inference," *J. Appl. Probab. Stat,* vol. 13, pp. 1–22, 2018.
10. A. F. B. Menezes, J. Mazucheli, and S. Dey, "The unit-logistic distribution: Different methods of estimation," *Pesqui. Operacional,* vol. 38, no. 3, pp. 555–578, 2018.
11. M. Ahsan-ul-Haq, S. Hashmi, K. Aidi, P. L. Ramos, and F. Louzada, "Unit Modified Burr-III Distribution: Estimation, Characterizations and Validation Test," *Ann. Data Sci.*, 2020.
12. R. A. R. Bantan *et al.*, "Some new facts about the unit-rayleigh distribution with applications," *Mathematics,* vol. 8, no. 11, pp. 1–23, 2020.
13. C. Chesneau, "Study of a unit power-logarithmic distribution," *Open J. Math. Sci.,* vol. 5, no. 1, pp. 218–235, 2021.

14. M. Ahsan-ul-Haq, M. Albassam, M. Aslam, and S. Hashmi, "Statistical Inferences on Odd Fréchet Power Function Distribution," *J. Reliab. Stat. Stud.,* vol. 14, no. 1, pp. 141–172, 2021.

15. M. Korkmaz and C. Chesneau, "On the unit Burr-XII distribution with the quantile regression modeling and applications," *Comput. Appl. Math.,* vol. 40, no. 1, pp. 1–26, 2021.

16. R. A. R. Bantan, C. Chesneau, F. Jamal, M. Elgarhy, W. Almutiry, and A. A. Alahmadi, "Study of a Modified Kumaraswamy Distribution," *Mathematics,* vol. 9, no. 21, p. 2836, 2021.

17. A. Krishna, R. Maya, C. Chesneau, and M. R. Irshad, "The Unit Teissier Distribution and Its Applications," *Math. Comput. Appl.,* vol. 27, no. 1, p. 12, 2022.

18. G. Martínez-Flórez, R. Tovar-Falón, and C. Barrera-Causil, "Inflated Unit-Birnbaum-Saunders Distribution," *Mathematics*, vol. 10, no. 4, p. 667, 2022.

19. M. S. Eliwa, M. Ahsan-ul-haq, A. Al-bossly, and M. El-morshedy, "A Unit Probabilistic Model for Proportion and Asymmetric Data : Properties and Estimation Techniques with Application to Model Data from SC16 and P3 Algorithms," Mathematical Problems in engineering 2022.

20. S. Sen, S. S. Maiti, and N. Chandra, "The xgamma distribution: Statistical properties and application," *J. Mod. Appl. Stat. Methods,* vol. 15, no. 1, pp. 774–788, 2016.

21. A. Z. Afify, A. M. Gemeay, and N. A. Ibrahim, "The heavy-tailed exponential distribution: risk measures, estimation, and application to actuarial data," *Mathematics,* vol. 8, no. 8, p. 1276, 2020.

22. N. M. Alfaer, A. M. Gemeay, H. M. Aljohani, and A. Z. Afify, "The extended log-logistic distribution: inference and actuarial applications," *Mathematics,* vol. 9, no. 12, p. 1386, 2021.

23. Z. Ahmad, E. Mahmoudi, M. Alizadeh, R. Roozegar, and A. Z. Afify, "The exponential TX family of distributions: properties and an application to insurance data," *J. Math.,* vol. 2021, 2021.

24. W. Glänzel, "A characterization theorem based on truncated moments and its application to some distribution families," in *Mathematical statistics and probability theory*, Springer, 1987, pp. 75–84.

25. A. Z. Afify and O. A. Mohamed, "A new three-parameter exponential distribution with variable shapes for the hazard rate: Estimation and applications," *Mathematics*, vol. 8, no. 1, p. 135, 2020.

26. A. Al Mutairi, M. Z. Iqbal, M. Z. Arshad, B. Alnssyan, H. Al-Mofleh, and A. Z. Afify, "A New Extended Model with Bathtub-Shaped Failure Rate: Properties, Inference, Simulation, and Applications," *Mathematics*, vol. 9, no. 17, p. 2024, 2021.

27. A. Z. Afify, H. M. Aljohani, A. S. Alghamdi, A. M. Gemeay, and A. M. Sarg, "A New Two-Parameter Burr-Hatke Distribution: Properties and Bayesian and Non-Bayesian Inference with Applications," *J. Math.*, vol. 2021, 2021.

28. S. Nadarajah and S. Kotz, "Moments of some J-shaped distributions," *J. Appl. Stat.*, vol. 30, no. 3, pp. 311–317, 2003.

Pakistan Academy of Sciences

Research Article

Class of Meromorphic Univalent Functions with Fixed Second Positive Coefficients Defined by q-Difference Operator

Zienab M. Saleh[1], and Adela O. Mostafa[2*]

Department of Mathematics, Faculty of Science, Mansoura University, Egypt

Abstract: In this paper using a q-difference operator, a class of meromorphic univalent functions with fixed second positive coefficients is defined. Coefficient estimates, some distortion theorems and other properties for this class are obtained. Various results obtained are sharp.

Keywords: Meromorphic, starlike, convex, fixed coefficient, radius of convexity.

1. INTRODUCTION

For $0 \leq \delta < 1$, let Σ_δ denote the class of univalent meromorphic functions of the form:

$$F(\varsigma) = \frac{1}{\varsigma - \delta} + \sum_{k=1}^{\infty} a_k \varsigma^k, F(\delta) = \infty,$$

defined in the desk $\mathcal{D}_\delta = \{\varsigma : \delta < |\varsigma| < 1\}$.
Also let $\Sigma_{\delta,\alpha}$, $0 < \alpha \leq 1$ be the subclass of functions F in Σ_δ which has the expansion:

$$F(\varsigma) = \frac{\alpha}{\varsigma - \delta} + \sum_{k=1}^{\infty} a_k \varsigma^k,$$

where $\alpha = Res(F, \delta)$, with $0 < \alpha \leq 1$, $\varsigma \in \mathcal{D}_\delta$.
The function F given in (1.1) was studied by Jinxi Ma [12]. The functions $F \in \Sigma_\delta$ is said to be meromorphically starlike (convex) functions of order β if and only if

$$-Re\left\{\frac{\varsigma F'(\varsigma)}{F(\varsigma)}\right\} > \beta, 0 \leq \beta < 1, \varsigma \in \mathcal{D}_\delta, \qquad (1.2)$$

$$-Re\left\{1 + \frac{\varsigma F''(\varsigma)}{F'(\varsigma)}\right\} > \beta, 0 \leq \beta < 1, \varsigma \in \mathcal{D}_\delta. \quad (1.3)$$

The class of such functions is denoted by $\Sigma_\delta^*(\beta)$ ($\Sigma_\delta^c(\beta)$). Note that the class $\Sigma_0^*(\beta)$ and various other subclasses of $\Sigma_\delta^*(0)$ had been studied by [5](see also [1, 2], [10], [13], [15], [17, 18, 19]).

Let $\Sigma_{\delta,\alpha}^+ \subset \Sigma_{\delta,\alpha}$ consisting of functions of the form:

$$F(\varsigma) = \frac{\alpha}{\varsigma - \delta} + \sum_{k=1}^{\infty} a_k \varsigma^k, (a_k \geq 0). \qquad (1.4)$$

It is known that the calculus without the notion of limits is called $q-$calculus which has influenced many scientific fields due to its important applications. Tang et al. [16] defined the $q-$derivative for meroromorphic functions $F \in \Sigma_0$ by:

$$(1.1)$$

$$\partial_q F(\varsigma) = \frac{F(\varsigma) - F(q\varsigma)}{(1-q)\varsigma} = -\frac{1}{q\varsigma^2} + \sum_{k=1}^{\infty} [k]_q a_k \varsigma^{k-1}, \qquad (1.5)$$

where

$$[j]_q = \frac{1-q^j}{1-q}. \qquad (1.6)$$

As $q \to 1^-$, $[j]_q = j$ and $\partial_q F(\varsigma) = F'(\varsigma)$.

For $F \in \Sigma_{\delta,\alpha}$, let:

$$\mathcal{M}_q^0 F(\varsigma) = F(\varsigma),$$

$$\mathcal{M}_q^1 F(\varsigma) = \varsigma \partial_q F(\varsigma) + \frac{\alpha((q+1)\varsigma - \delta)}{(\varsigma - \delta)(q\varsigma - \delta)},$$

$$\mathcal{M}_q^2 F(\varsigma) = \varsigma \partial_q (\mathcal{M}_q^1 F(\varsigma)) + \frac{\alpha((q+1)\varsigma - \delta)}{(\varsigma - \delta)(q\varsigma - \delta)},$$

---

and for $n \in \mathbb{N} = \{1,2,3,\dots\}$ we can write

$$\mathcal{M}_q^n F(\varsigma) = \varsigma \partial_q(\mathcal{M}_q^{n-1}F(\varsigma)) + \frac{\alpha((q+1)\varsigma - \delta)}{(\varsigma - \delta)(q\varsigma - \delta)}$$

$$= \frac{\alpha}{\varsigma - \delta} + \sum_{k=1}^{\infty} [k]_q^n a_k \varsigma^k. \qquad (1.7)$$

Note that:

(i) $\lim_{q \to 1^-} \mathcal{M}_q^n(\delta, \alpha) = \mathcal{M}^n(\delta, \alpha)$ (see [7, 8, 9]);

(ii) $\lim_{q \to 1^-} \mathcal{M}_q^n(0,1) = \mathcal{M}^n$ (see [6]).

Using the operator $\mathcal{M}_q^n$, and for $F \in \Sigma_{\delta,\alpha}$ we have:

Definition 1 *The function* $F \in \Sigma_q^n(\delta, \alpha, \beta)$ *if it satisfies*

$$\left| \frac{\varsigma q \partial_q(\mathcal{M}_q^n F(\varsigma))}{\mathcal{M}_q^n F(\varsigma)} + 1 \right| < \left| \frac{\varsigma q \partial_q(\mathcal{M}_q^n F(\varsigma))}{\mathcal{M}_q^n F(\varsigma)} + 2\beta - 1 \right| (n \in \mathbb{N}_0 =$$

$$\mathbb{N} \cup \{0\}), \qquad (1.8)$$

for some $\beta (0 \le \beta < 1)$.

For $q \to 1^-$, $\Sigma_q^0(\delta, 1, \beta)$ is the class of meromorphically starlike functions of order β and $\Sigma_q^0(\delta, 1, 0)$ gives the meromorphically starlike functions for all $\varsigma \in \mathcal{D}_\delta$.

Note that:

i. $\lim_{q \to 1^-} \Sigma_q^n(\delta, \alpha, \beta) = \Sigma^n(\delta, \alpha, \beta)$

$$= \left\{ F(\varsigma): \left| \frac{\varsigma(\mathcal{M}^n F(\varsigma))'}{\mathcal{M}^n F(\varsigma)} + 1 \right| < \left| \frac{\varsigma(\mathcal{M}^n F(\varsigma))'}{\mathcal{M}^n F(\varsigma)} + 2\beta - 1 \right| \right\}$$

(see [9]);

ii. $\Sigma_q^n(0, 1, \beta) = \Sigma_q^n(\beta)$

$$= \left\{ F(\varsigma): \left| \frac{\varsigma q \partial_q(\mathcal{D}^n F(\varsigma))}{\mathcal{D}^n F(\varsigma)} + 1 \right| < \left| \frac{\varsigma q \partial_q(\mathcal{D}^n F(\varsigma))}{\mathcal{D}^n F(\varsigma)} + 2\beta - 1 \right| \right\};$$

iii. $\lim_{q \to 1^-} \Sigma_q^n(0, 1, \beta) = \Sigma^n(\beta)$

$$= \left\{ F(\varsigma): \left| \frac{\varsigma(\mathcal{D}^n F(\varsigma))'}{\mathcal{D}^n F(\varsigma)} + 1 \right| < \left| \frac{\varsigma(\mathcal{D}^n F(\varsigma))'}{\mathcal{D}^n F(\varsigma)} + 2\beta - 1 \right| \right\}.$$

Let $\Sigma_q^n[\delta, \alpha, \beta] = \Sigma_q^0(\delta, \alpha, \beta) \cap \Sigma_{\delta,\alpha}^+$, where $\Sigma_{\delta,\alpha}^+$ is the class of functions of the form (1.4) that are analytic and univalent in $\mathcal{D}_\delta$.

Following Goodman [11] and Ruscheweyh [14], we begin by introducing here the N_δ −neighborhood for $F(\varsigma) \in \Sigma_\delta$ by

$$N_\delta(F, g) = \{g: g(\varsigma) \in \Sigma_\delta, g(\varsigma)$$

$$= \frac{1}{\varsigma} + \sum_{k=1}^{\infty} b_k \varsigma^k \text{ and } \sum_{k=1}^{\infty} k|a_k - b_k|$$

$$\le \delta\},$$

and for $e(\varsigma) = \frac{1}{\varsigma}$;

$$N_\delta(e, g) = \{g: g(\varsigma) \in \Sigma_\delta, g(\varsigma)$$

$$= \frac{1}{\varsigma} + \sum_{k=1}^{\infty} b_k \varsigma^k \text{ and } \sum_{k=1}^{\infty} k|b_k| \le \delta\}.$$

In [4] Aouf et al. (see also Madian and Aouf [3] (with $p = 1$)) defined the $N_{q,\delta}$ −neighborhood for $F(\varsigma) \in \Sigma_\delta$ by

$$N_{q,\delta}(F, g) = \{g: g(\varsigma) \in \Sigma_\delta, g(\varsigma) = \frac{1}{\varsigma} +$$

$$\sum_{k=1}^{\infty} b_k \varsigma^k \text{ and } \sum_{k=1}^{\infty} [k]_q |a_k - b_k| \le \delta_q\}, \quad (1.9)$$

and for $e(\varsigma) = \frac{1}{\varsigma}$;

$$N_{q,\delta}(e, g) = \{g: g(\varsigma) \in \Sigma_\delta, g(\varsigma) =$$

$$\frac{1}{\varsigma} + \sum_{k=1}^{\infty} b_k \varsigma^k \text{ and } \sum_{k=1}^{\infty} [k]_q |b_k| \le \delta_q\}. \quad (1.10)$$

2   MAIN RESULTS

Unless indicated, let $0 < q < 1$, $n \in \mathbb{N}_0$, $0 < \alpha \le 1$, $0 \le \beta < 1$, $\varsigma \in \mathcal{D}_\delta$.

Theorem 1 *Let $F(\varsigma)$ be defined by (1.4). Then $F \in \Sigma_q^n[\delta, \alpha, \beta]$ if and only if*

$$\sum_{k=1}^{\infty} [k]_q^n (q[k]_q + \beta)(1 - \delta)a_k \le \alpha(1 - \beta).$$
$$(2.1)$$

Proof. Assume that (2.1) holds true and let $|\varsigma| = 1$, by (1.8) we get

$$\left| \frac{\varsigma q \partial_q(\mathcal{M}_q^n F(\varsigma))}{\mathcal{M}_q^n F(\varsigma)} + 1 \right| - \left| \frac{\varsigma q \partial_q(\mathcal{M}_q^n F(\varsigma))}{\mathcal{M}_q^n F(\varsigma)} + 2\beta - 1 \right|$$

$$\le \frac{-2\alpha(1-\beta)}{|\varsigma||\varsigma - \delta|} - 2 \sum_{k=1}^{\infty} [k]_q^n (q[k]_q + \beta)a_k |\varsigma|^{k-1}$$

$$\le \frac{-2\alpha(1-\beta)}{1-\delta} - 2 \sum_{k=1}^{\infty} [k]_q^n (q[k]_q + \beta)a_k < 0.$$

We have

$$\sum_{k=1}^{\infty} 2[k]_q^n(q[k]_q + \beta)(1-\delta)a_k - 2\alpha(1-\beta)$$

$$< 0$$

Therefore, by the maximum modules theorem, we have $F \in \Sigma_q^n[\delta, \alpha, \beta]$.

Now, let $F \in \Sigma_q^n[\delta, \alpha, \beta]$, then

$$\left| \frac{\frac{\varsigma q \partial_q(\mathcal{M}_q^n F(\varsigma))}{\mathcal{M}_q^n F(\varsigma)} + 1}{\frac{\varsigma q \partial_q(\mathcal{M}_q^n F(\varsigma))}{\mathcal{M}_q^n F(\varsigma)} + 2\beta - 1} \right| < 1,$$

since $Re(\varsigma) \leq |\varsigma|$ for all ς, we get

$$Re\left\{ \frac{\frac{-\alpha\delta}{\varsigma(\varsigma-\delta)(q\varsigma-\delta)} + \sum_{k=1}^{\infty} [k]_q^n(q[k]_q+1)a_k\varsigma^{k-1}}{\frac{\alpha(2\beta-1)}{\varsigma(\varsigma-\delta)} - \frac{\alpha q}{(\varsigma-\delta)(q\varsigma-\delta)} + \sum_{k=1}^{\infty} [k]_q^n(q[k]_q+2\beta-1)a_k\varsigma^{k-1}} \right\} < 1.$$

Choose values of ς on real axis so that $\frac{\varsigma q \partial_q(\mathcal{M}_q^n F(\varsigma))}{\mathcal{M}_q^n F(\varsigma)}$ is real. Letting $\varsigma \to 1^-$ through real values, we have (2.1).

Corollary 1 *If $F \in \Sigma_q^n[\delta, \alpha, \beta]$, then we have*

$$a_k \leq \frac{\alpha(1-\beta)}{[k]_q^n(q[k]_q+\beta)(1-\delta)}. \tag{2.2}$$

Equality is attained for the function F:

$$F(\varsigma) = \frac{\alpha}{\varsigma-\delta} + \frac{\alpha(1-\beta)}{[k]_q^n(q[k]_q+\beta)(1-\delta)} \varsigma^k \tag{2.3}$$

Let $\Sigma_q^n[\delta, \alpha, \beta, c] \subset \Sigma_q^n[\delta, \alpha, \beta]$ consisting of functions:

$$F(\varsigma) = \frac{\alpha}{\varsigma-\delta} + \frac{\alpha(1-\beta)c}{(q+\beta)(1-\delta)}\varsigma + \sum_{k=2}^{\infty} a_k\varsigma^k, \tag{2.4}$$

with $0 \leq c < 1$.

Theorem 2 *Let $F(\varsigma)$ be defined by (2.4). Then $F(\varsigma) \in \Sigma_q^n[\delta, \alpha, \beta, c]$ if and only if*

$$\sum_{k=2}^{\infty} [k]_q^n(q[k]_q + \beta)(1-\delta)a_k \leq \alpha(1-\beta)(1-c). \tag{2.5}$$

Proof. Putting

$$a_1 = \frac{\alpha(1-\beta)c}{(q+\beta)(1-\delta)} \quad (0 < c < 1), \tag{2.6}$$

in (2.1), we have

$$c_1 + \sum_{k=2}^{\infty} \frac{[k]_q^n(q[k]_q+\beta)(1-\delta)}{\alpha(1-\beta)} a_k \leq 1, \tag{2.7}$$

which implies (2.5). The equality accurs for

$$F(\varsigma) = \frac{\alpha}{\varsigma-\delta} + \frac{\alpha(1-\beta)c}{(q+\beta)(1-\delta)}\varsigma + \frac{\alpha(1-\beta)(1-c)}{[k]_q^n(q[k]_q+\beta)(1-\delta)}\varsigma^k, \tag{2.8}$$

for $k \geq 2$.

Corollary 2 *If $F(\varsigma) \in \Sigma_q^n[\delta, \alpha, \beta, c]$, then*

$$a_k \leq \frac{\alpha(1-\beta)(1-c)}{[k]_q^n(q[k]_q+\beta)(1-\delta)}, \quad (k \geq 2). \tag{2.9}$$

The equality accurs for $F(\varsigma)$ given by (2.8).

Theorem 3 *If $F \in \Sigma_q^n[\delta, \alpha, \beta, c]$, then*

$$\sum_{k=2}^{\infty} a_k \leq \frac{\alpha(1-\beta)(1-c)}{[2]_q^n(q[2]_q+\beta)(1-\delta)}, \tag{2.10}$$

and

$$\sum_{k=2}^{\infty} [k]_q a_k \leq \frac{[2]_q\alpha(1-\beta)(1-c)}{[2]_q^n(q[2]_q+\beta)(1-\delta)}. \tag{2.11}$$

Proof. Let $F \in \Sigma_q^n[\delta, \alpha, \beta, c]$. Then, in view of (2.5), we have

$$[2]_q^n(q[2]_q + \beta)(1 - \delta) \sum_{k=2}^{\infty} a_k \leq \alpha(1 - \beta)(1 - c), \tag{2.12}$$

which immediately yields the first assertion

By appealing to (2.5), we have

$$[2]_q^n(1 - \delta) \sum_{k=2}^{\infty} q[k]_q a_k \leq \alpha(1 - \beta)(1 - c) - \beta[2]_q^n(1 - \delta) \sum_{k=2}^{\infty} a_k, \tag{2.13}$$

which in view of (2.10), can be putten in the form:

$$[2]_q^n(1 - \delta) \sum_{k=2}^{\infty} q[k]_q a_k \leq \alpha(1 - \beta)(1 - c) - \beta \frac{\alpha(1-\beta)(1-c)}{(q[2]_q+\beta)}. \tag{2.14}$$

Simplifying the right hand side of (2.14), we have (2.11).

Theorem 4 *Let $F(\varsigma) \in \Sigma_q^n[\delta, \alpha, \beta, c]$ for $0 < |\varsigma| = r < 1$.*

Then

$$\frac{\alpha}{|\varsigma - \delta|} - \frac{\alpha(1 - \beta)c}{(q + \beta)(1 - \delta)}|\varsigma|$$
$$- \frac{\alpha(1 - \beta)(1 - c)}{[2]_q^n(q[2]_q + \beta)(1 - \delta)}|\varsigma|^2$$

$$\leq |F(\varsigma)| \leq \frac{\alpha}{|\varsigma - \delta|} + \frac{\alpha(1-\beta)c}{(q+\beta)(1-\delta)}|\varsigma| + \frac{\alpha(1-\beta)(1-c)}{[2]_q^n(q[2]_q + \beta)(1-\delta)}|\varsigma|^2,$$

$$(2.15)$$

with equality for

$$F(\varsigma) = \frac{\alpha}{|\varsigma - \delta|} + \frac{\alpha(1-\beta)c}{(q+\beta)(1-\delta)}|\varsigma| + \frac{\alpha(1-\beta)(1-c)}{[2]_q^n(q[2]_q + \beta)(1-\delta)}|\varsigma|^2,$$

where $\alpha = Res(\varsigma, \delta)$, with $0 < c < 1$.

Proof. For $F(\varsigma) \in \Sigma_q^n[\delta, \alpha, \beta, c]$. Then

$$|F(\varsigma)| = \left| \frac{\alpha}{\varsigma - \delta} + \frac{\alpha(1-\beta)c}{(q+\beta)(1-\delta)}\varsigma + \sum_{k=2}^{\infty} a_k \varsigma^k \right|$$

$$\leq \frac{\alpha}{|\varsigma - \delta|} + \frac{\alpha(1-\beta)c}{(q+\beta)(1-\delta)}|\varsigma| + |\varsigma|^2 \sum_{k=2}^{\infty} a_k,$$

and

$$|F(\varsigma)| = \left| \frac{\alpha}{\varsigma - \delta} + \frac{\alpha(1-\beta)c}{(q+\beta)(1-\delta)}\varsigma + \sum_{k=2}^{\infty} a_k \varsigma^k \right|$$

$$\geq \frac{\alpha}{|\varsigma - \delta|} - \frac{\alpha(1-\beta)c}{(q+\beta)(1-\delta)}|\varsigma| - |\varsigma|^2 \sum_{k=2}^{\infty} a_k,$$

which in view of (2.10), we have (2.15).

Theorem 5 Let $F(\varsigma) \in \Sigma_q^n[\delta, \alpha, \beta, c]$ for $0 < |\varsigma| = r < 1$, then

$$\frac{\alpha}{|\varsigma - \delta||q\varsigma - \delta|} - \frac{\alpha(1-\beta)c}{(q+\beta)(1-\delta)} - \frac{\alpha(1-\beta)(1-c)}{[2]_q^{n-1}(q[2]_q + \beta)(1-\delta)}|\varsigma|$$

$$\leq |\partial_q F(\varsigma)| \leq \frac{\alpha}{|\varsigma - \delta||q\varsigma - \delta|} + \frac{\alpha(1-\beta)c}{(q+\beta)(1-\delta)} + \frac{\alpha(1-\beta)(1-c)}{[2]_q^{n-1}(q[2]_q + \beta)(1-\delta)}|\varsigma|,$$

with equality for

$$\partial_q F(\varsigma) = \frac{\alpha}{|\varsigma - \delta||q\varsigma - \delta|} + \frac{\alpha(1-\beta)c}{(q+\beta)(1-\delta)} + \frac{\alpha(1-\beta)(1-c)}{[2]_q^{n-1}(q[2]_q + \beta)(1-\delta)}|\varsigma|.$$

Proof. For $F(\varsigma) \in \Sigma_q^n[\delta, \alpha, \beta, c]$. Then

$$|\partial_q F(\varsigma)| = \left| \frac{-\alpha}{(\varsigma-\delta)(q\varsigma-\delta)} + \frac{\alpha(1-\beta)c}{(q+\beta)(1-\delta)} + \sum_{k=2}^{\infty} [k]_q a_k \varsigma^{k-1} \right|$$

$$\leq \frac{\alpha}{|\varsigma-\delta||q\varsigma-\delta|} + \frac{\alpha(1-\beta)c}{(q+\beta)(1-\delta)} + |\varsigma| \sum_{k=2}^{\infty} [k]_q a_k,$$

and

$$|\partial_q F(\varsigma)| = \left| \frac{-\alpha}{(\varsigma-\delta)(q\varsigma-\delta)} + \frac{\alpha(1-\beta)c}{(q+\beta)(1-\delta)} + \sum_{k=2}^{\infty} [k]_q a_k \varsigma^{k-1} \right|$$

$$\geq \frac{\alpha}{|\varsigma-\delta||q\varsigma-\delta|} - \frac{\alpha(1-\beta)c}{(q+\beta)(1-\delta)} - |\varsigma| \sum_{k=2}^{\infty} [k]_q a_k,$$

which in view of (2.11), we have the result.

Theorem 6 Let $F(\varsigma) \in \Sigma_q^n[\delta, \alpha, \beta, c]$. Then $F(\varsigma)$ is starlike of order v $(0 \leq v < 1)$ in $|\varsigma - \delta| < |\varsigma| < r_1$, where r_1 is the largest value for which

$$\frac{\alpha(3-v)(1-\beta)c}{(q+\beta)(1-\delta)}r^2 + \frac{\alpha(k_0+2-v)(1-\beta)(1-c)}{[k_0]_q^n(q[k_0]_q+\beta)(1-\delta)}r^{k+1}$$

$$\leq \alpha(1-v),$$

$$(2.16)$$

for $k \geq 2$. The result is sharp for the function $F(\varsigma)$ given by (2.8).

Proof. It is suffcient to show that

$$\left| \frac{(\varsigma-\delta)F'(\varsigma)}{F(\varsigma)} + 1 \right| \leq 1 - v, \quad (|\varsigma| < r_1). \quad (2.17)$$

We have

$$\left| \frac{(\varsigma - \delta)F'(\varsigma)}{F(\varsigma)} + 1 \right|$$

$$\leq \frac{\frac{2\alpha(1-\beta)c}{(q+\beta)(1-\delta)}|\varsigma| + \sum_{k=2}^{\infty}(k+1)a_k|\varsigma|^k}{\frac{\alpha}{|\varsigma - \delta|} - \frac{\alpha(1-\beta)c}{(q+\beta)(1-\delta)}|\varsigma| - \sum_{k=2}^{\infty} a_k|\varsigma|^k}.$$

$$(2.18)$$

Hence for $|\varsigma - \delta| < |\varsigma| < r$, (2.18) hold true if

$$\frac{\alpha(3-v)(1-\beta)c}{(q+\beta)(1-\delta)}r^2 + \sum_{k=2}^{\infty}(k+2-v)a_k r^{k+1}$$

$$\leq \alpha(1-v),$$

and it follow that from (2.5), we may take

$$a_k \leq \frac{\alpha(1-\beta)(1-c)\lambda_k}{[k]_q^n(q[k]_q+\beta)(1-\delta)}, \quad (k \geq 2),$$

where $\lambda_k \geq 0$ and $\sum_{k=2}^{\infty} \lambda_k \leq 1$.

For each fixed r, we choose the positive integer $k_0 = k_0(r)$ for which $\frac{\alpha(k_0+2-v)(1-\beta)(1-c)}{[k_0]_q^n(q[k_0]_q+\beta)(1-\delta)} r^{k_0+1}$, is maximal.

Then it follows that

$$\sum_{k=2}^{\infty} (k+2-v)a_k r^{k+1}$$
$$\leq \frac{\alpha(k_0+2-v)(1-\beta)(1-c)}{[k_0]_q^n(q[k_0]_q+\beta)(1-\delta)} r^{k_0+1},$$

then F is starlike of order v in $|\varsigma - \delta| < |\varsigma| < r_1$ provided that

$$\frac{\alpha(3-v)(1-\beta)c}{(q+\beta)(1-\delta)} r_1^2$$
$$+ \frac{\alpha(k_0+2-v)(1-\beta)(1-c)}{[k_0]_q^n(q[k_0]_q+\beta)(1-\delta)} r_1^{k_0+1}$$
$$\leq \alpha(1-v).$$

We find the value $r_1 = r_0(n, \alpha, \beta, c, v, k)$ and the corresponding integer $k_0(r_0)$ so that

$$\frac{\alpha(3-v)(1-\beta)c}{(q+\beta)(1-\delta)} r_0^2$$
$$+ \frac{\alpha(k_0+2-v)(1-\beta)(1-c)}{[k_0]_q^n(q[k_0]_q+\beta)(1-\delta)} r_0^{k_0+1}$$
$$= \alpha(1-v).$$

Then this value is the radius of starlikeness of order v for function F belong to class $\Sigma_q^n[\delta, \alpha, \beta, c]$.

Theorem 7 *Let $F(\varsigma) \in \Sigma_q^n[\delta, \alpha, \beta, c]$. Then $F(\varsigma)$ is covex of order v $(0 \leq v < 1)$ in $|\varsigma - \delta| < |\varsigma| < r_2$, where r_2 is the largest value for which*

$$\frac{\alpha(3-v)(1-\beta)c}{(q+\beta)(1-\delta)} r^2$$
$$+ \frac{\alpha k_0(k_0+2-v)(1-\beta)(1-c)}{[k_0]_q^n(q[k_0]_q+\beta)(1-\delta)} r^{k+1}$$
$$\leq \alpha(1-v), \qquad (2.19)$$

for $k \geq 2$. The result is sharp for the function $F(\varsigma)$ given by (2.8).

Proof. By using the same technique in the proof of Theorem 6 we can show that

$$\left| \frac{(\varsigma-\delta)F''(\varsigma)}{F'(\varsigma)} + 2 \right| \leq 1 - v, \quad (|\varsigma| < r_2), \qquad (2.20)$$

for $|\varsigma - \delta| < |\varsigma| < r_2$ with the aid of Theorem 2. Thus, we have the assertion of Theorem 7.

Theorem 8 *The class $\Sigma_q^n[\delta, \alpha, \beta, c]$ is closed under convex linear compination.*

Proof. Let $F(\varsigma)$ be defined by (2.4). Define the function $h(\varsigma)$ by

$$h(\varsigma) = \frac{\alpha}{\varsigma-\delta} + \frac{\alpha(1-\beta)c}{(q+\beta)(1-\delta)}\varsigma + \sum_{k=2}^{\infty} b_k \varsigma^k, \; b_k \geq 2. \; (2.21)$$

Suppose that $F(\varsigma)$ and $h(\varsigma)$ are in the class $\Sigma_q^n[\delta, \alpha, \beta, c]$, we only need to prove that

$$G(\varsigma) = \zeta F(\varsigma) + (1-\zeta)h(\varsigma) \quad (0 \leq \zeta \leq 1), (2.22)$$

also be in the class. Since

$$G(\varsigma) = \frac{\alpha}{\varsigma-\delta} + \frac{\alpha(1-\beta)c}{(q+\beta)(1-\delta)}\varsigma$$
$$+ \sum_{k=n+1}^{\infty} \{\zeta a_k + (1-\zeta)b_k\}\varsigma^k, \quad (2.23)$$

then

$$\sum_{k=2}^{\infty} [k]_q^n(q[k]_q+\beta)(1-\delta)\{\zeta a_k + (1-\zeta)b_k\}$$
$$\leq \alpha(1-\beta)(1-c), \qquad (2.24)$$

with the aid of Theorem 2. Hence $G(\varsigma) \in \Sigma_q^n[\delta, \alpha, \beta, c]$.

Theorem 9 *Let*

$$F_1(\varsigma) = \frac{\alpha}{\varsigma-\delta} + \frac{\alpha(1-\beta)c}{(q+\beta)(1-\delta)}\varsigma, \qquad (2.25)$$

and

$$F_k(\varsigma) = \frac{\alpha}{\varsigma-\delta} + \frac{\alpha(1-\beta)c}{(q+\beta)(1-\delta)}\varsigma + \frac{\alpha(1-\beta)(1-c)}{[k]_q^n(q[k]_q+\beta)(1-\delta)}\varsigma^k, \qquad (2.26)$$

for $k \geq 2$. Then $F(\varsigma) \in \Sigma_q^n[\delta, \alpha, \beta, c]$ iff

$$F(\varsigma) = \sum_{k=2}^{\infty} \eta_k F_k(\varsigma), \qquad (2.27)$$

where $\eta_k \geq 0$ $(k \geq 2)$ and

$$\sum_{k=2}^{\infty} \eta_k \leq 1. \qquad (2.28)$$

Proof. Let $F(\varsigma)$ be in the form (2.27). Then from (2.25), (2.26) and (2.28) we have

$$F(\varsigma) = \frac{\alpha}{\varsigma - \delta} + \frac{\alpha(1-\beta)c}{(q+\beta)(1-\delta)}\varsigma$$

$$+ \sum_{k=2}^{\infty} \frac{\alpha(1-\beta)(1-c)\eta_k}{[k]_q^n(q[k]_q+\beta)(1-\delta)}\varsigma^k. \qquad (2.29)$$

Since

$$\sum_{k=2}^{\infty} \frac{\alpha(1-\beta)(1-c)\eta_k}{[k]_q^n(q[k]_q+\beta)(1-\delta)} \cdot \frac{[k]_q^n(q[k]_q+\beta)(1-\delta)}{\alpha(1-\beta)(1-c)}$$

$$= \sum_{k=2}^{\infty} \eta_k = 1 - \eta_1 \leq 1, \qquad (2.30)$$

then, from Theorem 2, $F(\varsigma) \in \Sigma_q^n[\delta, \alpha, \beta, c]$. Conversely, let $F(\varsigma) \in \Sigma_q^n[\delta, \alpha, \beta, c]$ and satisfies (2.9) for $k \geq 2$, then

$$\eta_k = \frac{[k]_q^n(q[k]_q+\beta)(1-\delta)}{\alpha(1-\beta)(1-c)}a_k \leq 1, \qquad (2.31)$$

and

$$\eta_1 = 1 - \sum_{k=2}^{\infty} \eta_k. \qquad (2.32)$$

This compelets the proof of the Theorem 9.

Corollary 3 *The extreme points of the class* $\Sigma_q^n[\delta, \alpha, \beta, c]$ *are the functions* $F_k(\varsigma)$ $(k \geq 2)$ *given by (2.25) and (2.26).*

Theorem 10 *If* $F(\varsigma) \in \Sigma_q^n[\delta, \alpha, \beta, c]$, *then*

$$\Sigma_q^n[\delta, \alpha, \beta, c] \subset N_{q,\xi}(F; q), \qquad (2.33)$$

where the parameter ξ_q *is given by*

$$\xi_q = \frac{[2]_q\alpha(1-\beta)(1-c)}{[2]_q^n(q[2]_q+\beta)(1-\delta)}. \qquad (2.34)$$

Proof. For $F(\varsigma) \in \Sigma_q^n[\delta, \alpha, \beta, c]$, from (2.11) of Theorem 3 and in view of (1.10), we get (2.34).

3. ACKNOWLEDGEMENT

4. REFERENCES

1. M. K. Aouf, On a certain class of meromorphic univalent functions with positive coefficients, Rend. Mat. Appl., 7 (11) (1991), no. 2, 209-219.

2. M. K. Aouf and H. E. Darwish, Certain meromorphically starlike functions with positive and fixed second coefficients, Tr. J. of Mathematics., 21 (1997), 311- 316.

3. M. K. Aouf and S. M. Madian, Inclusion and properties neighbourhood for certain p-valent functions associated with complex order and q–p-valent Cătaş operator, J. Sci. Taibah Univer. Sci., 14(1) (2020) , 1226-1232.

4. M. K. Aouf, A. O. Mostafa and F. Y. AL-Quhali, Properties for class of β- uniformly univalent functions defined by Sălăgean type q-difference operator, Int. J. Open Probl. Complex Anal., 11 (2019), no. 2, 1–16.

5. J. Clunie, On meromorpic schlicht functions, J. Lond. Math.Soc., 34 (1959), 215-216.

6. B. A. Frasin and M. Darus, On certain meromorphic functions with positive coefficients, Southeast Asian Bull. Math., 28 (2004), 615-623.

7. F. Ghanim and M. Darus, On certain subclass of meromorphic univalent functions with fixed residue, Far East J. Math. Sci. (FJMS)., 26 (2007), 195- 207.

8. F. Ghanim and M. Darus, A new subclass of uniformly starlike and convex functions with negative coefficients, Int. J. Pure Appl. Math., 45 (4) (2008), 559-572.

9. F. Ghanim and M. Darus, On a certain subclass of meromorphic univalent functions with fixed second positive coefficients, Surveys in Mathematics and its Applications., 5 (2010), 49-60.

10. R. M. Goel and N. S. Sohi, On a class of meromorphic functions, Glas. Mat., 3. Ser., 17 (37) (1982), 19-28.

11. A.W. Goodman, Univalent functions and nonanalytic curves, Proc. Amer. Math. Soc., 8 (1957), 598-601.

12. Jinxi Ma, Extreme points and minimal outer area problem for meromorphic univalent functions, J. Math. Anal. Appl., 220 (2) (1998), 769-773.

13. J. Miller, Convex meromorphic mappings and related functions, Proc. Am. Math. Soc., 25 (1970), 220-228.

14. St. Ruscheweyh, Neighborhoods of univalent functions, Proc. Amer. Math. Soc., 81 (1981) 521-527.

15. H. M. Srivastava and S. Owa, Current Topics In Analytic Functions Theory, World Scientific, Singapore, 1992.

16. H. Tang, H. M. Zayed, A. O. Mostafa and M. K. Aouf, Fekete-Szegö problems for certain classes of meromorphic functions using q-derivative operator, J. Math. Resear. Appl., 38 (2018), no. 3, 236-246.

17. B. A. Uralgaddi and M. D. Ganigi, A certain class of meromorphically starlike functions with positive coefficients, Pure Appl. Math. Sci., 26 (1987), 75-81.

18. B. A. Uralegaddi and C. Somanatha, Certain differential operators for meromorphic functions, Houston J. Math., 17 (1991), 279-284.

19. B. A. Uralegaddi and C. Somanatha, New criteria for meromorphic starlike univalent functions, Bull. Austral. Math. Soc., 43 (1991), 137-140.

Pakistan Academy of Sciences

Research Article

Root Finding Methods Through GUI in Spreadsheets

Atteeq Razzak[1], Muhammad Hani Zaheer[2], Muhammad Bilal Khan[2], and Zaheer Uddin[2]

[1]Department of Mathematics, University of Karachi, Karachi, Pakistan
[2]Department of Physics, University of Karachi, Karachi, Pakistan

Abstract: Root finding Methods like the Bisection Method, Newton Raphson Method, Secant Method, and False Position Method have been revisited through a new approach. EACH METHOD'S user-friendly GUI computer programs have been developed on an Excel spreadsheet. A root locator graph is introduced in the spreadsheets, which helps identify the initial guess(es) required to calculate root using these methods. All real roots are now easily calculable by any of the four methods. The detailed steps to calculate roots are also shown on the spreadsheet. The spreadsheet can be made ready for the next calculation with a single click. We have developed a technique for Excel that helps accept polynomial in variable 'x' without directly mentioning cell location.

1. INTRODUCTION

Mathematics students find numerical computing and root-finding methods very boring; as mathematics and physics teachers, we have tried to find them a convenient and new method to find roots through GUI. Several numerical methods approximate the real roots of transcendental and higher-order polynomial functions. These methods use several iterations to converge a set of values to a natural root. Such methods include Newton-Raphson Method, Bisection Method, False Position Method, and Secant Method.

Spreadsheets are used to organize and analyze statistical data in bulk amounts. Microsoft Excel is the most widely used spreadsheet application. Different programs can be made on Excel for different purposes. It is ubiquitous and available to most students at educational institutions. It has an easily accessible and very user-friendly GUI. Excel has been widely used in teaching data-based subjects, and various researches have been done on this use [1-4]. In her paper "Microsoft Excel in the Physics classroom," Khan described how Excel could teach students Physics in a classroom setting

using the example of an oscillating pendulum. She expressed success when her educational institute introduced Excel as part of the Mathematics curriculum [5]. Webb experimented with using Microsoft Excel to teach students Physics. In her paper, she gave an example of how Kepler's Third Law can be analyzed using Excel. Using Excel decreased the time and effort of students in repetitive tasks that took away from actually learning Physics [6]. Cooke, in his paper, explained the advantages of using spreadsheets over computer programs. He argued that teaching Physics Excel is a user-friendly environment and very accessible. He gave an example of how to generate random numbers in spreadsheets. He furthered mapped electric potentials and fields [7]. Healy and Sutherland researched using spreadsheets with the teaching of Mathematics. They gave examples of spreadsheet activities on mathematical problems for students. They mentioned that the Bisection Method and Newton Raphson Method could be done using spreadsheets such that the process of using this method is visible for students [8]. Wrong and Barford analyzed the potential and advantages of teaching programming to Engineering students using Excel Visual Basic for Applications (VBA).

They used problems and demonstrations to show the advantages of using Excel VBA for programming [9]. Lilley proposed introducing students to programming on VBA by using Numerical Methods. She used standard methods like Cramer's Rule for two by two (2 x 2) matrices and Newton Raphson Method to achieve this task. She mentions the availability and accessibility of Excel for such purposes [10]. Zaheer et al. showed that spreadsheets could be used as a simulation tool; they simulated wind data on spreadsheets and used spreadsheets to explain Lissajous figures and Damped Harmonic Oscillator [11, 12].

Previous research points towards the accessibility above and ease of access that Microsoft Excel offers as a tool for teaching Physics. Some have used numerical methods, including various root-finding methods for teaching Physics. There was even a mention of making a program such that the process was visible for students first encountering such numerical approaches to problems. Our aim is not to teach VBA programming but to create accessible Excel spreadsheets for various root-finding methods that students typically learn in Numerical Analysis or Numerical Methods courses. The iterative process is visible for students. A better understanding can be developed this way. The following sections have given a brief introduction and Algorithm of four root-finding methods (Bisection, Secant, False Position, and Newton Raphson). An example of each of these methods is also given using the

function $f(x) = 8x^3 - 6x^2 - 261x + 3$.

2. ROOT FINDING METHODS

We have made an excel program to automatically draw graphs without doing calculations separately. Instead of giving direct values, it is possible in the program to enter a mathematical expression of the function. The Draw graph button executes the program and plots the graphs. This is something new in drawing graphs in excel. Fig. 1. shows the screenshot of the program to draw the graph. The mathematical expression is written in A7; upper and lower limits of abscissa are given in A3 and A5, respectively.

In the following section, we discuss four numerical methods of root-finding; an Algorithm and an example of each method are also given.

2.1 Bisection Method

The Bisection Method is an approximation method used for finding the real roots of functions [1, 13-15]. It essentially works by guessing an interval from the domain within which a root of the function may be found. The interval is smaller in successive iterations until the resulting interval is sufficiently small to give a real root with the desired accuracy. The procedure is easy to perform but takes several iterations to answer with errors low enough to be acceptable.
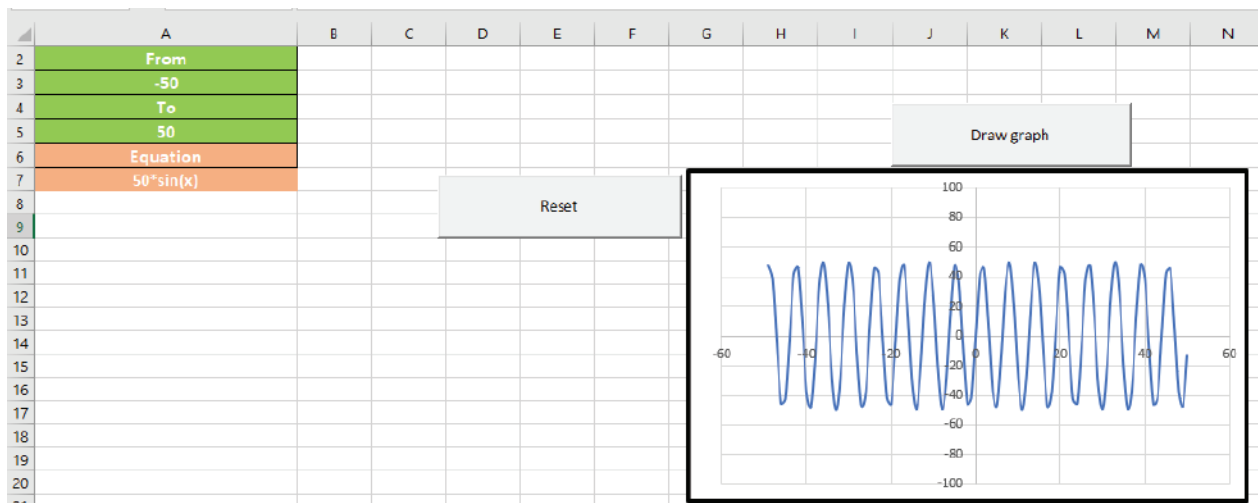

Fig. 1. Screenshot of the program to draw the graph.

**Algorithm and an example of Bisection Method
The Algorithm is given below:**

Step 1. For a function $f(x)$ consider an interval (x_o, x_1) in which $f(x)$ is continuous, find $f(x_o)$ and $f(x_1)$, if $f(x_o) = 0$ then x_0 is the root or if $f(x_1) = 0$ the $x_1 = 0$ is the root. or check if $f(x_o) * f(x_1) < 0$, if yes, continue to step; otherwise, next select a suitable interval.

Step 2. Take the midpoint.
$x_2 = (x_o + x_1) / 2$

Step 3. Find $f(x_2)$, if $f(x_2) = 0$, or $f(x_2) < \epsilon$, (ϵ is the predefined acceptable error) then x_2 is the root,

Step 4. If ((i) $f(x_o) * f(x_2) < 0$ then roots lies between (x_o, x_2) otherwise, the root lies between (x_1, x_2).

Step 5. Use new interval and repeat all steps from step 2 until $f(x_2) < \epsilon$.

In fig. 2. The bisection method procedure is shown. The root lies within the interval (-2,2). The first iteration gives midpoint 0; now root lies in the interval (0,2). The second iteration gives midpoint 1; the root lies between (1,2). The third iteration gives midpoint 1.5, which coincides with the root, so $x = 1.5$ is one of the roots of a function.

2.2 Secant Method

In Secant Method [1, 13-15], a secant line is drawn on the curve, and the value of x is found where the secant line cuts the x-axis (the root of the secant line). A new secant line is drawn with the help of the root of the previous secant line. The process continues until the secant line converges to a tangent

line at the root of the function. The Secant Method can be regarded as a discrete approximation of the Newton Raphson Method. The Secant Method uses the same formula as the False Position Method. However, it does not have the condition that the value of the function at the points chosen to be of opposite polarity. Hence in the Secant Method, the zeros do not always converge to a root.

Algorithm and an example of Secant Method

The Algorithm of Secant Method is as follows:

Step 1. For a function $f(x)$ consider two points $x = x_o$ and $x = x_{x1}$.

Step 2. Calculate $f(x_o)$ and $f(x_1)$, if either is zero or $f(x_2) < \epsilon$ the root is at the corresponding x value.

Step 3. Otherwise, find the point x_2 where secant line joining $x = x_o$ and $x = x_1$ meets x-axis. To find x_2 following formula is used.

$x_2 = x_1 - f(x_1) (x_1 - x_o) / (f(x_1) - f(x_o))$

Step 4. If $f(x_2)$ is zero $f(x_2) < \epsilon$, x_2 is the root. Otherwise,

Step 5. Replace x_o by x_1 and x_1 and x_2. Repeat steps 2 to 4 until $f(x_2) < \epsilon$.

Let $x_0 = -4$ and $x_1 = 4$ be the initial guess interval. The first iteration gives $x_2 = 2.1203$, the second iteration gives 0.2068. Even though the second iteration seems to take the value away from the root, the third iteration gives a decent close approximation $x_2 = 1.5840$. In this case, the iterations make the approximation converge to the root, whose actual value is 1.5.
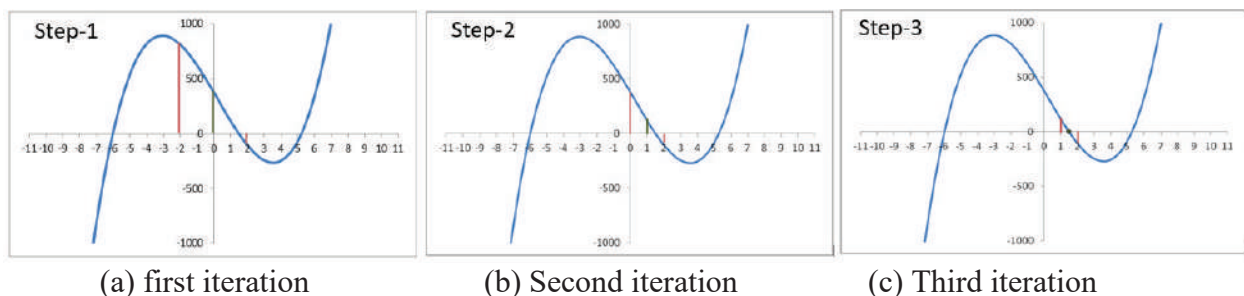

|(a) first iteration | (b) Second iteration | (c) Third iteration |

Fig. 2. Root finding by bisection method

2.3 False Position Method

False Position Method is essentially a combination of the Bisection Method and the Secant Method [1, 13-15]. Two initial guesses are chosen such that the function changes the sign between them. A secant line is drawn, which passes through the initial guesses. A new interval is taken whose one point is the root of the secant line such that sign changes between them. The secant line with each iteration approaches a tangent line whose root coincides with the function under consideration. Because of this extra condition, this method is more generally applicable than the Secant Method. Further, the convergence in the False Position Method is faster than in the Bisection Method.

Algorithm and an example of False position method The Algorithm of the False Position Method is as follows:

Step 1. For a function $f(x)$, choose x_0 and x_1 such that $f(x_o) * f(x_1) < 0$.

Step 2. If either of $f(x_o)$ or $f(x_1)$ are zero or $f(x_o)$ or $f(x_1) < \epsilon$, then x_0 or x_1 is root respectively.

Step 3. A secant line is drawn, and its root x_2 is located.

The root of the secant line x_2 is found by the following formula

$x_2 = x_1 - f(x_1)(x_1 - x_0) / (f(x_1) - f(x_0))$

Step 4. Find $f(x_2)$, if $f(x_2) = 0$, or $f(x_2) < \epsilon$, (ϵ is the predefined acceptable error) then x_2 is the root,

Step 5. If ((i) $f(x_0) * f(x_2) < 0$ then roots lies between (x_o, x_2) otherwise, the root lies between (x_o, x_1).
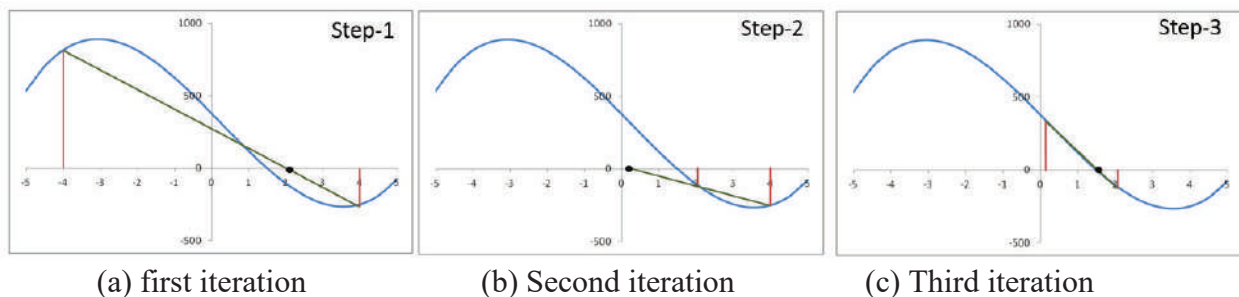
Step 6. Use new interval and repeat all steps from step 2 until $f(x_2) < \epsilon$.

Fig. 4. illustrates the False Position Method of the root finding procedure. Let $x_0 = -4$ and $x_1 = 4$ be the initial guesses. Each iteration gets the value closer to the root of the function. The third iteration gives 1.5198, which is very close to the actual value of the root.

2.4 Newton Raphson Method

Root finding by Newton Raphson Method takes a single initial guess compared to the other three methods that take two points as initial guesses [1, 13-16]. A tangent line is drawn to the curve at that point. A new tangent line is drawn on the curve at the root of the tangent line. This process continues. If the initial guess is good enough, the points converge to the root of the function considered. This convergence is quadratic. The convergence is linear if the desired root has a multiplicity higher than one. If the initial guess is a stationary point, then the method fails. Another failure appears where two points yield each other in an infinite cycle.

Algorithm and an example of Newton Raphson Method

The Algorithm of Newton Raphson method is as follows:

Step 1. Guess an initial root x_o and find $f(x_o)$.

Step 2. If $f(x_o) = 0$ or $f(x_2) < \epsilon$ then x_o is the root, otherwise,

Step 3. Calculate $f'(x_o)$.

Step 4. If $f'(x_o) = 0$ then take a new x_o.

Step 5. Draw a tangent line at x_o and find out x_1

(a) first iteration   (b) Second iteration   (c) Third iteration

Fig. 3. Root finding by Secant Method

where it cuts the x-axis, the point is found by

$$x_1 = x_o - f(x_o) / (f'(x_o))$$

Step 6. Replace x_o by x_1 and repeat from step 2 until $f(x_2) < \epsilon$.

Fig. 5. gives an example of the Newton Raphson Method. Let $x_o = -1$ be the initial guess for the root. The tangent line at $x_o = -1$ cuts x-axis at $x = 1.7777$. The new tangent line at $x_o = 1.7777$ is drawn, and the new value of x_o is extremely close to the actual root which is 1.5.

3. RESULTS AND DISCUSSION

We have used a spreadsheet to develop a program for calculating roots by four methods: Bisection Method, Newton Raphson Method, Secant Method, and False Position Method. All these methods, as GUI, are developed on spreadsheets. In each program, there are three buttons. The first button is labelled "Draw graph," which draws a graph that locates all the real roots. The graph of the equation is given in cell A7. For the first time, we have introduced a method that allows one to write

a function's equation in variables' x's or 'X' rather than cell location. This gives the user freedom to use any function whose roots are determined. The equation is plotted with the help of intervals given in the A3 and A5. The values in cells A3 and A5 can be changed if the roots lie outside the given interval; the same button can draw a new graph. Once the graph is drawn, the approximate position of the roots can be seen; these approximated positions help choose the initial values of the guess for the calculation. The initial guess is in cell locations A10 and A12. The termination criterion can also be set by inserting its value in cell position A14. Once all these cells occupy appropriate values, a second button, "Calculate root," is used to calculate the root. The button also displays each calculation step in columns C to H. The root value is displayed in a message box on reaching the termination criterion. The third button, "Reset," is used to get the spreadsheet to find the next root. Four spreadsheets are also available with this paper.

(i) Several programs on Bisection and other methods were developed on a spreadsheet by various people [17-21]; our program is different from an entire root-finding, a single button
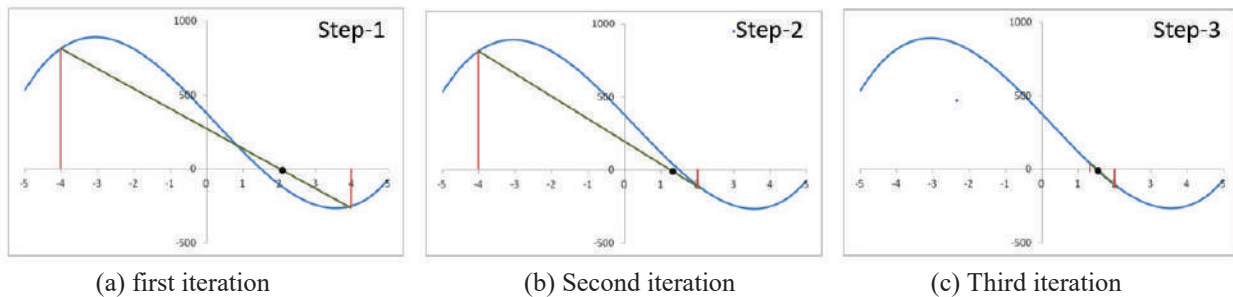

| (a) first iteration | (b) Second iteration | (c) Third iteration |

Fig. 4. Root finding by False Position Method

| (a) first iteration | (b) Second iteration |

Fig. 5. Root finding by Newton Raphson Method

Bisection Method

Graph Range
From: -50
To: 50
Equation: 8*x^3-6*x^2-261*x+378
x1: 0
x2: 3.5
Termination limit: 0.0001
Start Time: 9:23:47 PM
End Time: 9:23:50 PM

x1	x2	f(x1)	f(x2)	x3	f(x3)
0.00000	3.50000	378.00000	-266.00000	1.75000	-54.25000
0.00000	1.75000	378.00000	-54.25000	0.87500	150.39063
0.87500	1.75000	150.39063	-54.25000	1.31250	43.18945
1.31250	1.75000	43.18945	-54.25000	1.53125	-7.00171
1.31250	1.53125	43.18945	-7.00171	1.42188	17.75742
1.42188	1.53125	17.75742	-7.00171	1.47656	5.28981
1.47656	1.53125	5.28981	-7.00171	1.50391	-0.87845
1.47656	1.50391	5.28981	-0.87845	1.49023	2.20012
1.49023	1.50391	2.20012	-0.87845	1.49707	0.65944
1.49707	1.50391	0.65944	-0.87845	1.50049	-0.10986
1.49707	1.50049	0.65944	-0.10986	1.49878	0.27470
1.49878	1.50049	0.27470	-0.10986	1.49963	0.08240
1.49963	1.50049	0.08240	-0.10986	1.50006	-0.01373
1.49963	1.50006	0.08240	-0.01373	1.49985	0.03433
1.49985	1.50006	0.03433	-0.01373	1.49995	0.01030
1.49995	1.50006	0.01030	-0.01373	1.50001	-0.00172
1.49995	1.50001	0.01030	-0.00172	1.49998	0.00429
1.49998	1.50001	0.00429	-0.00172	1.49999	0.00129
1.49999	1.50001	0.00129	-0.00172	1.50000	-0.00021
1.49999	1.50000	0.00129	-0.00021	1.50000	0.00054
1.50000	1.50000	0.00054	-0.00021	1.50000	0.00016
1.50000	1.50000	0.00016	-0.00021	1.50000	-0.00003

Draw graph
Calculate root
Reset

Fig. 6. Screenshot of GUI program of Bisection Method

controls process.

(ii) Usually, available software on these methods calculates one root; new guesses are required for others, which may take longer. In our method, we have added a 'visual root locator.' This locator shows the approximate position of the root by a single line that crosses the x-axis on a graph. With the use of this locator, one can easily choose the initial guess(s).

(iii) These methods can find all real roots in a relatively more straightforward manner.

(iv) Besides the value of roots, a chart is also developed that shows all the process steps.

(v) It also shows the start time and finishes time.

(vi) Some of the available online root calculators by Newton's Raphson Method need an expression of the function's derivative [22], which is not straightforward in most cases. Also, most available calculators fail to calculate roots at stationary points [22, 23]. In our program, we have added a step in which the program first finds out whether the point is stationary or not. If stationary, it changes the initial guess to a neighboring point and finds the root.

(vii) Source file can be made available online for users of all standards and level.

4. CONCLUSION

In this paper, we have developed computer programs for numerical root-finding methods. We developed programs for four root-finding methods (Bisection Method, Newton Raphson Method, Secant Method, and False Position Method). The programs are developed on an Excel spreadsheet. There is a variety of software that find a real root using these methods, but our programs have some new features:

- They have root locators, which help choose initial guess(es).
- All the real roots of the equation can be found.
- The programs are GUIs.
- The programs are suitable for those who don't have any background in computer languages.

5. DECLARATION OF INTEREST

The authors declare that they have no known competing for financial and conflict of interests or personal relationships that could have appeared to influence the work reported in this paper.

6. REFERENCES

1. H. S. Drier, T*eaching and learning mathematics with interactive spreadsheets. School science and mathematics,* 2001. 101(4): p. 170-179.

2. J. B. Soper, J.B. and M.P. Lee, *Spreadsheets in teaching statistics. Journal of the Royal Statistical Society: Series D (The Statistician),* 1985. 34(3): p. 317-321.

3. J. C. Nash, *Teaching statistics with Excel 2007 and*

other spreadsheets. Computational Statistics & Data Analysis, 2008. 52(10): p. 4602-4606.

4. K. Jones, *Using spreadsheets in the teaching and learning of mathematics: A research bibliography. MicroMath*, 2005. 21(1): p. 30-31.

5. S. A. Khan *Microsoft Excel in the physics classroom. in The Third Annual Conference for Middle East Teachers of Mathematics, Science and Computing, The Petroleum Institute, Abu Dhabi.* 2007.

6. L. Webb, *Spreadsheets in physics teaching. Physics Education,* 1993. 28(2): p. 77.

7. B.A Cooke, *Some ideas for using spreadsheets in physics. Physics Education*, 1997. 32(2): p. 80.

8. Healy, L. and R. Sutherland, *The use of spreadsheets within the mathematics classroom. International Journal of Mathematical Education in Science and Technology,* 1990. 21(6): p. 847-862.

9. K. W. Wong and J.P. Barford, *Teaching Excel VBA as a problem solving tool for chemical engineering core courses. Education for Chemical Engineers,* 2010. 5(4): p. e72-e77.

10. D. Lilley *Excel/VBA for Numerical Methods Education, Calculations and Applications in Energy Engineering. in 44th AIAA Aerospace Sciences Meeting and Exhibit.* 2006.

11. A. Uddin, M. Ahsanuddin, and D.D. Khan, *Teaching physics using microsoft excel. Physics Education,* 2017. 52(5): p. 053001.

12. Z. Uddin and M.H. Zaheer, *Simulating Physics Experiments in Spreadsheets–Experimenting with Ohm's Law.* The Physics Teacher, 2019. 57(3): p. 182-183.

13. S. K. Gupta, *Numerical methods for engineers.* 1995: New Age International.

14. E. J. Billo, *Excel for scientists and engineers: numerical methods.* 2007: John Wiley & Sons.

15. Authors, *Teaching physics online through spreadsheets in a pandemic situation.* Physics Education, 2020. 55(6): p. 063006.

16. M. Iqbal, et al., *Teaching physics online through spreadsheets in a pandemic situation.* Physics Education, 2020. 55(6): p. 063006.

17. LearnChemE. *Bisection Example/Excel.* 2012 [cited 2012 May 8, 2012]; Available from: https://www.youtube.com/watch?v=q6WdsIJVl9M.

18. H. Arshad *Bisection Method in Excel.* 2017 [cited 2017 Apr 18, 2017]; Available from: https://www.youtube.com/watch?v=fmDa-1h5ONo.

19. Arshad, H. *Newton raphson method using MS Excel.* 2017 [cited 2017 Apr 17, 2017]; Available from: https://www.youtube.com/watch?v=VuAqKL2hYeE.

20. Mohammed, M. *Excel for Chemical Engineers | 38 | False Position Method.* 2016 [cited 2016 Feb 29, 2016]; Available from: https://www.youtube.com/watch?v=VuAqKL2hYeE.

21. L. F Stojanovska. *Secant Method - Ex. 2 (spreadsheet).* 2013 [cited 2013 Feb 1, 2013]; Available from: https://www.youtube.com/watch?v=nF4xakajgvY.

22. Calculator, K.O., *Newton method f(x),f'(x) Calculator.* 2021.

23. Mathematics, G.i. *Newton-Raphson Method.* 2010 [cited 2010 Aug 1, 2010]; Available from: http://www.wolframalpha.com/widgets/view.jsp?id=7366b7a89fc9d6c90e308d633d63884f.

Pakistan Academy of Sciences

Research Article

Higher Order Modeling of Reactor Regulating System and Nonlinear Neural Model Predictive Controller Design for a Nuclear Power Generating Station

Arshad H. Malik[1*], Aftab A. Memon[2], and Feroza Arshad[3]

[1]Department of Maintenance Training, Pakistan Atomic Energy Commission, A-104, Block-B, Kazimablad, Model Colony, Karachi, Pakistan
[2]Department of Telecommunication Engineering, Mehran University of Engineering and Technology, Jamshoro, Sindh, Pakistan
[3]Department of Management Information System, Pakistan Atomic Energy Commission, B-63, Block-B, Kazimablad, Model Colony, Karachi, Pakistan

Abstract: In the existing instrumentation and control system of an operating Pressurized Heavy Water Reactor (PHWR) based nuclear power plant, conventional controllers are used to control the reactor power. A new idea of Nonlinear Neural Model Predictive Controller (NNMPC) is introduced in this research work. The new 17th order nonlinear higher order model of Reactor Regulating System (RRS) is developed under different plant operating modes and various parametric conditions in Single Input Multi Output (SIMO) configuration with special emphasis on Helium Control Valve Dynamics (HCVD) and Coupled Nonlinear Iodine and Xenon Dynamics (CNIXD). The SIMO RRS model is developed based on first principle. The 17th order model is reduced to 9th order lower dynamic model using Balanced Truncation Method (BTM). The Reduced Order SIMO RRS (RO-SIMO-RRS) model is programmed, simulated and validated in SIMULINK environment. The plant Neural SIMO RRS (N-SIMO-RRS) model is developed using innovative data generated from RO-SIMO-RRS simulations. The plant neural N-SIMO-RRS model is optimized using Levenberg-Marquardt Algorithm (LMA). Using the identified N-SIMO-RRS model, the Nonlinear Neural Model Predictive Controller (NNMPC) is designed, trained, verified, validated, and finally optimized using the backtracking technique in the SIMULINK environment. The optimized results are obtained from designed closed loop RRS and found within the acceptable design limits. The performance of the proposed closed loop RRS is also tested in reference tracking mode with excellent fast tractability near the optimal target demanded power level.

Keywords: SIMO Modelling, Reactor Regulating System, Model Reduction, Nonlinear Neural Predictive Control, Helium Control Valve Dynamics, PHWR, Nuclear Power Plant

1. INTRODUCTION

MIn this research work, a Pressurized Heavy Water Reactor (PHWR) type nuclear power plant system is focused which is associated with reactor power control system known as Reactor Power Regulating System (RPRS) or simply Reactor Regulating System (RRS) [1].

A robust H-Infinity controller has been designed for current PHWR in [2] which is also under consideration in this research. A state space based Model Predictive Controller (MPC) has been designed for reactor power control systems for a different Pressurized Water Reactor (PWR) type nuclear power generating station in [3]. A data driven composite MPC has been captured for current PHWR Reactor Power Controller (RPC) in [4]. A nonlinear higher order model of RRS of operating PHWR type nuclear power generating station has been developed in [5] and Linear Matrix Inequalities (LMI) based Fast Output Sampling (FOS) controller has been designed. The higher order dynamics of an Advanced Heavy

Water Reactor (AHWR) have been reduced using Balanced Truncation Method (BTM) under reactor transient conditions for controller design purposes in [6]. A Genetic Algorithm (GA) tuned Proportional Integral Derivative (PID) controller has been designed for reactor kinetics of PWR in [7]. A fuzzy PID controller has been identified for PWR in load following mode in [8]. A robust H-Infinity mixed sensitivity controller has been proposed for small PWR with parametric uncertainties in [9]. A robust Linear Quadratic Gaussian (LQG) controller has been synthesized for the PWR type nuclear power plant [10]. A Multi-Layer Perceptron compensated output feedback PD controller has been designed for Gas Cooled Reactor (GCR) in [11]. A neural network based MPC has been designed for Single Input Single Output (SISO) power converter in [12]. A reactor power change constrained based fuzzy logic controller has been designed for a nuclear research reactor in [13]. A fuzzy logic-based MPC controller has been designed for the reactor power control of the PWR type nuclear power plant [14]. A decentralized fuzzy MPC has been proposed for PWR with xenon dynamics in [15]. A MLP based model free MPC has been designed for nuclear steam supply system in [16].

In this research work, a new multi-objective optimized Single-Input Multi-Output (SIMO) Nonlinear Neural Network based Model Predictive Controller (NNMPC) SIMO-NNMPC is proposed for a Novel Full Higher Order Integrated SIMO Reactor Regulating System (NFHOI-SIMO-RRS) and Reduced Order SIMO RRS (RO-SIMO-RRS) models with special emphasis on Helium Control Valve Dynamics (HCVD) and Coupled Nonlinear Iodine and Xenon Dynamics (CNIXD). The proposed NNMPC is designed, for the first time, for PHWR type nuclear power generating station with substantially reduced online computational requirements as compared to conventional MPC techniques. The computational effort involved in the NNMPC training depends mainly on the artificial neural network complexity, and not on the length of the control horizon. This makes it feasible to design a controller with a longer control horizon.

2. MATERIALS AND METHODS

2.1 Reactor Regulating System

SReactor Regulating System (RRS) is designed to regulate the reactor power. RRS is a fine reactivity control system using Helium Gas (HG) Control Valve (CV) as modulating element. In RRS, there are two power channels known as Regulating Channel-A and Regulating Channel-B respectively. Both channels act like redundant systems. There are two Helium Gas Control Valves (HGCV1 and HGCV2) installed between the upper and lower Calandria in PHWR type CANDU Nuclear Power Plant [1].
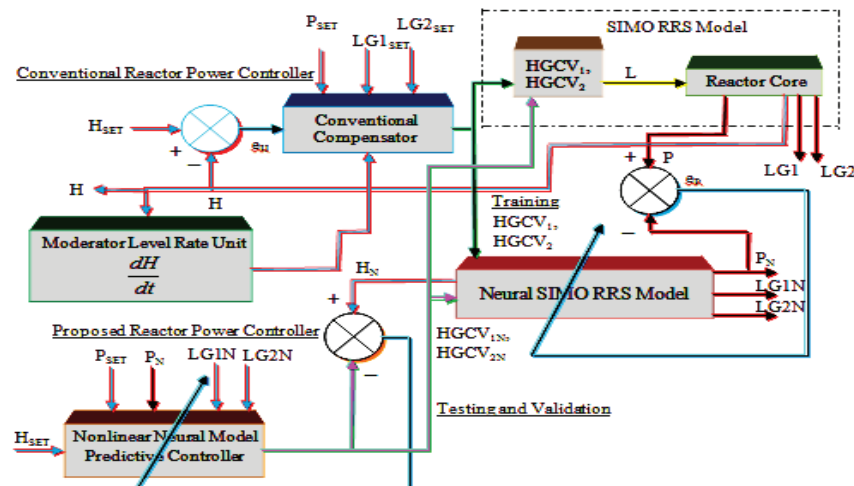

Fig. 1. Closed loop design architecture of existing and proposed RRS.

2.2 Existing Reactor Power Controller

Two Reactor Power Controllers (RPC) control Regulating Channel-A and Regulating Channel-B. At a time, reactor power is controlled by one RPC while second RPC works as Backup Controller in tracking mode. The existing controller is a digital controller known as AC132 controller. The reactor power is normalized and expressed in %. In this research paper, the plant operation is considered in Reactor Following Mode (RFM) also known as Neutron Power Mode (NP-Mode). In RFM, there are four set points designated as moderator level set point (HSET), reactor power set point (PSET), logarithmic of reactor power set point (LG1SET) and rate of change of logarithmic of reactor power set point (LG2SET). Similarly, there are four corresponding measured variables designated as moderator level (H), reactor power (P), logarithmic of reactor power (LG1) and rate of change of logarithmic of reactor power (LG2). Therefore, four sub controllers will be considered for design and analysis, in detail, in subsequent sections. RPC is basically a conventional compensator technology implemented on Programmable Logic Controllers (PLCs) [1]. The closed loop architecture of existing RRS is shown in Fig.1.

2.3 Proposed Reactor Power Controller

The proposed reactor power controller is basically Nonlinear Neural Model Predictive Controller (NNMPC). Therefore, two major milestones are required to achieve in this research work. Firstly, a Neural SIMO RRS (N-SIMO-RRS) model is required to developfor NNMPC. Such a N-SIMO-RRS model is extracted from Reduced Order SIMO-RRS (RO-SIMO-RRS) modelusing data driven technique. RO-SIMO-RRS model is developed after implementing dimension reduction technique on Full Higher Order SIMO-RRS (FHO-SIMO-RRS) model. The closed loop architecture of proposed RRS is shown in Fig.1.

NNMPC1 consists of N-SIMO-RRS model and the optimizer. The optimizer computes controller signal u^' that minimizes the controller cost function JC which is given as [16]:

$$J_C = Y(t) - \rho U(t) \qquad (1)$$

Where

$$U(t) = \sum_{j=1}^{N_U} \left(u'(t+j-1) - u'(t+j-2) \right)^2$$

$$Y(t) = \sum_{j=N_1}^{N_2} \left(y_r(t+j) - y_m(t+j) \right)^2$$

Where N_1, N_2 and Nu define the minimal and maximal prediction horizons of controlled output of RO-SIMO-RRS and prediction horizon of controller signal. The u^'is the predicted NNMPC controller signal, yr is the desired response of RO-SIMO-RRS model and ym is the network model response of N-SIMO-RRS model. The ρ value determines the contribution of the sum of the squares of the control increments that has an impact on the performance index.

Since, four sub controllers are configured for *H, P, LG1* and *LG2* separately in SISO form for HGCV1, therefore, four separate cost functions are defined against the same input L as:

$$J_{C11} = Y_{11}(t) - \rho_{11}U_{HGCV1}(t) \qquad (2)$$

$$J_{C12} = Y_{12}(t) - \rho_{12}U_{HGCV1}(t) \qquad (3)$$

$$J_{C13} = Y_{13}(t) - \rho_{13}U_{HGCV1}(t) \qquad (4)$$

$$J_{C14} = Y_{14}(t) - \rho_{14}U_{HGCV1}(t) \qquad (5)$$

The structure of neural MPC of reduced order plant model is shown in Fig. 2.

Similarly, cost functions are designed for HGCV2. Constraints are imposed on input, change in input, output and change in output for each sub controllers for HGCV$_1$ and HGCV$_2$.

2.4 Nonlinear Neural MPC Optimization

2.4.1 Backtracking Technique

A one-dimensional (1D) linear cost function minimization technique that works on a linear search algorithm is called backtracking. It uses step multiplier and backtracks, till the quadratic approximation of controller cost function which is a function of step multiplier and current point is minimized in the search direction. If the quadratic approximation based cost function is not sufficiently reduced then a cubic approximation is used and

minimized.

2.4.2 Stopping Criteria

When training of NNMPC is accomplished with minimum error then this represents that the maximum number of iterations (epochs) reached. Minimum mean square error of the epoch is the square root of the sum of squared differences between the NNMPC predicted outputs and actual existing RPC outputs divided by the number of training samples of controller.

2.5 NewNonlinear Higher Order Dynamics of SIMO RRS Model

2.5.1. Choice of Reference Model

The reference model is adopted from an already conducted and established research [5] which is a Single Input and Multi-Output RRS model that includes Nuclear Reactor Dynamics (NRD) and Helium Control Valve Dynamics (HCVD) in electrical form for reactivity management for the current PHWR under consideration. The assumptions taken into account for higher order modelling as reference model are that six precursor groups are chosen, reactor power is only controlled by Helium control valves and moderator level is not entered in the band of reactor regulating control rods. This non-linear 15th order SIMO-RRS model is linearized and transformed into state equation model form as [5]:

$$\dot{x}(t) = A\,x(t) + B\,u(t) \qquad (6)$$
$$y(t) = C\,x(t) \qquad (7)$$

where $A \in R^n$, $B \in R^m$ and $C \in R^p$ are the matrices of appropriate dimensions.

2.5.2. Coupled Nonlinear Iodine and Xenon Dynamics

In a reactor power system, nuclear fission reactions take place. In nuclear reactions, fission fragments are produced and all fission products absorb neutrons to some extent, so are known as reactor poisons. Most fission product poisons simply build up slowly as the fuel burns up and are accounted for as a long-term reactivity. The neutron absorbing fission products Xenon-135 and Samarium-149 have particular operational importance. Their concentrations can change quickly, produces major changes in neutron absorption on a relatively short time scale. Each arises from the decay of a precursor fission product, which controls their production rate, but, because they have large absorption cross-sections, their removal changes quickly with changes in thermal neutron flux $\emptyset_T$.

Xenon-135 (often simply referred to just as xenon) is the most important fission product poison. It has a very large absorption cross-section and high production rate.

Xenon is a strong neutron absorber so its presence in the fuel creates a large negative reactivity in the core. The reactivity worth of the Xe-135 is known as the Xenon load. Therefore, the relationship between Xenon load and reactor power is inverse, as the Xenon load increases, the reactor power decreases. Similarly, the iodine load is the
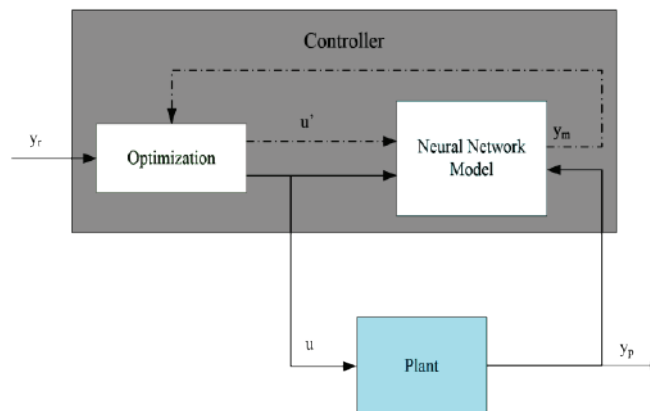

Fig. 2. Structure of neural MPC of reduced order plant model.

reactivity that it would insert into the reactor, if all the iodine present suddenly changes into xenon [1].

Iodine dynamics is represented by the following expression in PHWR [15]:

$$\frac{dI(t)}{dt} = \gamma_I \Sigma_f \phi_T - \lambda_I I - \sigma_{aI} I \tag{8}$$

Where I is the concentration of I-135 (atoms/cm3), γ_I is the effective yield of I-135 (atoms per fission), Σf is the thermal fission cross-section, ϕ_T is the reactor neutron flux, λ_I is the decay constant for I-135, and σ_{aI} is the I-135 absorption cross-section.

Xenon dynamics is represented by the following expression in PHWR [15]:

$$\frac{dX(t)}{dt} = \gamma_X \Sigma_f \phi_T + \lambda_I I - \lambda_X X - \sigma_{aX} \phi_T X \tag{9}$$

Where X is the concentration of Xe-135, γ_x is the effective yield of Xe-135, λ_x is the decay constant for Xe-135, and σa_X is the absorption cross-section for Xe-135.

The thermal flux and reactor power are correlated by the following expression for an operating PHWR[1]:

$$\phi_T = p(\%) \times \frac{137 MWe}{100} \times 3.12 \times 10^{10} \frac{fissions}{watt.\sec}$$
$$\times \frac{1}{\Sigma_f V} \tag{10}$$

2.5.3 Integrated SIMO RRS Model

The nonlinear poison model of 2nd order developed in this research work is then linearlized and integrated with alrealy developed linearlized 15th order SIMO RRS model. The new Higher Order Integrated SIMO-RRS (HOI-SIMO-RRS) model is highly precise and state of the art.

Now, the continuous time state space model of SIMO-RRS expressed equations (6) and (7) is appended with Xenon poison dynamics. The appended higher order model is then restructured for Helium Control Valve Dynamics (HCVD) and transformed into non-electrical form and finally represented in state space form as:

$$\dot{x}(t) = A_{AR} x(t) + B_{AR} u(t) \tag{11}$$

$$y(t) = C_{AR} x(t) \tag{12}$$

Where $A_{AR} \epsilon\ R^r$, $B_{AR} \epsilon\ R^m$ and $C_{AR} \epsilon R^p$ are the appended and restructured matrices of appropriate dimensions (r>n).

The integrated appended dimensionality of input vectors for both control valves in the proposed design 17×1.

The input vector, state vector and output vector of a PHWR model described in equations (6) and (7) are as follows:

$$u(t) = L$$

$$x(t) = \begin{bmatrix} \delta P & \delta\overline{C} & \delta L & \delta\overline{G}_{12} & \delta\overline{R}_{12} & \delta\overline{L} & \delta Q_M & \delta\overline{X}_I \end{bmatrix}^T$$

Where

$$\delta\overline{C} = \begin{bmatrix} \delta C_1 & \delta C_2 & \delta C_3 & \delta C_4 & \delta C_5 & \delta C_6 \end{bmatrix}^T$$

$$\delta\overline{G}_{12} = \begin{bmatrix} \delta LG1 & \delta LG2 \end{bmatrix}^T$$

$$\delta\overline{L} = \begin{bmatrix} \delta L_1 & \delta L_2 \end{bmatrix}^T$$

$$\delta\overline{X}_I = \begin{bmatrix} \delta X & \delta I \end{bmatrix}^T$$

$$y(t) = \begin{bmatrix} y_1 & y_2 & y_3 & y_4 \end{bmatrix}^T = \begin{bmatrix} H & P & LG1 & LG2 \end{bmatrix}^T$$

where H, P, LG1 and LG2 are moderator level, power, log power and rate log power respectively.

2.5.4 Reduced Order SIMO RRS Model

The 17th order SIMO RRS model is reduced by Balanced Truncation Method [6] and the Reduced 9th Order SIMO RRS (RO-SIMO-RRS) model is obtained from equations (11) and (12) based on optimal value of tolerance value of error bound for RO-SIMO-RRS model as:

$$\dot{x}(t) = A_R x(t) + B_R u(t) \tag{13}$$

$$y(t) = C_R x(t) \tag{14}$$

where $A_R \epsilon\ R^d$, $B_R \epsilon\ R^m$ and $C_R \epsilon R^p$ are the matrices

of appropriate dimensions (d<r).

The input vector, state vector and output vector of RO-SIMO-RRS model described in equations (13) and (14) are as follows:

$$u(t) = L$$

$$x(t) = [\delta x_1 \ \delta x_2 \ \delta x_3 \ \delta x_4 \ \delta x_5 \ \delta x_6 \ \delta x_7 \ \delta x_8 \ \delta x_9]^T$$

$$y(t) = [y_1 \ y_2 \ y_3 \ y_4]^T = [H \ P \ LG1 \ LG2]^T$$

Where H, P, LG1 and LG2 are moderator level, power, log power and rate log power respectively. The error bound for RO-SIMO-RRS model in frequency domain is defined as:

$$\|G_{RO-SMO-RRS}(s) - G_{HOI-SMO-RRS}(s)\| = \varepsilon \quad (15)$$

Where ε is tolerance value.

2.6 Neural SIMO RRS Model

2.6.1 Choice of Neural Inputs and Outputs

Assuming for $HGCV_1$, the dataset D_i contains Q number of data patterns and d_i is an $(n_u + n_t)$ dimensional vector containing nu number of inputs and n_t number of outputs defined as:

$$d_i = \{u_{HGCV1}, t_P, t_H, t_{LG1}, t_{LG2}\}$$

Similarly, assuming for $HGCV_2$, the dataset D_j contains number of data patterns and dj is an $(n_u + n_t)$ dimensional vector containing nu number of inputs and nt number ofoutputs defined as:

$$d_j = \{u_{HGCV2}, t_P, t_H, t_{LG1}, t_{LG2}\}$$

2.6.2 Optimization of N-SIMO-RRS Model

N-SIMO-RRS model is divided into four sub N-SISO-RRS models. N-SISO1-RRS, N-SISO2-RRS, N-SISO3-RRS and N-SISO4-RRS sub models are optimized in distributed parallel computing fashion using standard Levenberg-Marquardt algorithm implemented in MATLAB.

2.6.3 Formulation of MSE for N-SIMO-RRS Model

Now, if where t_{nt} is the desired outputs of SIMO-RRS model for each input pattern and yntis the actual

output produced by each N-SISO-RRS model, then Mean Square Error (MSE) is a dimensionless value computed to deduce the N-SISO-RRS model performance for training, testing and validation for each n_t.

For moderator level (H), MSEs can be defined as:

$$MSE_{Training} = \sum_{q=1}^{Q_{tr}}(t_1 - y_1)^2 = \sum_{q=1}^{Q_{tr}}(H - H_N)^2$$

$$MSE_{Testing} = \sum_{q=1}^{Q_{te}}(t_1 - y_1)^2 = \sum_{q=1}^{Q_{te}}(H - H_N)^2$$

$$MSE_{Validation} = \sum_{q=1}^{Q_{va}}(t_1 - y_1)^2 = \sum_{q=1}^{Q_{va}}(H - H_N)^2$$

Similarly, all rest of the MSEs can be defined for P, LG1 and LG2.

The structure of N-SIMO-RRS model for training, testing and evaluation is shown in Fig. 2.

3. RESULTS AND DISCUSSION

The simulations and analysis of 15th order SIMO-RRS model described in equations (1) and (2) were discussed in detail in [5]. Now, in this research work, a new addition of coupled dynamics of Iodine and Xenon described in equations (8), (9) and (10) are modeled in Simulink environment in MATLAB as shown in Fig. 3. This model is very useful for long term dynamic studies of nuclear reactor dynamics. All the constants and parameters are properly modeled for dynamic analysis purposes. The impact of Xenon dynamics is considered and integrated with reference model [5].

Basically, the Xenon dynamics is highly nonlinear in nature and helpful for power dynamics on large time-scale, especially in power transients. The power transient consists of reactor power maneuvering in either direction depending on the power demand changes.

3.1 Estimation and Implementation of RO-SIMO-RRS

The new 17th order SIMO-RRS (HOI-SIMO-RRS) model is reduced using BTM in MATLAB

and a reduced 9th order RO-SIMO-RRS model is obtained as described in equations (13) and (14). The comparison of frequency responses of HOI-SIMO-RRS and RO-SIMO-RRS models is shown in Fig. 4.

The error bound is computed using equation (15) and found 10-4, which shows a very good agreement. The RO-SIMO-RRS model is implemented in Simulink environment as shown in Fig. 5.

3.2 Estimation and Implementation of NNMPC-1 and NNMPC-2

The Configuration of redundant NNMPC-1 and NNMPC-2 interfaced with RO-SIMO RRS model is shown in Fig. 6.

This configuration is basically designed for Automatic / Manual (AUTO/MAN) operation of an operating PHWR type nuclear power plant. The

advantage of proposed redundant controllers is that when the controlling controller is failed then tracking controller is configured as backup controller in a bump less manner. In this research work, MAN mode is selected for dynamic parametric studies embedded with four sub controllers in Neutron Power Reactor Control Mode (NP-Mode) [1]. NP-mode is a mode before Steam Pressure Mode (SP-Mode).

An innovative dataset of 9000 samples is generated very sophisticatedly from RO-SIMO-RRS model at a sample time T_s = 0.16 second. 5400 samples are used for training, 1800 for testing and 1800 for validation of N-SIMO-RRS model. All the training, testing and validation of N-SIMO-RRS model are carried out in MATLAB Simulink environment. All the design parameters of N-SIMO-RRS model are estimated using methodology discussed in section 2.3 and are tabulated in Table 1.
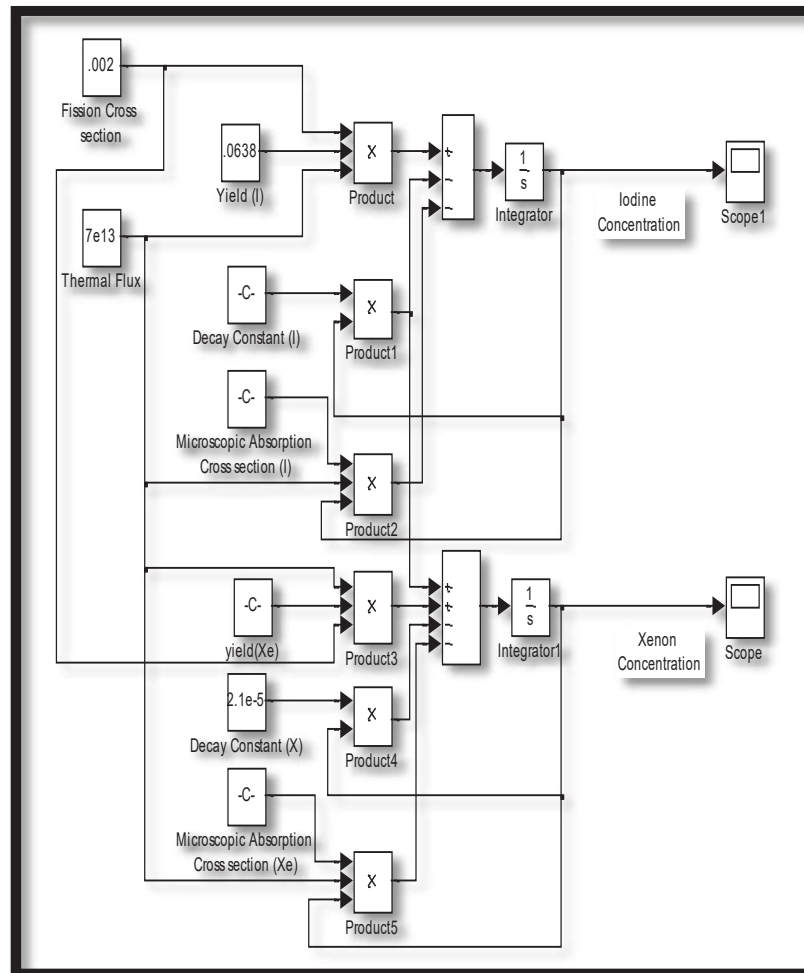
Fig. 3. Coupled Simulink model of Xenon and Iodine dynamics.
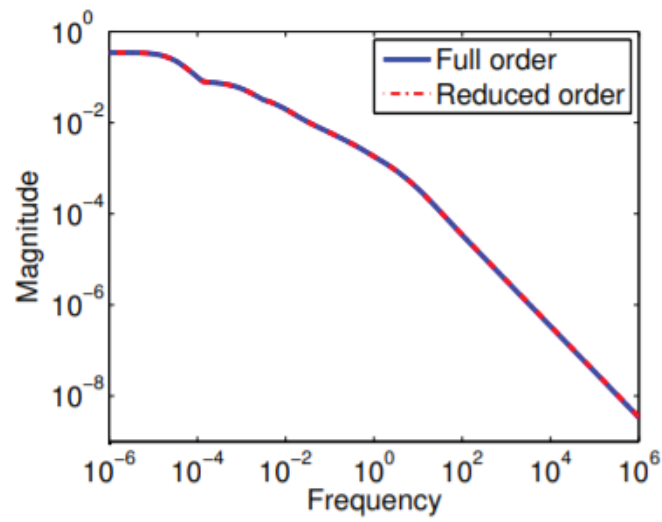
Fig. 4. Comparison of frequency responses of HOI- SIMO-RRS and RO-SIMO-RRS models.
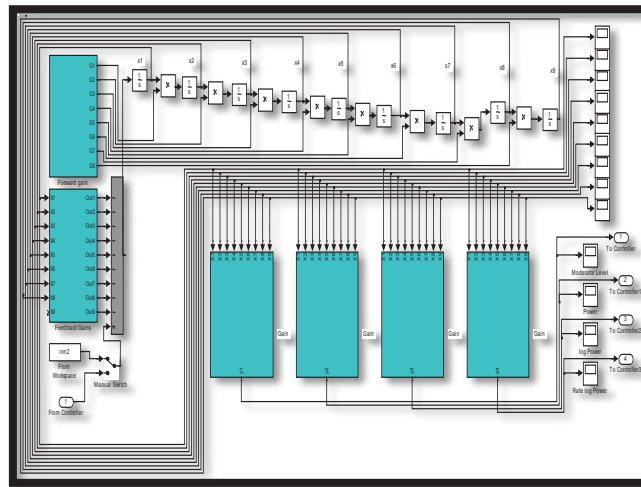
Fig. 5. Simulink model of RO-SIMO-RRS model
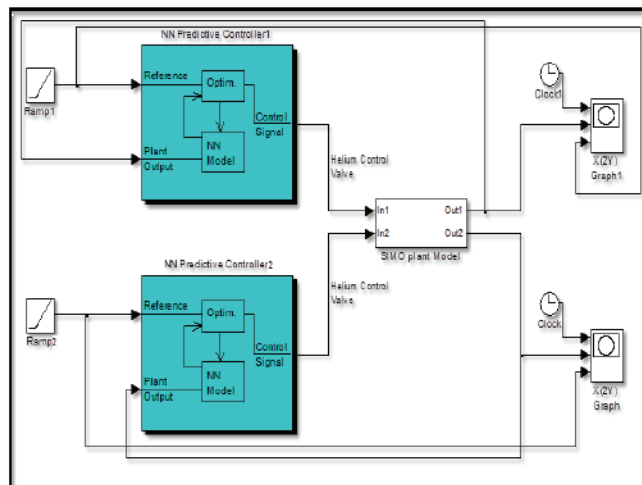
Fig. 6. Configuration of redundant NNMPC-1 and NNMPC-2 interfaced with RO-SIMO RRS model

Table 1. Parameters of N-SIMO-RRS model

Parameters	Design Values
Number of Input (n_u)	1
Number of Outputs(n_t)	4
No of hidden layers	9
No of neurons in hidden layer (n_h)	25
Sampling Interval (seconds)	0.16
Total Samples (Q)	9000
Training Samples (Q_{tr})	5400
Testing Samples (Q_{te})	1800
Validation Samples (Q_{va})	1800
Mu Value (μ)	0.0001
Training Epochs	200
Performance	$1.8 \times 10\text{-}6$

Four sub controllers NNMPC11, NNMPC12, NNMPC13 and NNMPC14 are configured in distributed parallel computing framework in Simulink environment using equations (2) to (5). The parameters of designed sub controller of NNMPC11 for moderator levelare tabulated in Table (2) for reference purposes.

Table 2. Parameters of NNMPC11 for moderator level

Parameter Name	Design Value
Minimal Cost Horizon (N1)	1
Maximal Cost Horizon (N2)	7
Control Horizon (Nu)	2
Control Weighting Factor (ρ_{11})	0.1
Search Parameter (α_{11})	0.02
Iterations per sample time	2

Similarly, the design parameters of rest of three sub controllers NNMPC12, NNMPC13 and NNMPC14 for HGCV1and four sub controllers NNMPC21, NNMPC22, NNMPC23 and NNMPC24 HGCV2are evaluated in NP-mode.

3.3 Closed Loop Simulation Scenarios for Validation of Proposed NNMPC

Two case studies are considered in this research work that shall be discussed in the subsequent sections.

3.3.1 Rule based Reactor Power Rising Scenario from 0% to 75%

In this first case study, reactor power rising transient is considered with RO-SIMO-RRS model

and NNMPC. The reactor power is increased from 0% to 75% as per procedure as laid down in [1]. This procedure is known as rule based transient in engineering language. The rule base scenario is a predefined combination of steps, ramps, checks, permissives and interlocks. The behaviour of Helium control valve controller and corresponding changes in moderator level, reactor power, logarithmic reactor power and rate of logarithmic reactor power are simulated and analyzed as shown in Fig.7 to Fig. 11 respectively.

All the parametric behavior is well controlled and well within the design constraints imposed on closed loop RRS [1, 5]. The Helium control valve signal is observed highly nonlinear in nature and remained within 100% throughout the power rising transient. The moderator level rises from 35 inches to 175 inches which is well within 190 inches control limit. The reactor power increases from 0% to 75% without any overshoot which is one of most important design basis of RRS[1, 5].The logarithmic reactor power is quite well because rate oflogarithmic reactor power is within 4%RP/sec design limit.
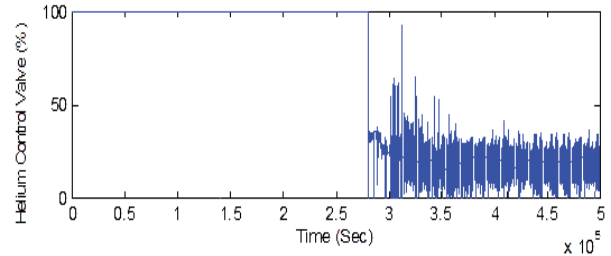

Fig. 7. Helium control valve controller signal during power rising transient.
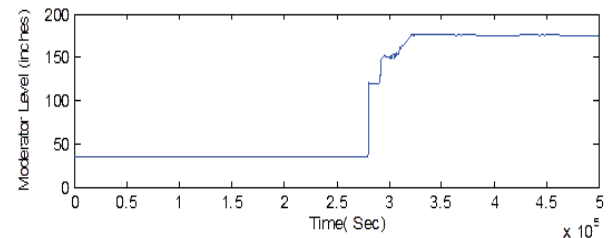

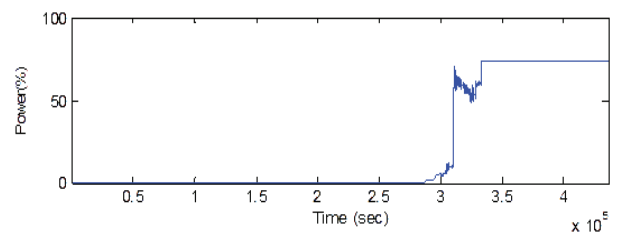**Fig. 8.** Moderator level during power rising transient.

Fig. 9. Reactor power during power rising transient.

3.3.2 Reactor Power Rising Scenario from 0% to 50% in Reference Tracking Mode

In this second case study, reactor power rising transient is considered with HOI-SIMO-RRS model and NNMPC in reference tracking mode. In this mode, plant is to follow the reference command signal which is implemented as per plant design procedure. Such design studies are carried with any of the redundant channel that replicates the actual plant operating configuration. The proposed NNMPC is configured with HOI-SIMO-RRS model as shown in Fig. 12.

The reactor power is increased from 0% to 50% in reference tracking mode in NP-mode. This procedure is known as ramp transient in engineering language. The behavior of HOI-SIMO-RRS model with special emphasis on Xenon dynamics, the behavior of Iodine concentration, Xenon concentration, moderator level as a result of Helium control valve controller signal variation and corresponding changes in reactor power are simulated and compared with reference signal as patent ramp transient as shown in Fig. 13 to Fig. 16 respectively.All the parametric behavior is well controlled and well within the design constraints imposed on closed loop RRS in reference tracking mode in a reactor following transient.

There is no overshoot observed in any of the parameter. Moderator level and reactor power as key parameters of interest are observed smooth andfast with leading dynamics and reached the target moderator level of 175 inches and reactor power of 50%. The moderator level is found within design limits even with Xenon load. Hence, the proposed closed loop SIMO-RRS is sufficiently stable and found robust in reference tracking mode.
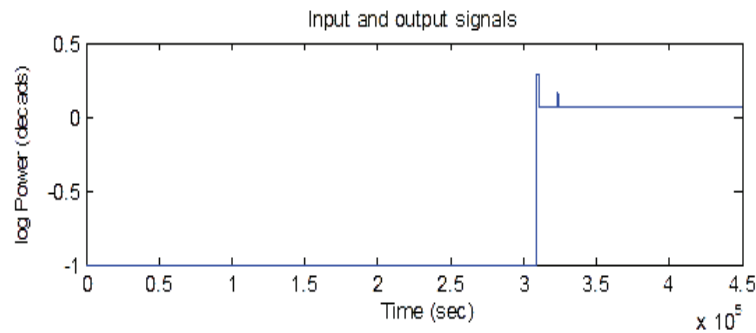
Fig. 10. Log reactor power during power rising transient.
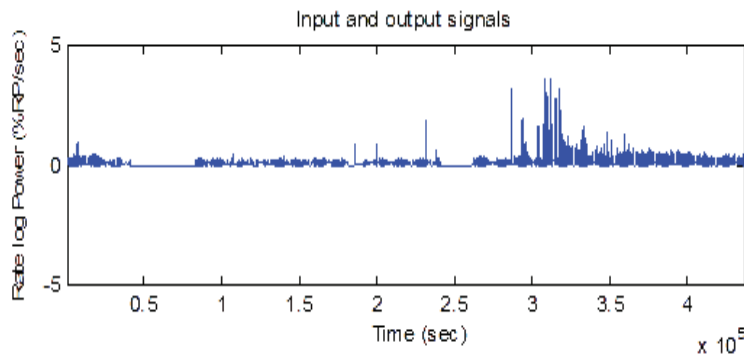
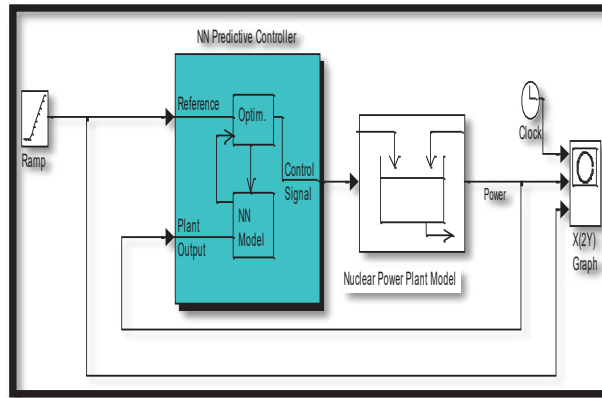**Fig. 11.** Rate log reactor power during power rising transient.

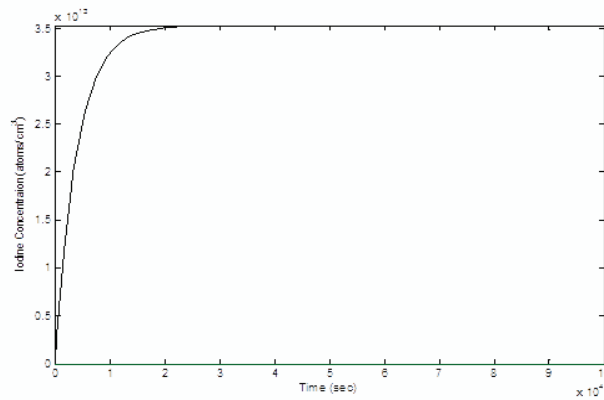**Fig. 12.** Structure of NNMPC interfaced with HOI-SIMO-RRS model.

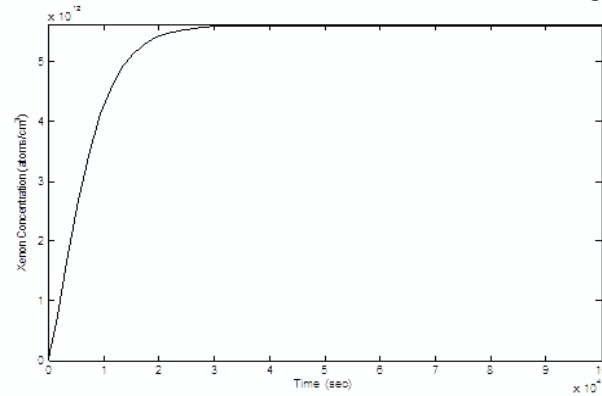**Fig. 13.** Variation of Iodine concentration in reference tracking mode.

Fig. 14. Variation of Xenon concentration in reference tracking mode.
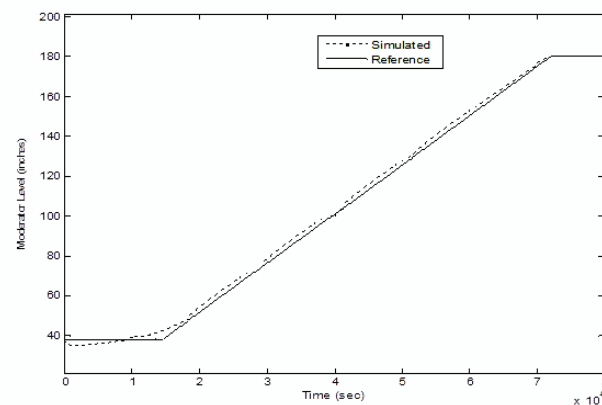

Fig. 15. Performance of proposed closed loop RRS moderator level in reference tracking mode.
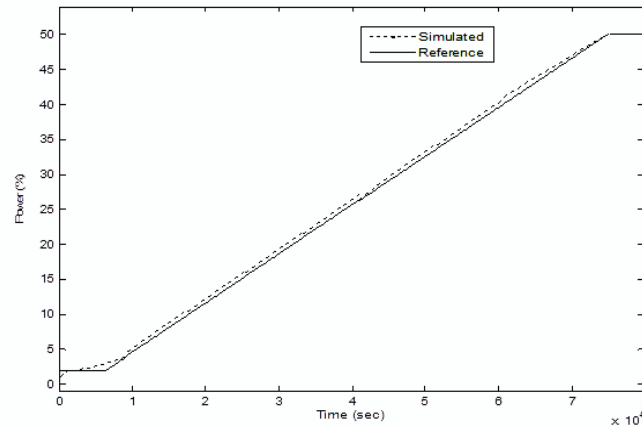
Fig. 16. Performance of proposed closed loop RRS reactor power in reference tracking mode.

4. CONCLUSIONS

In this research work, a new nonlinear neural model predictive controller has been designed as new innovative replacement of conventional compensator of RRS. The performance of NNMPC has been tested and evaluated with RO-SMO-RRS model under rule based reactor power transient and with HOI-SIMO-RRS model under reference tracking mode and found smooth, faster and robust in closed loop configuration. All the parametric trends prove that the proposed closed loop SIMO-RRS model with NNMPC is realistic and within design bounds.

5. ACKNOWLEDGEMENTS

6. REFERENCES

1. A. H. Malik. Nuclear reactor instrumentation and control. *KINPOE, PAEC, Pakistan* (2017).
2. A. H. Malik,, A. A. Memon, and M. R. Khan. Synthesis of model based robust stabilizing reactor power controller for nuclear power plant. *Mehran University Research Journal of Engineering and Technology* 30 (2): 265-276 (2011).
3. W. Guoxu, B. Zeng, Z. Xu., W. Wu. and X. Ma. State-space model predictive control method for core power control in pressurized water reactors nuclear power stations. *Nuclear Engineering and Technology* 49 (1): 134-140 (2017).
4. A. H. Malik,, A. A. Memon, and M. R. Khan. Synthesis of reference tracking multivariable composite controller for PHWR. Proceedings of Pakistan Academy Sciences 47 (4): 245-252 (2010).
5. A. H. Malik, A. A. Memon, and M. R. Khan. Dynamic modeling and controller design for nuclear power plant. *Journal of Engineering and Applied Sciences* 29 (2): 19-33 (2010).
6. R. S. Ananthoju, E. Tiwari, A. P. and M. N. Belur. Model Reduction of AHWR space time kinetics using balanced truncation. *Annals of Nuclear Energy* 102: 454-464 (2017).
7. S. M. H. Mousakazemi. Comparison of error-integral performance indexes in a GA-tuned PID controlling system of a PWR-type nuclear reactor point-kinetics model. *Progress in Nuclear Energy* 132: 1412-1423 (2021).
8. Z. Wenjie, Q. Jiang, Jinsen X. and T. Yu. A functional variable universe fuzzy PID controller for load following operation of PWR with the multiple model. *Annals of Nuclear Energy* 140: 1-6 (2020).
9. X. Y. Pengfei, P. Wang, J. Qing, S. Wu and F. Zahao. Robust power control design for small pressurized water reactor using H infinity mixed sensitivity method. *Nuclear Engineering and Technology* 52: 1443-1451 (2020).
10. V. Vajpayee, V. Becerra, N. Bausch, J. Deng, S. R. Shimjith and A. J. Arul. Robust-optimal integrated control design technique for pressurized water-type nuclear power plant. *Progress in Nuclear Energy* 131: 1-14 (2021).
11. Zhe, D. An artificial neural network compensated output feedback power control for modular high temperature gas-cooled reactors. *Energies* 07: 1149-

1170 (2014).

12. S. Sanaz, R. Heydari., M. Mohiti., M. Savaghebi. and J. Rodriguez. Model-free neural network-based predictive control for robust operation of power converter. *Energies* 14: 01-12 (2021).

13. S. M. Mohd, N. A. M. Subha., F. Hassan., and A. Ahmad. Application of fuzzy logic for power change rate constraint in core power control at reactor TRIGA PUSPATI. IOP Conference Series: Material Science and Engineering 785: 1-18 (2020).

14. L. Xiangie, and M. Wang. Nonlinear fuzzy model predictive control for a PWR nuclear power plant. *Mathematical Problems in Engineering* 2014: 1-10 (2014).

15. L. Xiangjie, Di. Jiang., and K. Y. Lee. Decentralized fuzzy MPC on special power control of a large PHWR. *IEEE Transactions on Nuclear Science* 63 (4): 1-10 (2016).

16. Z. Dong, Z. Zhang., Y. Dong., and X. Huang. Multi-layer perception based model predictive control for thermal power of nuclear superheated-steam supply systems. *Energy* 151: 116-125 (2018).

Pakistan Academy of Sciences

Research Article

Two-Phase CS0 for Introductory Programming

Muhammad Shumail Naveed[1*], and Muhammad Sarim[2]

[1]Department of Computer Science & Information Technology, University of Balochistan, Quetta, Pakistan
[2]Department of Computer Science, Federal Urdu University of Arts, Science & Technology, Karachi, Pakistan

Abstract: Computer programming is the heart of computer science and thereby an important skill of the students. However, comprehending programming is extremely hard and introductory courses on programming are notorious to cause issues and challenges for learners, which affect their motivation and consequently cause high dropouts and low retention. This paper introduced CS0 as a precursor programming course to teach beginners, the fundamental notions of programming before the first course on programming. The proposed CS0 is grounded on two-phase learning strategy and equipped with a collaboration strategy. The results of the initial evaluation of proposed course are reasonably encouraging to motivate and prepare the novices for the first course on programming. The statistical significance of a proposed course is observed in improving the academic outcomes of novices in a first programming course. The normality of data was checked using the Kolmogorov-Smirnov and Shapiro-Wilk tests. The findings were analyzed with one-way ANOVA test and Kruskal–Wallis H test, indicating that the suggested course is statistically significant in enhancing the academic achievements of beginners in their first programming course.

Keywords: Programming, introductory programming, pair programming, CS0, motivation.

1. INTRODUCTION

MComputer Programming is one of the important abilities of computer science students [1, 2]. However, comprehending programming is extremely difficult for novice students [3,4], and therefore introductory courses on programming are generally very difficult. Appropriate problem-solving skills are necessary for programming [5], but the syntax and denotations of computer languages are mostly hard for novices [6]. It is commonly believed that complicated syntax, the span of time to construct a computer program and isolation during coding and learning are the prime factors for the sophistication to learn and understand the programming [7]. In [8], it is opined that the inherent difficulty of the programming and a lack of motivation in novices are the core reasons of their failure.

The first course on computer programming is usually called a CS1 [9]. The first programming language is immensely important for students since it forms the tone for all the successive classes of computer education [10]. However, the requirement of problem-solving abilities, complicated syntax, strange semantic and dense logic disturbs students' learning curve in a first course on programming [11]. These actualities have caused novice students to scare from programming and form wrong judgment regarding their education in programming [12].

An initial disappointment of learning fundamental concepts affects the confidence and increase dropout of students in CS1. Educators and mentors are being asked to determine the beneficial intermingle of technology and pedagogy to aid students in CS1 [13]. Different studies are organized to control these problems yet the failure rates and dropout in introductory courses on programming are still very high [8, 14, 15, 16, 17].

Several studies have attempted to analyze and determine the aspects that predict success of students in a first course on programming. In [18], it is argued that the performance of students is strongly affected by their learning strategy. Motivation is extremely important for successful instruction [19]. Settle et al. [14], identified the positive correlation between the motivation and success to learn the programming.

Anderson et al. [20] described that learning in programming is affected by students' low motivation. Likwise, Nikula et al. [21] argued that lack of motivation increased the failure rates in a first programming course. Similarly, it is widely believed and reported that prior experience of programming strongly affects students' outcome in the introductory courses of programming [22].

The rest article is organized as follows. Related work is presented in the next section. Section 3 described the research approach and methods. Section 4 includes the evaluation and discussed the initial results. Finally, the conclusion is described in section 5.

2.   RELATED WORK

Several programming environments and approaches have been introduced to control the difficulties of introductory programming.

Visual programming language is a programming language that helps students in learning programming concepts by allowing figures and graphical objects to write the programs [23]. These languages allow the drag-and-drop features to develop a program. Scratch is a language developed to teach programming to novice students. It supports to develop interactive stories, computer animation, interactive stories, and other multimedia projects. Blockly is a client-side library developed by Google for JavaScript. It eases the programming by supporting drag-and-drop of components to develop the programs. Sub-clauses of instructions and placeholders for identifiers are supported in Blockly [24]. With Blockly novices concentrating on algorithm semantics and relaxed from the rigid syntax of a language.

Seraj et al [25], compared and analysed the impact of Scratch and Blockly in increasing the programming capabilities of students. The study reported the significance of Scratch over the Blockly. However, Blockly is found useful in increasing the interest of students in future programming.

Alice is a programming language for educational purpose. It follows an object-oriented style of programming and developed by Carnegie Mellon University. Alice supports beginners in learning elementary concepts like variables, arrays, objects & classes, and recursionbeginners in elementary concepts like variables, arrays, objects & classes, recursion, and inheritance. In [26], the four-component instructional model and Alice are proposed for initial programming learning and results suggested that the use of Alice in programming learning has the positive effects.

The transition from visual to textual languages is another main concern of introductory programming [27]. In a landmark study [28], Alice is critically analysed. The study described that drag and drop feature in Alice separates the learning of syntax from comprehending the semantics. It is also identified that Alice rises the confidence, but this confidence vanished when students shifted from Alice to the traditional text-based languages. It is widely believed that visual tools help novice students in the initial stages, but these tools should not be assumed as a universal panacea [29].

Bakar et al. [30], proposed a VJava module which includes submodules comprised of multiple sections that cover the elementary areas of programming. MJava library is included in a module that permits the computer programs to construct visual outputs. The contents, design and usability aspects of VJava are corroborated with the experts' validation process.

In [31], the impacts of exercises-only approach with lectures combined with exercises in introductory programming was compared. The study reported that both methodologies are fruitful in introductory programming, but the exercise-only approach is more effective than the other approach. The study also identified that prior programming knowledge and grade expectation are important antecedents of learning performance in programming.

Malik et al. [32], developed an application called PROBSOL to increase the skills of beginners in the introductory courses of programming. PROBSOL is centered on pseudo code techniques and supports web application and mobile app which is available from Google store. The application of PROBSOL showed that their use promotes students' engagement, logic and problem solving skills. However, the mobile based framework is recommended by novices over the web based dialect.

The CS0 is a doable methodology to prepare the novices for the introductory courses in programming. The CS0 courses provide a system for novices to get a background which is essential for CS1 [33]. The CS0 course is offered as a pre-programming course with no explicit prerequisites. The majority of CS0 courses use programming tools to introduce the novice students to the introductory concepts of computer programming.

In [34], a CS0 course for students has introduced. The course embraces GameMaker and C# to introduce programming and covers elementary topics like sequences, operators, conditions, loops, arrays and functions. The prime goal was to attract the students and provide them with an elementary knowledge of computer programming. The views received from learners reported that pedagogy is helpful to prepare students for real programming.

Dyne and Braun [35] define and evaluated a course that supports methods and techniques for resolving problems and critical reasoning to aid beginners with the essentials required for successfully completing CS1. The preliminary results of inducting the course are very reasonable in improving students' academic outcomes.

Uludag proposed a course that used web application development environment, Lego Mindstorms with block-based language and aimed to support the students in programming courses and initially found very effective in learning the introductory programming [36].

Haungs et al. [37] introduced a CS0 course that covers multiple tracks that students can select (for example, gaming, mobile apps and music,

robotics). This allows the beginners to comprehend the fundamental of programming and teamwork.

Gudmundsen et al. [38], introduced a CS0 course for introductory programming. The course covers Visual Logic in first stage and then switched to Python. The initial results are reasonably encouraging in increasing the performance and commitment of students.

Naveed and Sarim [39] defined an algorithmic style programming language and introduced before the CS1 to illuminate the beginners about the fundamental concepts of novice programming. The language is very similar to natural language based algorithmic description. It also supports the generation of equivalent source programs in Python, Java, C++ and C from the input source program. The initial application of LPL is very encouraging in increasing students' performance and retention rate.

Dawson et al. [40], developed a CS0.5 course to improve students' attitude, satisfaction and achievement in CS1. The course was offered as a unified and reduced-face interval course. The students' were assigned pre-class work comprising of reading material and problem solving using new notions. Students' feedback revealed that the designed course successfully improved students' outcomes. Similarly, Wood et al. [41] conducted a very comprehensive study by comparing different pedagogical approaches of precursor courses and reported that CS0 has a productive impact on students' attitudes and performance.

3. DESIGN AND METHODS

The novice students without some previous understanding of programming need to equipped with methods to resolve the problem and employ a computer programming language as a framework to attempt the problem concurrently [42]. These manifold preconditions naturally increase the cognitive load [43] and for that reason, the first course on programming frequently necessities to introduce platform for novice students.

In this research, a CS0 course for novice students of CS1 has proposed and its effectiveness is investigated as it is widely accepted that CS0 course

is a crucial element of education [44]. Principally, the proposed CS0 does not refute the prevailing precursor courses, but solely mingle their coherent elements in an innovative fashion. The central aim of the proposed course is to support novice students by providing prior knowledge of programming and improve their academic outcomes in a first course on programming. The proposed CS0 is based on two-phase learning and equipped with a collaboration strategy. In two-phase learning the fundamentals of programming are introduced to students in two stages.

In the first phase of the proposed course, the novices are introduced to elementary theories of foundational programming without compelling them to concentrate on the rigid structure of languages because adjourning actual in introductory level would provide fair learning opportunity to students [45]. This phase merely presents the plain concepts of novice programming. So in the first phase, the fundamental concepts of programming are introduced through the visual language which is unanimously recognized as a feasible approach to engage and support the students.

The visual language offered in the first phase of a proposed CS0 presents the basics of programming by representing the difficult theories with graphical support and fostering their enthusiasm but presenting no actual familiarity with concrete programming. Klassen [46] defined that graphical language like Alice in CS0 is not enough to prepare the students for CS1. So CS0 must involve actual programming and should follow a meticulous approach.

The second phase of proposed CS0 presents the elementary concepts with a text-oriented language. The text-based platform is recognized as an operational podium for novice students to explicitly deal with actual computer programming [47]. In [48], it is identified that the algorithmic approach is desirable to foundational programming. So, the second phase is designed to cover the programming with easy, clear and self-explanatory statements like in Python.

Students commonly encounter nervousness while learning programming; so in a proposed CS0, the novices are persuaded to work in a pair as it is positive for students and may increase their academic outcomes. Pair programming has been found very effective in introductory programming courses [49, 50] and in other academic courses [51].

The extensive examination of the literature revealed that several ways have been introduced to address the difficulties of introductory programming. Table 1 compares some of the most notable methods for introductory programming courses.

Several solutions have been suggested to overcome the challenges of beginning programming, according to the discussion in Table 1. Each method provided is focused on a certain domain and programming language. The significance of beginning programming cannot be overlooked, as it is a requirement for pursuing higher level courses [59].

4. RESULTS

In order to ascertain the actual effectiveness of proposed CS0 course a small study is conducted. The study analyzed the impact of using the two-phase CS0 course in improving the academic achievement of novices in the first course on programming.

During the study 148 students have participated which are randomly clustered into four groups. To the first group, no CS0 course is offered before offering the first course on programming. Python is introduced as a CS0 to a second group, Blockly is offered to a third group, whereas the proposed CS0 is offered to the fourth group of a study. Blockly is used in the first phase, Blockly is a visual block language that enables the rapid creation of programs. In introductory programming environments, block-based programming has proven popular for teaching programming to young students. Blockly has been recognized as a valuable tool for improving students' coding skills and changing their attitudes about programming. Python is used in the second phase of a proposed CS0 course

The study was performed on the undergraduate students of computer science in 2018 and the subjects voluntarily contributed in the study. All the learners declare that they have no previous acquaintance of actual programming.
Later, a course on programming is offered as a CS1

Table 1. Comparison of Programming Environments & Approaches

Sr. No.	Environment + Approaches	Merits & Demerits
1	Visual Languages	A visual programming language is one that allows to create programs using graphical elements and images. Visual languages increased learners' knowledge of basic programming principles while also increasing their self-efficacy [52,53]. In visual languages the learners are relieved from the burden of difficult syntax. When a learner transitions from a visual language to a real language with intricate syntax, their experience with visual languages frequently diminishes.
2	Learners Programming Language	The complexity of programming languages is exacerbated by the complicated and peculiar syntax of programming languages. A simple syntax-based programming language has been introduced that supports algorithmic type constructs for program development. The majority of them are still in the early stages of development and are only helpful in learning a limited number of programming languages [39].
3	Blended Learning	Blended learning is a form of teaching that blends conventional place-based classroom methods with online educational materials and chances for online participation. Several studies have sought to use blended skills to develop their students' performance in beginning programming courses [54]. Although the technique has proven to be quite efficient, it does necessitate regular hardware support for utilizing online teaching content, which is almost impossible in every educational system.
4	Didactic Strategies	To make programming easier for novices, several didactic strategies are introduced. The strategies often included approaches and techniques such as preceding courses, use of doodles, and pair programming [55]. These tactics are usually developed for a specific sort of programming course and a specific group of students or learning environment.
5	Intelligent Tutoring System	Intelligent tutoring is a smart learning method designed to improve student scores, pass rates, and teacher efficiency. Over multiple academic years, a set of technology-based instructional practices was adopted in an introductory programming course, and the data demonstrate that the grade distributions have significantly improved [56]. However, most of the experimental studies on intelligent tutoring systems are conducted on a small number of subjects. It is widely observed that supplemental assistance in intelligent tutoring simply increases learners' cognitive load.
6	Descriptive Errors Presentation	The difficulty of debugging source programs has an impact on a novice's ability to learn programming. In development environments, descriptive error messages are used to make debugging easier. However, it was discovered that the simplicity of error messages has a significant impact on debugging score, but there is no association between debugging and programming scores [57].
7	Gamification	Different studies have demonstrated the educational benefits of digital gaming. The adaptation of game characteristics to non-game environments is referred to as gamification. Various studies have demonstrated that when used correctly, gamification may establish a learning environment and lead to significant improvements in students' interest in programming. However, according to a study on the impact of gamification on programming, gamification does not improve students' performance while increase their engagement [58].

by a same team of instructors to all the groups of study and C language is covered during the course. In all groups the same teaching methodology, material and programming environments are followed.

After the completion of CS1 all subjects are internally evaluated and results are shown in Table 2.

High mean marks are observed in the fourth group (pass rate = 61%), followed by a third group (pass rate = 49%), third second group (pass rate= 41%) and first group (pass rate= 36%), respectively. The mean score of each group in a study can be analyzed with a mean plot shown in Fig. 1.
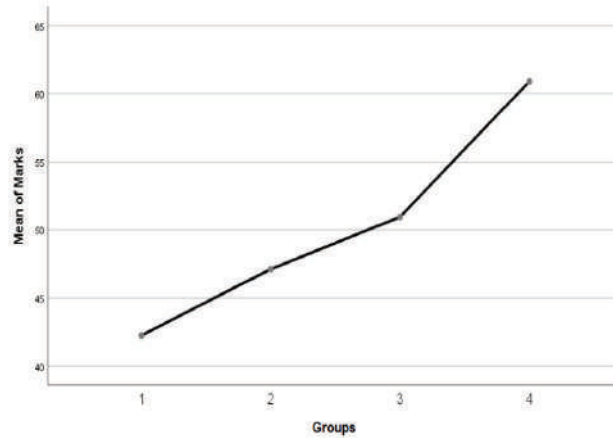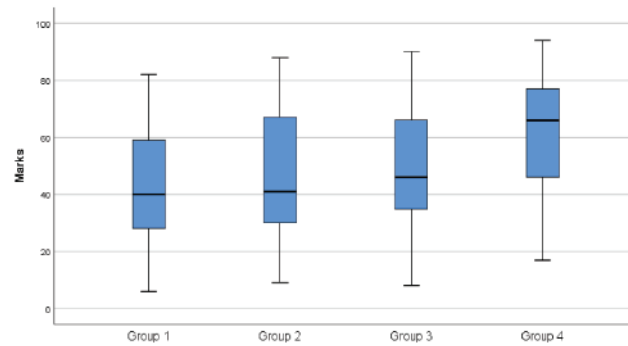
Fig 1. Mean plot of marks

Fig 2. Box plot of marks

The mean plot shown in Fig. 1 illustrates how the mean of score varies across different groups in a study and the least mean score is observed in the first group and the highest mean score in the fourth group. Fig. 2 shows the boxplot of the marks obtained by the groups involved in the study.

The median, minimum and maximum marks illustrated in the box plot declare the fourth group as highest and the first group being the last in securing the marks in the first programming course and the second and third groups' lies among them.

For further analysis, the normality tests were conducted on the score of students and results are shown in Table 3.

Kolmogorov-Smirnov test indicates that the mark secured by all groups of study follows a normal distribution. Similarly, the Shapiro-Wilk test shows that secured scores of all the involved groups in a study follows a normal distribution.

For better illustration a normal probability (Q-Q) plot of the marks is shown Fig. 3 and depicted the distribution of data against the expected normal distribution.

Table 2. Score of students in CS1

Groups	Mean	Std. Deviation	Std. Error	Min	Max
1	42.24	20.55	3.38	6	82
2	47.11	21.29	3.50	9	88
3	50.95	20.76	3.41	8	90
4	60.89	20.62	3.39	17	94

Table 3. Normality test on the score of students in CS1

Groups	Kolmogorov-Smirnov			Shapiro-Wilk		
	Statistic	df	Sig.	Statistic	df	Sig.
1	0.090	37	.200	0.974	37	0.542
2	0.126	37	0.143	0.954	37	0.127
3	0.108	37	.200	0.975	37	0.573
4	0.138	37	0.071	0.954	37	0.125

A one-factor analysis of variance (ANOVA) was conducted on all groups of study and the results showed that there was a significant difference between study groups in a first programming course remembered at the $p < 0.05$ for the conditions $[(3,144) = 5.347, p = 0.002]$.

Concerning the students' retention, the study assessed their responses to the following questions: "In next semester semester, I am willing in another course on programming". Subjects replied on 5-item Likert scale and the results are illustrated in

Fig. 4.

The study revealed that high interest in another course on programming is observed in those students who have attended a two-phase CS0 course before the CS1. For further analysis a Kruskal–Wallis H test is conducted on the feedback of subjects and results are shown in Table 4.

The fourth group is identified as top with highest mean value, followed by group two, three and one respectively. The significant differences
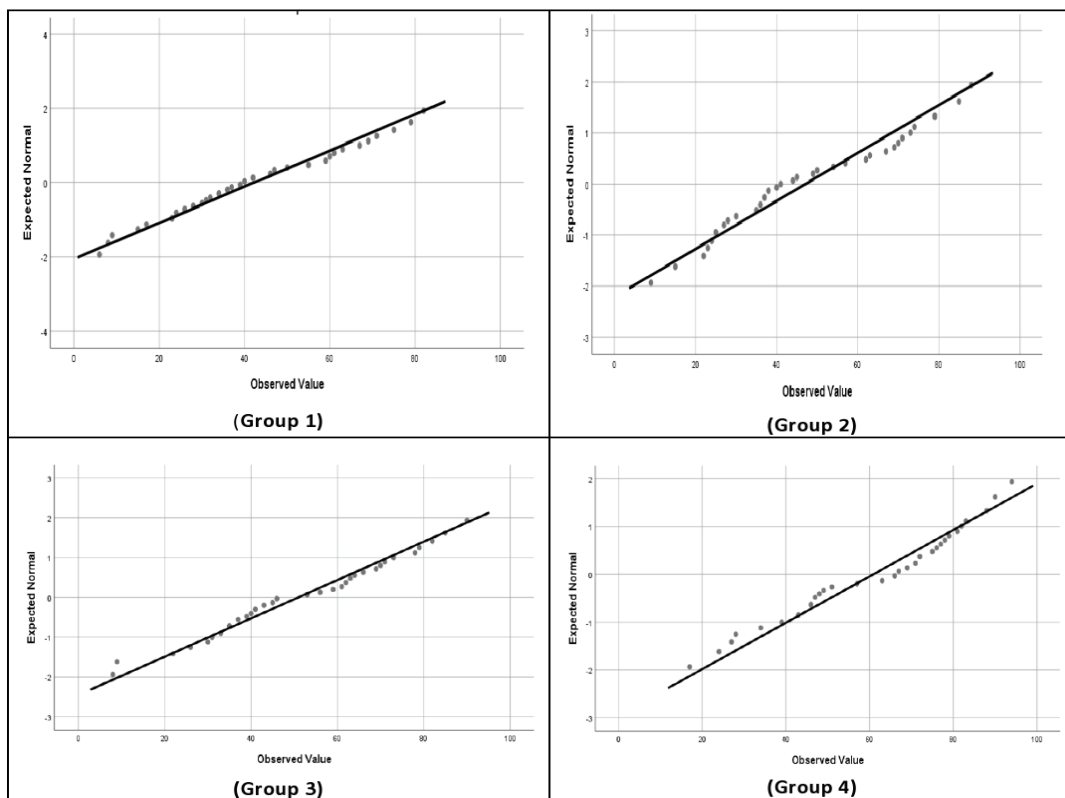
Fig 3. Normal Q-Q Plot of Groups
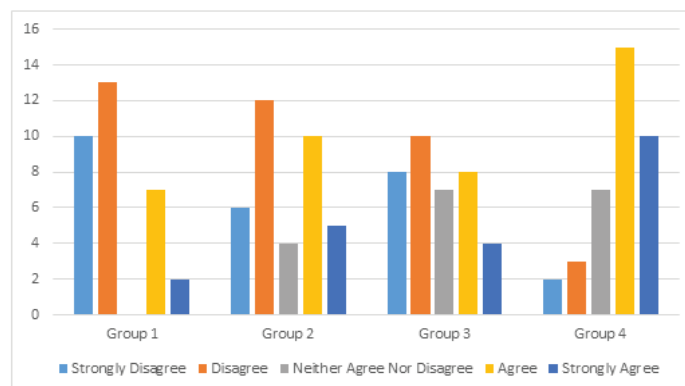
Fig 4. Students' willingness in another course on programming

Table 4. Ranks of groups in study

Group	Size	Mean Rank
1	37	57.70
2	37	72.86
3	37	67.76
4	37	99.68

Table 5. Comparison of learning strategies for CS1

S.No	Study	Method	Results
1	Seraj et al. [25]	Comparative analysis of Scratch and Blockly	Scratch is more helpful than Blockly, $F(1,22) = 28.02$, $p < 0.001$
2	Bakar et al. [30]	Expert validation Process.	VJava module is confirmed suitable, with score ranged from 3.67 to 5.00 on 5-point Likert scale.
3	Zhang et al. [31]	Comparative analysis of two teaching approaches	The exercise only approach is more useful than lectures combined with exercises in introductory programming, $df = 34$, $t = 2.320$, $p < 0.05$
4	Malik et al. 2019 [32]	Development and application of pseudocode-based application with two modes, web-based and mobile-based	3% of positive improvement in higher category as well as in medium achiever category
5	Panitz et al. [34]	Survey and feedback from students	GameMaker and C# based CS0 is effective in attracting and preparing students for programming
6	Naveed et al. [39]	Comparative analysis of different precursor courses	Textual programming language with the support of high-level source code generation is supportive to prepare novices for CS1
7	Dawson et al. [40]	Survey and appreciative inquiry	CS 0.5 is helpful to improve the students' outcome in CS1 and increased their personal interest: $t(515.0) = 8.96$, $p < 0.001$
8	Wood et al. [41]	Comparative study of pedagogical methods in CS0	CS0 course is helpful in CS1 yet no pedagogical method in CS0 is better than other methods, p-value = 0.449
9	Parham-Mocello et al. [45]	Comparative analysis of code-first versus using stories	Using stories is useful in introductory programming, especially for females, with 95% confidence, $\alpha <= .05$
10	Proposed CS0	Comparative analysis of different pattern of CS0 courses.	Two-phase CS0 is more helpful than single language based CS0 and also fruitful in preparing students for CS1, $F = 5.35$, $df = 3$, $p = .002$

(Kruskal-Wallis = 20.404, $p < .05$, $df = 3$) were found among the four groups of study.

5. DISCUSSIONS

An important aspect of introductory programming courses is the development of a good way of thinking [60]. This article presents a two-phase learning technique that is accompanied by a cooperation strategy.

These results suggested that the amalgamation of graphical and textual environment in CS0 is better than using a single environment-based CS0 course. Moreover, the two-phase CS0 course is more useful in improving the performance of students in CS1 as well as by increasing their retention in the other course of programming.

The results obtained from the initial evaluation of two-phase CS0 are further compared with other studies and the results are shown in Table 5.

The results illustrated in Table 4 opined that the proposed CS0 course is quite fruitful and supportive in increasing the academic outcomes of novices

in a first course on programming and therefore comparable with other topical strategies.

The novelty of proposed CS0 resides in an amalgamated approach that unified the two modes of programming systems in a single precursor course with an agile collaboration strategy to prepare the novices for the first course on programming. The statistical significance of initial evaluation suggests the viability of the proposed course. To our knowledge, none of any study has been conducted or at least reported on the subjects of Pakistan.

6. CONCLUSIONS

The first course on programming is infamously complex for novice students. These complexities are typically exhibited in the form of weak performance and low rates in retention. In this article two-phase CS0 is introduced to boost the academic achievements of novice students in a first course on programming.

The proposed course is initially evaluated and preliminary results suggested that the lack of previous knowledge of programming is one of a main reason behind the hardness of introductory programming. Likewise, a CS0 course that introduced elementary programming without forcing the students to understand the grammar of a specific programming language and then introduce the concepts of programming with a simple textual programming is a suitable methodology to prepare students for a first course on programming and ultimately improve their performance and retention. However, in current form, the study has several limitations. First, the sample size is not very large and the subjects in each group of the study are randomly selected. Second, the impact of CS0 is evaluated on the performance of students in CS1, but not in the subsequent programming courses. Third, the demographic parameters of students are not considered during the analysis.

7. ACKNOWLEDGEMENTS

8. REFERENCES

1. J. O'Kelly, and J. P. Gibson. RoboCode & Problem-based Learning: A Non-prescriptive Approach to Teaching Programming. *ACM SIGCSE Bulletin* 38(3): 217-221 (2006).

2. M. V. McCracken., D. D. Almstrum., M. Guzdial., D. Hagan., Y. B. Kolikant., C. Laxer., L. Thomas., I. Utting, and T. Wilusz. A Multi-national, Multi-institutional Study of Assessment of Programming Skills of First year CS Students. *ACM SIGCSE Bulletin* 33(4):125-180 (2001).

3. B. Sabitzer, and S. Pasterk. Brain-based programming continued: Effective teaching in programming courses. *Proceedings of IEEE Frontiers in Education Conference*: 1-6 (2014).

4. C. Ott. Decoding Feedback: Improving feedback practices for students in introductory programming courses. *PhD thesis*, University of Otago, Dunedin, New Zealand: (2014).

5. S. M. Taheri., M. Sasaki, and H. T. Ngetha. Evaluating the Effectiveness of Problem Solving Techniques and Tools in Programming. *Proceedings of Science and Information Conference:* 928-932 (2015).

6. A. Sen. Using Code Analysis Tool in Introductory Programming Class. *Issues in Information Systems* 15(1): 1-10 (2014).

7. A. Ali, and D. Smith. Teaching an Introductory Programming Language in a General Education Course. *Journal of Information Technology Education: Innovations in Practice* 13: 57-67 (2014).

8. G. Gárcia-Mateos, and J. L. Fernández-Alemán. A Course on Algorithms and Data structures using On-line Judging. *ACM SIGCSE Bulletin* 41(3):45-49 (2009).

9. M. Brown., C. Hu., C. Burch, and M. Nooner. CS0: Why, What, and How?: Panel Discussion. *Journal of Computing Sciences in Colleges* 25 (5):79-81 (2010).

10. K. Howell. First Computer Languages. *Journal of Computing Sciences in Colleges* 18(4):317-331 (2003).

11. A. Riker. Natural Language in Programming An English Syntax-based Approach for Reducing the Difficulty of First Programming Language Acquisition. *Master's thesis,* Department of Computer Science, Graduate School of Arts and Sciences, Brandeis University: (2010).

12. M. Konecki. Introductory Programming Education

for Visually Impaired. *International Journal of Research in Engineering and Technology* 3(17): 65-70 (2014).

13. K. Price, and S. Smith. Improving Student Performance in CS1. *Journal of Computing Sciences in Colleges* 30(2): 157-163 (2014).

14. A. Settle., A. Vihavainen, and J. Sorva. Three Views on Motivation and Programming. *Proceedings of the 2014 Conference on Innovation & Technology in Computer Science Education*: 321-322 (2014).

15. A. Robins. Learning edge momentum: a new account of outcomes in CS1. *Computer Science Education* 20(1): 37-71 (2010).

16. R. H. Sloan, and P. Troy. CS 0.5: A Better Approach to Introductory Computer Science for Majors. *ACM SIGCSE Bulletin* 40(1): 271-275 (2008).

17. A. Robins. Novice programmers and introductory programming, *S. A. Fincher & A. V. Robins (Eds.), the Cambridge Handbook of Computing Education Research. Cambridge, UK: Cambridge University Press*: 327-376 (2019).

18. P. Y. Amoako., K. A. Sarpong., J. K. Arthur, and C. Adjetey. Performance of Students in Computer Programming: Background, Field of Study and Learning Approach Paradigm. *International Journal of Computer Applications* 77(12): 17-21 (2013).

19. L. M. Serrano-Camara., M. Paredes-Velasco., C. Alcover, and J. A. Velazquez-Iturbide. An evaluation of students motivation in computer supported collaborative learning of programming concepts. *Computers in Human Behavio*r 31: 499-508 (2014).

20. R. Anderson., M. D. Ernst., R. Ordonez., P. Pham, and S. A. Wolfman. Introductory Programming Meets the Real World: Using Real Problems and Data in CS1. *Proceedings of the 45th ACM Technical Symposium on Computer Science Education, pages*: 465-466 (2014).

21. U. Nikula., O. Gotel, and J. Kasurinen. A Motivation Guided Holistic Rehabilitation of the First Programming Course. *ACM Transactions on Computing Education* 11(4): 24:1-24:38 (2011).

22. A. Tafliovich., J. Campbell, and A. Petersen. A Student Perspective on Prior Experience in CS1. *Proceeding of the 44th ACM Technical Symposium on Computer Science Education*: 239-244 (2013).

23. K. Al-Tahat. The Impact of a 3D Visual Programming Tool on Students' Performance and Attitude in Computer Programming: A Case Study in Jordan. *Journal of Cases on Information Technology* 21(1): 52-64 (2019).

24. A. Marron., G. Weiss, and G. Wiener. A Decentralized Approach for Programming Interactive Applications with JavaScript and Blockly. *Proceedings of the 2nd Edition on Programming Systems, Languages and Applications Based on Actors, Agents, and Decentralized Control Abstractions*: 59-70 (2012).

25. M. Seraj., E. Katterfeldt., K. Bub., S. Autexier, and R. Drechsler. Scratch and Google Blockly: How Girls' Programming Skills and Attitudes are Influenced. *Proceedings of the 19th Koli Calling International Conference on Computing Education Research*: 1-10 (2019).

26. J. M. Costa, and G. L. Miranda. Using Alice Software with 4C-ID Model: Effects in Programming Knowledge and Logical Reasoning, *Informatics in Education* 18(1): 1-15 (2019).

27. Y. Matsuzawa., T. Ohata., M. Sugiura, and S. Saka. Language Migration in non-CS Introductory Programming Through Mutual Language Translation Environment. *Proceedings of the 46th ACM Technical Symposium on Computer Science Education:* 185-190 (2015).

28. K. Powers., S. Ecott, and L. M. Hirshfield. Through the Looking Glass: Teaching CS0 with Alice. *ACM SIGCSE Bulletin* 39(1):213-217 (2007).

29. A. Stefik, and S. Siebert. An Empirical Investigation into Programming Language Syntax. *ACM Transactions on Computing Education* 13(4): 19:1-19:40 (2013).

30. M. A. Bakar., M. Mukhtar, and F. Khalid, The Development of a Visual Output Approach for Programming via the Application of Cognitive Load Theory and Constructivism. *International Journal of Advanced Computer Science and Applications* 10(11): 305-312 (2019).

31. X. Zhang., C. Zhang., T. F. Stafford, and Ping Zhang. Teaching Introductory Programming to IS Students: The Impact of Teaching Approaches on Learning Performance. *Journal of Information Systems Education* 24(2): 147-155 (2013).

32. S. I. Malik., R. Mathew., R. Al-Nuaimi., A. Al-Sideiri, and J. Coldwell-Neilson. Learning problem solving skills: Comparison of E-learning and M-learning in an introductory programming course. *Education and Information Technologie*s 24: 2779-2796 (2019).

33. C. Farrell. Predicting (and Creating) Success in CS1. *Issues in Information Systems* 7(1): 259-263 (2006).

34. M. Panitz., K. Sung, and R. Rosenberg. Game Programming in CS0: A Scaffolded Approach. *Journal of Computing Sciences in Colleges* 26(1):

126-132 (2010).

35. M. V. Dyne, and J. Braun. Effectiveness of a Computational Thinking (CS0) Course on Student Analytical Skills. *Proceedings of the 45th ACM Technical Symposium on Computer Science Education*: 133-138 (2014).

36. S. Uludag., M. Karakus, and S. W. Turner. Implementing IT0/CS0 with Scratch, App Inventor For android, and Lego Mindstorms. *Proceedings of the 2011 Conference on Information Technology Education*: 183-190 (2011).

37. M. Haungs., C. Clark., J. Clements, and D. Janzen. Improving First-year Success and Retention Through Interest-based CS0 Courses. *Proceedings of the 43rd ACM Technical Symposium on Computer Science Education*: 589-594 (2012).

38. D. Gudmundsen., L. Olivieri, and N. Sarawagi. Using Visual Logic: Three Different Approaches in Different Courses - General Education, CS0, and CS1. *Journal of Computing Sciences in Colleges* 26(6): 23-29 (2011).

39. M. S. Naveed., M. Sarim, and K. Ahsan. Learners Programming Language a Helping System for Introductory Programming Courses. *Mehran University Research Journal of Engineering & Technology* 35(3): 347-358 (2016).

40. J. Q. Dawson., M. Allen., A. Campbell, and A. Valair. Designing an Introductory Programming Course to Improve Non-Majors' Experiences. *Proceeding of 49th ACM Technical Symposium on Computer Science Education*: 26-31 (2018).

41. Z. J. Wood., J. Clements., Z. Peterson., D. Janzen., H. Smith., M. Haungs., J. Workman., J. Bellardo, and B. DeBruhl. Mixed Approaches to CS0: Exploring Topic and Pedagogy Variance After Six Years of CS0. *Proceedings of the 49th ACM Technical Symposium on Computer Science Education*: 20-25 (2018).

42. S. Mishra., S. Balan., S. Iyer, and S. Murthy. Effect of a 2-week Scratch Intervention in CS1 on Learners with Varying Prior Knowledge. *Proceedings of the 2014 Conference on Innovation & Technology in Computer Science Education*: 45-50 (2014).

43. J. J. Merrienboer, and J. Sweller. Cognitive load theory and complex learning: Recent developments and future directions. *Educational Psychology Review* 17(2): 147-177 (2005).

44. T. Babbitt., C. Schooler, and Kyle King. Punch Cards to Python: A Case Study of a CS0 Core Course. *Proceedings of the 50th ACM Technical Symposium on Computer Science Education*: 811-

817 (2019).

45. J. Parham-Mocello., M. Erwig, and E. Dominguez. To Code or Not to Code? Programming in Introductory CS Courses. *Proceeding of IEEE Symposium on Visual Languages and Human-Centric Computing*: 187-191 (2019).

46. M. Klassen. Visual Approach for Teaching Programming Concepts. *Proceedings of the 9th International Conference on Engineering Education*: M4H-5-M4H-10 (2006).

47. V. Isomoottonen., A. Lakanen, and V. Lappalainen. K-12 Game Programming Course Concept Using Textual Programming. *Proceedings of the 42nd ACM Technical Symposium on Computer Science Education*: 459-464 (2011).

48. R. Garlick, and E. C. Cankaya. Using Alice in CS1: A Quantitative Experiment. *Proceedings of the Fifteenth Annual Conference on Innovation and Technology in Computer Science Education*:165-168 (2010).

49. L. Jarratt., N. A. Bowman., K. C. Culver, and A. M. Segre. *Proceedings of the 2019 ACM Conference on Innovation and Technology in Computer Science Education*: 176-181 (2019).

50. M. Ayub., O. Karnalim., R. Risal., W. F. Senjaya, and M. C. Wijanto. Utilising pair programming to enhance the performance of slow-paced students on introductory programming. *Journal of Technology and Science Education* 9(3): 357-367 (2019).

51. M. S. Naveed, and M. Sarim. Didactic Strategy for Learning Theory of Automata & Formal Languages, Pakistan Academy of Sciences, *A. Physical and Computational Sciences* 55 (2): 55–67 (2018).

52. C. Tsai. Improving students' understanding of basic programming concepts through visual programming language: The role of self-efficacy, *Computers in Human Behavior* 95: 224-232 (2019).

53. M. Noone, and A. Mooney. Visual and textual programming languages: a systematic review of the literature, *Journal of Computers in Education* 5: 149-174 (2018).

54. M. N. Demaidi, M. Qamhieh, and A. Afeefi. Applying Blended Learning in Programming Courses, *IEEE Access* vol. 7: 156824-156833, (2019).

55. M. S. Naveed, M. Sarim, and A. Nadeem. C in CS1: Snags and Viable Solution, *Mehran University Research Journal of Engineering & Technology* 37(1): 1-14 (2018).

56. J. Figueiredo, and F. J. García-Peñalvo. Intelligent Tutoring Systems approach to Introductory

Programming Courses. *Proceedings of the Eighth International Conference on Technological Ecosystems for Enhancing Multiculturality*: 34-39 (2020).

57. M. S. Naveed, and M. Sarim. Analyzing the Effects of Error Messages Presentation on Debugging and Programming, *Sukkur IBA Journal of Computing and Mathematical Sciences* 4(2): 38-48 (2020).

58. S. Papadakis, and M. Kalogiannakis. Using Gamification for Supporting an Introductory Programming Course. The Case of ClassCraft in a Secondary Education Classroom, *Lecture Notes of the Institute for Computer Sciences, Social Informatics and Telecommunications Engineering* 229: 366-375 (2018).

59. U. Omer, M. S. Farooq, and A. Abid. Introductory programming course: review and future implications, *PeerJ Computer Science* 7: e647 (2021).

60. T. Teodosiev, and A. Nachev, Some Pitfalls in Introductory Programming Courses. *Informatics in Education* 11(2): 241-255 (2012).

Pakistan Academy of Sciences

Research Article

Advanced Multi-Modeling of PWR Dynamics and Deep Learning based Computational Tool in SIMULINK and LabVIEW

Arshad H. Malik[1*], Aftab A. Memon[2], and Feroza Arshad[3]

[1]Department of Maintenance Training, Pakistan Atomic Energy Commission, A-104, Block-B, Kazimablad, Model Colony, Karachi, Pakistan
[2]Department of Telecommunication Engineering, Mehran University of Engineering and Technology, Jamshoro, Sindh, Pakistan
[3]Department of Management Information System, Pakistan Atomic Energy Commission, B-63, Block-B, Kazimablad, Model Colony, Karachi, Pakistan

Abstract: The reactivity monitoring, prediction, and investigation is the most important parameter to ensure the safety and reliable operation of a nuclear power plant. This parameter is gained further importance in Pressurized Water Reactor (PWR) due to more sophisticated reactivity insertion mechanisms and innovative reactor core fuel loading scheme. Based on deterministic internal and external dynamics and neutronics analysis of Advanced PWR, all the reactivity feedback effects such as Doppler effect, moderator effect, control rod effect, liquid boron effect and reactor poisons effect are investigated, modeled and stochastically optimized using deep artificial intelligence. Advance Pressurized Water Reactor (APWR) of 600 MWe rating (AP-600) is used as a reference reactor model and based on the dynamics of AP-600, an Advanced Pressurized Water Reactor Dynamics and Intelligent Stochastic Optimization based Deterministic Neutronics Simulation (APD-ISO-DNS) Code is developed in the hybrid SIMULINK and LabVIEW environments. AP-600 reactor model is fine-tuned and adjusted for 300 MWe PWR (P-300) and 1070 MWe Advanced Chinese PWR (ACP-1000) using neutronics parameters and operational dynamic data of operating PWR nuclear power plants in Pakistan. Various load reduction transient experiments are conducted and dynamic transient simulations of P-300, AP-600 and ACP-1000 are evaluated in SIMULINK and in LabVIEW environments and found as per design basis.

Keywords: Multi-Model PWR Dynamics, Deterministic Reactor Neutronics, Deep Stochastic Optimization, Artificial Intelligence, Hybrid Simulation

1. INTRODUCTION

In this research work, a Pressurized Water Reactor (PWR) dynamics and neutronics are considered for state-of-the-art code development for P-300, AP-600 and ACP-1000.

A reactor dynamics model is developed based on the Point Reactor Kinetics Model (PRKM) with sixprecursor groups, internal reactivity feedbacks, and control rod reactivity [1]. The PRKM model with all internal and external reactivity feedbacks are models in [2]. This model is comprehensive and used for full fuel cycle modeling of nuclear reactor.

The PWR dynamics are further appended with decay heat for simulator development [3]. The practical aspects of 600 MWe PWR dynamics and neutronics for analyzer development for educational purposes are explored by micro simulation technology in [4]. A TRIGA research reactor and AP1000 PWR dynamics are evaluated for accident analysis in [5]. A TRIGA research reactor and VVER1000 PWR dynamics are evaluated for safety and transient accident analysis in [6]. The thermal hydraulics modeling of AP1000 PWR dynamics is carried out in RELAP code and compared with AP1000 using PCTRAN in [7]. A data driven ANN based PHWR dynamics is modeled with moderator level

---

reactivity and control rod reactivity feedbacks in [8]. A fuzzy multi-model PWR dynamics is modeled for different power levels using control rod reactivity feedback in [9]. A research reactor PRKM neutronics is modeled and simulated with control rod reactivity feedback using LabVIEW in [10]. Further research is carried out in which web-based Graphical User Interface (GUI) is developed for PWR RELAP code in LabVIEW in [11]. A 3D neutron diffusion code for PWR fuel depletion and burn-up analysis is developed in [12]. A modelling approach using Deep Artificial Neural Network (DANN) optimized by a stochastic decent gradient algorithm is identified in [13]. Further research is carried out in [14, 15] in which deterministic data driven models are developed using PID based stochastic decent gradient optimizers. In [16], a hybrid simulation platform of MATLAB and LabVIEW is used to develop ANN models.

In this research work, a novel state-of-the-art hybrid simulation platform of Simulink and LabVIEW is used for designing, deterministic modeling, fine-tuning and Improved Stochastic Gradient Decent (ISGD) with Momentum (ISGD-M) based Optimization of Advanced Multi-PWR Dynamics and Neutronics of P-300, AP-600 and ACP-1000 for APD-ISO-DNS Code development. Therefore, this research work is one step ahead in the direction of advanced PWR dynamics and neutronics with most modern improved stochastic optimization used, for the first time, in nuclear industry. The proposed hybrid code is robust against parametric uncertainties and a highly accurate tool for advanced PWR dynamics and neutronics studies and nuclear reactor analysis, emphasising fuel cycle modelling of nuclear reactors.

2. MATERIALS AND METHODS

2.1 PWR Reactor Dynamics

There are hundreds of fission fragments in PWR, but 24 fission fragments or precursors are considered of comparable half-lives. Nuclear reactor kinetics is concerned with time dependent reactor power behavior caused by precursor concentration changes while the nuclear reactor dynamics is concerned with reactor power transients in which reactivity feedbacks caused by reactivity changes due to the

power change plays a vital role in over-all reactor behaviour.

2.2 Deterministic Modeling PWR Reactor Dynamics and Neutronics

The study of reactor kinetics and reactor dynamics is known as reactor neutronics.

In reactor core, reactor power is generated 93% by nuclear fission and 7% by decay heat, which can be modeled as [3]:

$$P(t) = P_{Fission}(t) + P_{Decay}(t) \tag{1}$$

Fission power is produced by fission fragments using multiple precursor groups. Fission power computed for six precursor groups is reported in [2], which is appended for 24 precursor groups in this research work as:

$$\frac{dP_{Fission}(t)}{dt} = \frac{\rho(t) - \beta}{\Lambda} P_{Fission}(t) + \sum_{m=1}^{24} \lambda_m C_m(t) \tag{2}$$

$$\frac{dC_m(t)}{dt} = \frac{\beta_m}{\Lambda} P_{Fission}(t) - \lambda_m C_m(t) \tag{3}$$

Where the symbols having their usual meanings.

Therefore, 25th order coupled reactor kinetics model is developed for short time scale modeling of nuclear reactor.

Decay heat is calculated using three decay product groups, which is calculated as [3]:

$$P_{Decay}(t) = \phi_T - \sum_{n=1}^{3} (\gamma_n \phi_T - D_n(t)) \tag{4}$$

$$\frac{dD_n(t)}{dt} = \lambda_n (\gamma_n \phi_T - D_n(t)) \tag{5}$$

Where the symbols having their usual meanings.

The decay heat is used to calculate fuel and moderator temperatures. Therefore, 4th order coupled decay heat model is developed.

The heart of this research work is the sophisticated higher order coupled reactivity feedbacks model which is developed using all internal and external reactivity feedbacks taken into account.

The total reactivity is modeled as:

$$\rho(t) = \rho_{INTERNAL}(t) + \rho_{EXTERNAL}(t) \qquad (6)$$

A very complex functional formulation of total internal reactivity as a function of internal reactivity feedbacks, initial reactor Po and demanded reactor power PD, Current reactor power and transient power (rate of change of power) such that ϵ {Po, PD}is given by [2, 5]:

$$\rho_{INTERNAL}(t) = f\left(\begin{array}{l} \dfrac{dP(t)}{dt}, \dfrac{dT_F(t)}{dt}, \dfrac{dT_M(t)}{dt}, \\ \dfrac{d\rho_{Xe}(t)}{dt}, \dfrac{d\rho_{Sm}(t)}{dt}, P(t), P_0, P_D \end{array}\right) \qquad (7)$$

Where the symbols having their usual meanings.

Similarly, the very complex functional formulation of total external reactivity as a function of external reactivity feedbacks is given by [2, 5]:

$$\rho_{EXTERNAL}(t) = g\left(\begin{array}{l} \dfrac{dP(t)}{dt}, \dfrac{d\rho_B(t)}{dt}, \dfrac{d\rho_{CR}(t)}{dt}, \\ P(t), P_0, P_D \end{array}\right) \qquad (8)$$

Where the symbols having their usual meanings.

Therefore, overall, a higher order highly nonlinear dynamic model is developed for long time scale modeling of PWR reactor core.

2.3 Framework of APD-ISO-DNS Code

The Reactivity measurement and investigation is one of the challenges in PWR type nuclear power plants because the reactivity of the nuclear power reactor is not measured directly in PWRs. It is computed with dedicated nuclear reactor codes. Therefore, this research aims to design and develop an innovative computational tool for virtual total reactivity and reactivity feedback.

The analytical deterministic computational model developed for PWR transient dynamics is fine-tuned and simulated for P-300, AP-600 and ACP-1000 PWR-based nuclear power plants using plant operational data and reactor design data. Therefore, P-300, AP-600 and ACP-1000 reactor cores have higher order deterministic different

neutronics models.

The developed transient nuclear reactor model APD-ISO-DNS Code has three modules APD-ISO-DNS-300, APD-ISO-DNS-600 and APD-ISO-DNS-1000 for P-300, AP-600 and ACP-1000 PWR respectively as shown in Fig.1.
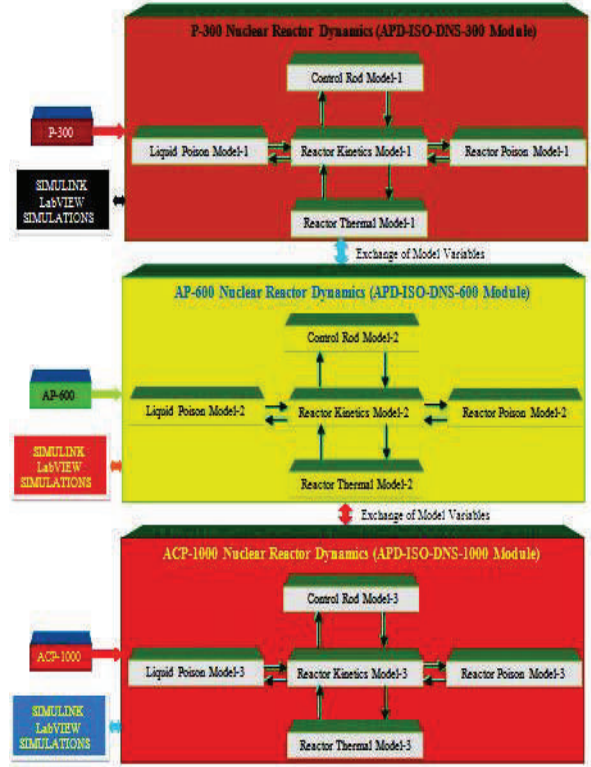
Fig. 1. Overall design of APD-ISO-DNS code.

Each module comprises four models known as reactor kinetics model, reactor poison model, liquid poison model, and control rod model. Reactor kinetics model is further composed of fission fragments dynamics and decay product dynamics. Reactor poison model is composed of Xenon and Samarium dynamics. Liquid poison model is composed of boron dynamics with different fuel conditions such as burn-up of fuel and different conditions of reactor core like Beginning of Core (BOC), Middle of Core (MOC) and End of Core (EOC) as shown in Fig. 2. Control rod model is composed of different control banks and overlapping logics.

The innovative reactor dynamics data is generated from the developed fine-tuned transient reactor dynamics models for APD-ISO-DNS-300, APD-ISO-DNS-600 and APD-ISO-DNS-1000

modules. These modules are used to design and develop an intelligent reactor dynamics code, now designated as APD-ISO-DNS Code. This code has an excellent reverse engineering capability to produce reactor power from reactivity feedback. After fine tuning, the APD-ISO-DNS code is modified to produce reactivity feedback and total reactivity directly from measured data of P-300, AP-600 and ACP-1000. The PWR neutronics tool is deterministic in nature which is optimized by stochastic technology.

2.4 Deep Artificial Intelligence

2.4.1 Concept of Deep Learning

Deep Artificial Neural Network (DANN) is an excellent intelligent tool for nonlinear pattern mapping or dataset. The term deep is used in the sense of dense or depth or more number of hidden layers with number of nodes in each hidden layer in an artificial neural network having multi-step processing. A neural network with more than three layers including input and output layer is considered for deep learning process. Deep learning is basically unsupervised learning capable to produce a highly accurate model.

2.4.2 Selection of Optimization Algorithm

Improved Stochastic Gradient Decent Momentum (ISGD-M) optimization based DANN is selected in this research work, which converges quickly and accurately. So, it is an Intelligent Stochastic Optimization (ISO) method for DANN. SGD is simply a Proportional Controller with gain KP. SGD plus Momentum term (SGD-M) is a Proportional plus Integral Controller with gains K_P and K_I. There is a problem of overshoot associated with SGD-M optimizer, which is resolved by introducing a future prediction feature through Derivative Controller with gain K_D. K_D is called hyper-parameter. Now, SDM-M with hyper-parameter is designated as ISGD-M. Therefore, a PID controller based optimization is adopted for deep ANN training known as PID optimizer for DANN, which uses past, present and change of gradient for updating DANN weights [14].

In this DANN, input is mapped with output through a parameter θ. θ(t) is the weight o PID

optimizer. DANN is a three-layer deep ANN with two hidden layers in this research work. If Wji, Wkj and Wlk are layer weights between input layer and first hidden layer, first hidden layer and second hidden layer and second hidden layer and output layer respectively, then $\theta = \{ W_{ji}, W_{kj}, W_{lk} \}$, where i, j, k and l are the number of nodes or neurons in input, first hidden, second hidden and output layers respectively [15].

The difference between the desired actual reactivity feedback as an output parameter and deep ANN output as an predicted reactivity feedback is computed through loss function or error function L. $\partial L/\partial \theta$ is called gradient. In fact, in this research work, $\partial L/\partial \theta$ is $\partial L(\theta, P(t), \dot{P}(t))/\partial \theta$ because $P(t)$ and are inputs for all reactivity feedbacks. The gradient in deep ANN is basically having the similar concept as the error $e(t)$ in PID controller.

The gradient between input layer and first hidden layer is given by:

$$e_{ji}(t) = \partial L(\theta(W_{ji}, W_{kj}, W_{lk}), (P(t), \dot{P}(t))/\partial \theta(W_{ji})$$

The gradient between first hidden layer and second hidden is given by:

$$e_{kj}(t) = \partial L(\theta(W_{ji}, W_{kj}, W_{lk}), (P(t), \dot{P}(t))/\partial \theta(W_{kj})$$

The gradient between second hidden layer and output hidden is given by:

$$e_{lk}(t) = \partial L(\theta(W_{ji}, W_{kj}, W_{lk}), (P(t), \dot{P}(t))/\partial \theta(W_{lk})$$

The gradient in deep ANN works on the principle of moving average of gradients. The concept of feedback in PID controller is basically the back propagation in deep ANN. Therefore, as long as the gradient exists, weight is updated.

Learning rate (r) is the most important parameter for deep ANN in this optimisation process. The optimal values of PID controller for DANN are $K_p = 2r$; $K_I = K_D = r$ [15]. There is one more important design parameter α, which is known as balancing factor. This balancing factor is defined between past and current gradients. The derivative gain (K_D) of PID is the most dominant parameter for stochastic optimization process.

The ideal value of hyper-parameter K_D is computed as [15]:

$$K_D = 0.5 + 0.25r + (1 + \frac{16}{9}\pi^2)\Big/r \qquad (9)$$

2.5 IntelligentModeling of PWR Dynamics and Neutronics

2.5.1 Choice of Design Matrices ,Vectors and Activation Functions for Sub DANN

Now, intelligent modeling of PWR neutronics is accomplished with DANN using stochastic optimization technique. Suppose Hjiand Hkj are the weight matrices of first and second hidden layers comprised of Wji and Wkj weights respectively. In that case, Mlk is the weight matrix of output layer comprised of Wlk weights. Bj, Bk and Bl are bias vectors of first hidden, second and output layers respectively then Ψj (.), Ψk (.) and Ψl (.) are nonlinear activation functions, linear activation function of first hidden layer, second hidden layer and output layer respectively.

2.5.2 Modeling of Sub DANN for Reactivity Feedbacks

Now, all reactivity feedbacks for six sub ISO-DANN are modeled as:

$$\rho_F(t) = \Psi_l^F [M_{lk}^F \Psi_k^F \{H_{kj}^F \Psi_j^F (H_{ji}^F (P(t), \dot{P}(t))$$
$$+ B_j^F) + B_k^F\} + B_l^F] \qquad (10)$$

$$\rho_M(t) = \Psi_l^M [M_{lk}^M \Psi_k^M \{H_{kj}^M \Psi_j^M (H_{ji}^M (P(t), \dot{P}(t))$$
$$+ B_j^M) + B_k^M\} + B_l^M] \qquad (11)$$

$$\rho_{Xe}(t) = \Psi_l^{Xe} [M_{lk}^{Xe} \Psi_k^{Xe} \{H_{kj}^{Xe} \Psi_j^{Xe} (H_{ji}^{Xe} (P(t), \dot{P}(t))$$
$$+ B_j^{Xe}) + B_k^{Xe}\} + B_l^{Xe}] \qquad (12)$$

$$\rho_{Sm}(t) = \Psi_l^{Sm} [M_{lk}^{Sm} \Psi_k^{Sm} \{H_{kj}^{Sm} \Psi_j^{Sm} (H_{ji}^{Sm} (P(t), \dot{P}(t)$$
$$+ B_j^{Sm}) + B_k^{Sm}\} + B_l^{Sm}] \qquad (13)$$

$$\rho_{CR}(t) = \Psi_l^{CR} [M_{lk}^{CR} \Psi_k^{CR} \{H_{kj}^{CR} \Psi_j^{CR} (H_{ji}^{CR} (P(t), \dot{P}(t)$$
$$+ B_j^{CR}) + B_k^{CR}\} + B_l^{CR}] \qquad (14)$$

$$\rho_B(t) = \Psi_l^B [M_{lk}^B \Psi_k^B \{H_{kj}^B \Psi_j^B (H_{ji}^B (P(t), \dot{P}(t))$$
$$+ B_j^B) + B_k^B\} + B_l^B] \qquad (15)$$

3. RESULTS AND DISCUSSION
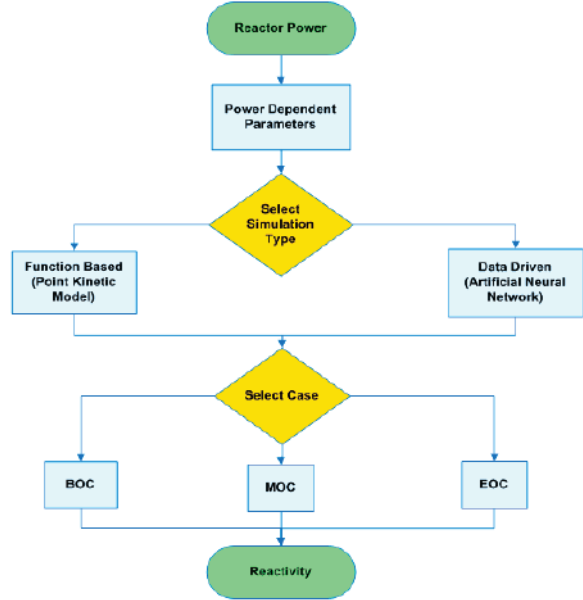
Fig. 2. Selection scheme for fuel burn-up along the fuel cycle length in APD-ISO-DNS code.

PCTRAN is obtained from micro-simulation technology and is a product of International Atomic Energy Agency (IAEA). The process of obtaining the power dependent reactivity components or reactivity feedbacks using artificial intelligence is shown in Fig. 3.
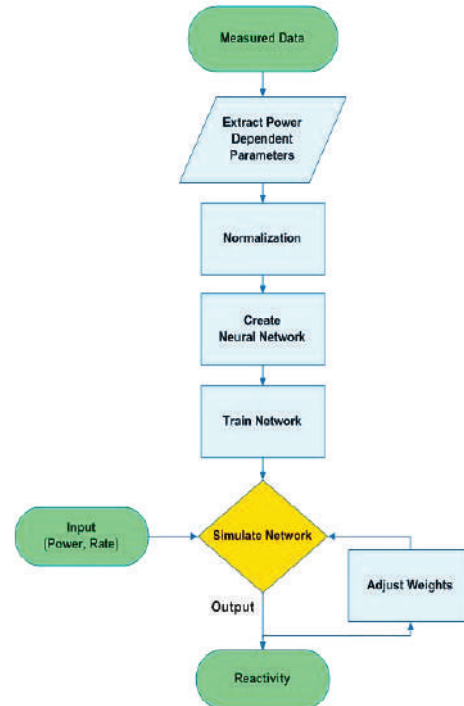
Fig. 3. Structure of intelligent data flow in APD-ISO-DNS code.

Therefore, the APD-ISO-DNS-600 module is best tuned and adjusted and used as a reference module or model for APD-ISO-DNS-300 and APD-ISO-DNS-1000 modules. APD-ISO-DNS-300 and APD-ISO-DNS-1000 modules are fine-tuned and adjusted using operational and design data of P-300 and ACP-1000. APD-ISO-DNS code is developed in hybrid Simulink and LabVIEW environments.

3.1 Evaluation of APD-ISO-DNS Code in SIMULINK

In this research work, APD-ISO-DNS code is developed for the first time for nuclear industry using ISGD-M optimized DANN in Simulink environment. There are six DANN designed for each reactivity feedback. The processing of data flow in all six Sub ISO-DANN is in parallel distributed fashion. The coupling scheme of all six Sub ISO-DANN in APD-ISO-DNS code is shown in Fig. 4.

The APD-ISO-DNS code is designed and developed using equations (10) through (16) optimized by hyper-parameter defined in equation (9). The Simulink model transient dynamics framework of APD-ISO-DNS code is shown in Fig. 5.

Eighteen design parameters of APD-ISO-DNS code are computed and optimized for P-300, AP-600 and ACP-1000. The detailed design parameters for moderator reactivity are tabulated in Table 1 for reference purposes. The optimized hyper-parameters for the entire six sub ISO-DANN for P-300, AP-600 and ACP-1000 are tabulated in Table 2.

In this research work, APD-ISO-DNS-600 module is evaluated for a load reduction transient in which reactor power is reduced from 100% to 60% in a sequence of 4 steps with a 10% step size using control rods as external reactivity mechanism because AP-600 is a base load nuclear power plant and its reactivity control is designed for 10% step change. Each step is executed at a rate of 2.31%/min embedded in the transient design. Practically, all step changes are designed with embedded ramp transients in AP-600. Since the reactor is 600 MWe PWR with medium scale nuclear power plant category, so ramp rate is 2.31%/min adopted in this transient. The innovative transient data which is specially generated using analytical model data, plant operational data and design data is now designated as "Experimental Data". The training of fuel reactivity, moderator reactivity and control rod reactivity are shown in Fig. 6, Fig.7 and Fig. 8 respectively.
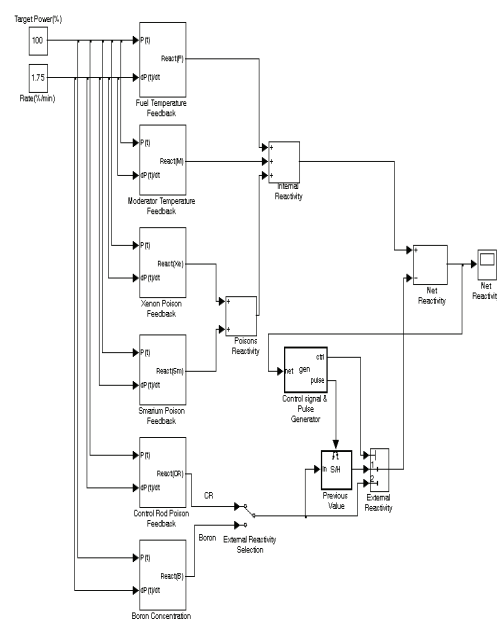

Fig. 4. Coupling of intelligent dynamic feedback design of APD-ISO-DNS code.

Fig. 5. Simulink model of APD-ISO-DNS code

Table 1. Parameters of APD-ISO-DNS-300 code for moderator reactivity

Reactor Type	Hyper-parameters of Different Variables	Design Values
P-300	Fuel Reactivity	10
P-300	Moderator Reactivity	12
P-300	Xenon Reactivity	18
P-300	Samarium Reactivity	16
P-300	Control Rod Reactivity	15
P-300	Boron Reactivity	11
AP-600	Fuel Reactivity	10
AP-600	Moderator Reactivity	12
AP-600	Xenon Reactivity	17
AP-600	Samarium Reactivity	15
AP-600	Control Rod Reactivity	14
AP-600	Boron Reactivity	11
ACP-1000	Fuel Reactivity	17
ACP-1000	Moderator Reactivity	13
ACP-1000	Xenon Reactivity	16
ACP-1000	Samarium Reactivity	15
ACP-1000	Control Rod Reactivity	29
ACP-1000	Boron Reactivity	22

Table 2. Optimized Hyper-parameter of APD-ISO-DNS

Intelligent Code Design Parameters	Design Values
Number of Nodes of Input Layer (i)	2
Number of Nodes of First Hidden Layer (j)	177
Number of Nodes of Second Hidden Layer (k)	177
Number of Nodes of Output Layer (l)	1
Number of training patterns (N)	25000
Number of Epochs	600
Balancing factor (α)	1
Initial Learning Rate (r)	0.15
Optimal Hyper-parameter (K_D)	12
Final Learning Rate (r)	1.68
Performance gradient	0.001
Standard deviation	0.0005
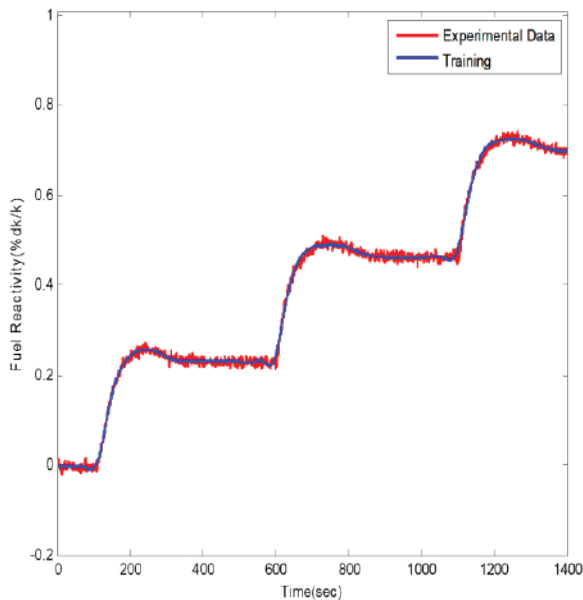
Fig. 6. Fuel reactivity of P-600 during learning phase of APD-ISO-DNS code.
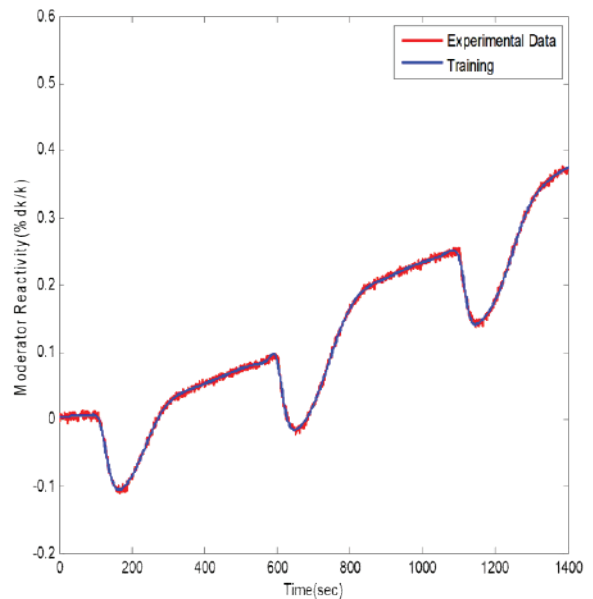
Fig. 7. Moderator reactivity of P-600 during learning phase of APD-ISO-DNS code.

There are six data sets for reactivity parameters. Therefore, in fact, there are six trends for training phase and six trends for validation phase. But due to space limitation and scope of this research work, three trends are shown for validation purposes. In validation phase, the pattern of error between predicted and experimental output is also realized. The fuel reactivity, moderator reactivity, control rod reactivity and total reactivity for validation phase are shown in Fig. 9, Fig.10, Fig. 11 and Fig. 12 respectively.

In this case study, it is observed that as the reactor power is reduced in steps, fuel reactivity and moderator reactivity increases as shown in Fig. 9 and Fig.10. This is because the fuel and moderator reactivity coefficients are negative.

Since the fuel and moderator reactivities are increased against reactor power reduction in steps, therefore, to cater this increase in total internal reactivity, control rod reactivity is decreased which in turn decreases the total external reactivity as shown in Fig. 11.

The validation is proved successfully because the total reactivity moves around zero that completely and safe ensures reactor criticality throughout the load reduction transient as shown in Fig. 12.

All the results of APD-ISO-DNS-600 are as per specifications and reactivity bounds as laid down in [4].

Later, APD-ISO-DNS-300 module is evaluated for a load reduction transient in which reactor power is reduced from 100% to 75% at a rate of 5%/min because P-300 is a base load nuclear power plant of small scale category and its reactivity control is designed for maximum upto 5%/min embedded ramp rate. All the reactivity feedbacks are shown collectively in Fig. 13.

The variations of reactivity feedbacks are exactly similar to those in APD-ISO-DNS-600 module. All the results of APD-ISO-DNS-300 are as per specifications and reactivity bounds as laid down in Final Safety Analysis Report of P-300 which is standard report from the designer as a benchmark.

3.2 Evaluation of APD-ISO-DNS Code in LabVIEW

Now, in this research work, APD-ISO-DNS code is developed again for the first time in nuclear industry using ISGD-M optimized DANN in LabVIEW environment. PID optimizer based intelligent DANN VIs are designed and developed in LabVIEW for APD-ISO-DNS LabVIEW code as
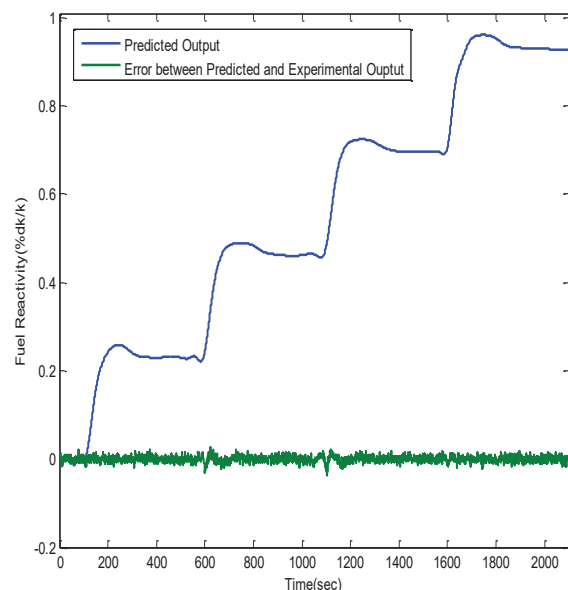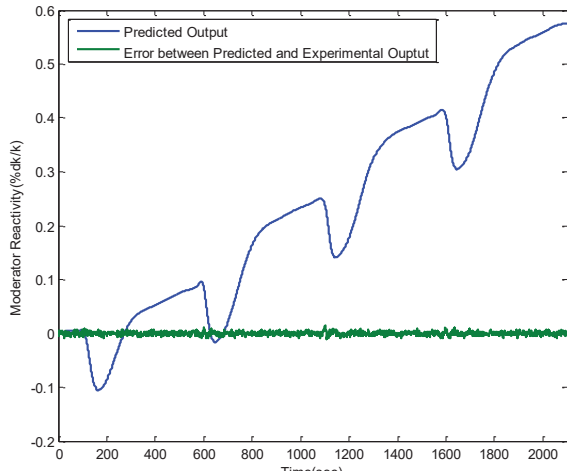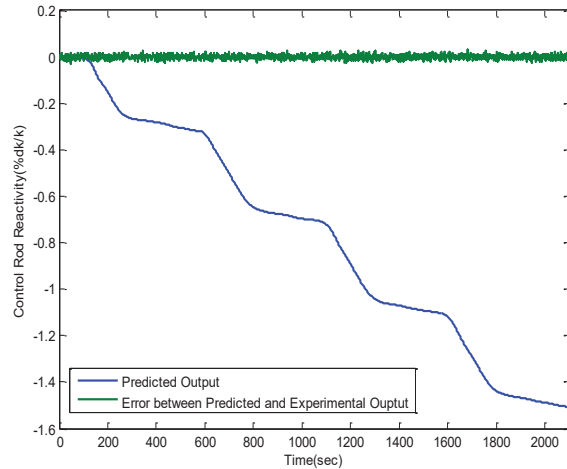

Fig. 8. Control rod reactivity of P-600 during learning phase of APD-ISO-DNS code.

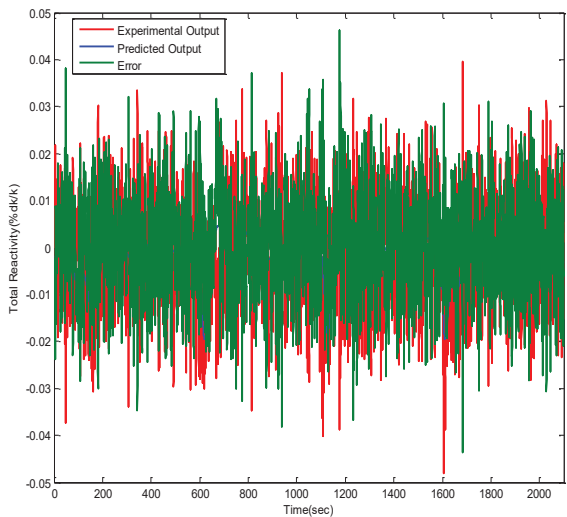**Fig. 9.** Fuel reactivity of P-600 during validation phase of APD-ISO-DNS code.

shown in Fig. 14.

The LabVIEW block diagram code is developed for APD-ISO-DNS code that integrates transient dynamic Simulink model of APD-ISO-DNS code as shown in Fig. 15.

APD-ISO-DNS-1000 module is evaluated for a load reduction transient in which reactor power is reduced from 100% to 20% in a sequence of 4 steps with a 20% step size using control rods as external reactivity mechanism for the compensation of total internal reactivity because it is load following nuclear power plant of large scale category. In this

transient, each after 20% change in reactor power, it is held constant for 9 hours. Each step is executed at a 0.166%/min rate embedded in the transient design. A front panel is shown in Fig. 16, in which all the reactivity feedbacks are shown. The variations of reactivity feedbacks are exactly similar to those in APD-ISO-DNS-600 module.

All the results of APD-ISO-DNS-1000 are as per specifications and reactivity bounds as laid down in Final Safety Analysis Report (FSAR) of ACP-1000 which is standard report from designer as a benchmark.

Fig. 10. Moderator reactivity of P-600 during validation phase of APD-ISO-DNS code.

Fig. 11. Control reactivity of P-600 during validation phase of APD-ISO-DNS code.

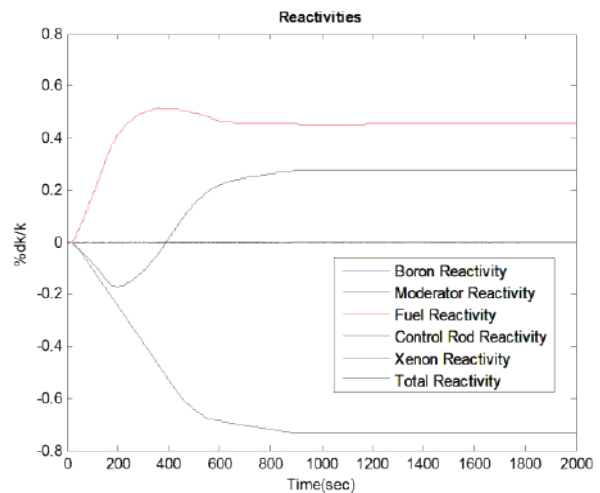**Fig. 12.** Total reactivity of P-600 during validation phase of APD-ISO-DNS code.

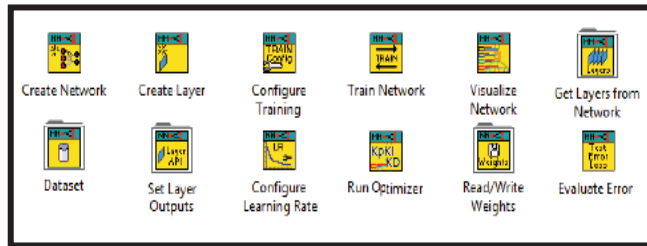**Fig. 13.** Reactor dynamics of P-300 during validation phase of APD-ISO-DNS code..

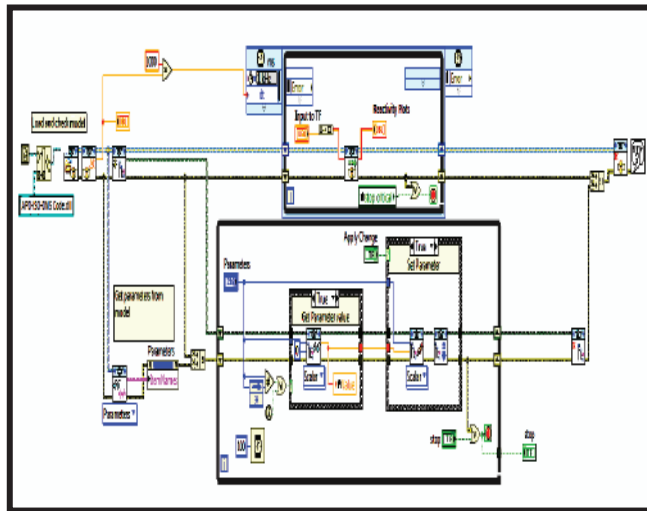**Fig. 14.** PID optimizer based intelligent DANN VIs in APD-ISO-DNS LabVIEW code.

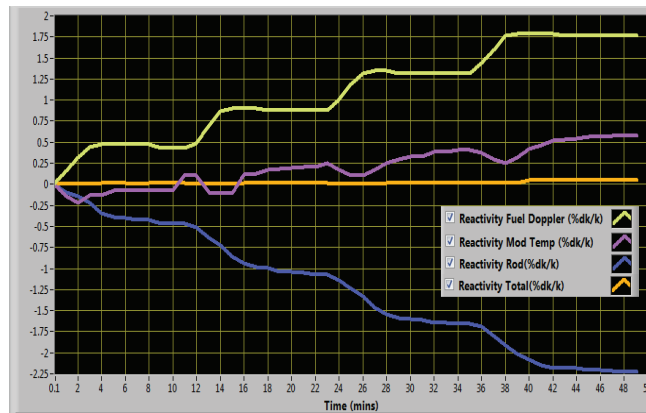**Fig. 15.** Block Diagram of APD-ISO-DNS LabVIEW Code.

Fig. 16. Front Panel of Reactor dynamics of ACP-1000 during validation phase in APD-ISO-DNS Code.

4. CONCLUSIONS

The reactor neutronics of three different generations of PWR based nuclear power plants have been considered in this research work. A state-of-the-art advanced multi-model PWR Dynamics and Intelligent Neutronics Simulation Code has been modeled, fine-tuned and simulated for P-300, AP-600 and ACP-1000 PWR based nuclear power plants. The developed computational transient analysis code for advanced multi-model PWR emerged as APD-ISO-DNS Code has three modules APD-ISO-DNS-300, APD-ISO-DNS-600 and APD-ISO-DNS-1000 which are evaluated under various load change transient conditions with different combinations of reactivity mechanisms in normal operation of PWR and reactor criticality is maintained and ensured as per benchmarks of Final Safety Analysis Reports (FSARs). Simulations have been conducted and performance of APD-ISO-DNS Code has been evaluated in a hybrid SIMULINK and LabVIEW environments and found optimal for future development of innovative advanced PWR nuclear power plant dynamics and accident analysis codes.

5. ACKNOWLEDGEMENTS

6. REFERENCES

1. M. Subekti, S. Bakhri, and G. R. Sunaryo.The simulator development for RDE reactor. *Journal of Physics* 962: (2018).

2.. M. Johnson, S. Lucas, and P. Tsvetkov. Modeling of reactor kinetics and dynamics.Idaho National Laboratory, Report Idaho Falls, Idaho 83415, *U.S. Department of Energy, Canad*a (2010).

3. W. K. Lam. Advanced pressurized water reactor simulator. *IAEA Workshop on NPP Simulators for Education, Bucharest, Romania* (2006).

4. L. C. C. Po. PCTRAN/PWR. Report Montville, New Jersey 07045, *IAEA Workshop on NPP Simulators for Education, Bucharest, Romania* (2006).

5. L. C. C. Po. PC-based simulator for education in advanced nuclear power plant construction. *International Symposium on the Peaceful Application of Nuclear Technology in the GCC Countries* (2008).

6. A. S. Mollah. Education tool for simulation of safety and transient analysis of a pressurized water reactor. *International Journal of Integrated Sciences & Technology* 03: 01-10 (2018).

7. S. M. A. Ibrahim. Thermal hydraulic simulations of a PWR nuclear power plant. *International Journal of Safety and Security* 013 (01): 31-520 (2019).

8. A. H. Malik,, A. A. Memon, and M. R. Khan. Identification of nonlinear dynamics of nuclear power reactor using adaptive feedforward neural network. *Proceedings of Pakistan Academy Sciences* 47 (2): 111-120 (2010).

9. Z. Wenjie, Q. Jiang, Jinsen X. and T. Yu. A functional variable universe fuzzy PID controller for load following operation of PWR with the multiple model. *Annals of Nuclear Energy*140: 1-6 (2020).

10. S. U. E. Hakim, A. Abimanyu, and Sutanto. Simulator design of Kartini reactor based on LabVIEW. *Journal forum Nukir* 12 (1): 29-41 (2018).

11. L. A. Macedo, W. M. Torres, G. Sabundjian, D. A. Andrade, A. B. Junior, P. E. Umbehaun, T. N. Conti, R. N. Mesquita, P. H. F. Masotti, and G. Angelo. Development of a LabVIEW web-based simulator for RELAP. *International Nuclear Atlantic Conference, Brazil*: 01-13 (2011).

12. J. Park, J. Jang, H. Kim, .Choe, D. Yun, and P. Zhang.RAST-K V2-Three-Dimentional nodal diffusion code for pressurized water reactor core analysis. *Energies* 13: 01-21 (2020).

13. X. Cui, W. Zhang, Z. Tuske, and M. Picheny. Evolutionary stochastic gradient decent for optimization of deep neural networks. *32 Conference on Neural Information Processing Systems, Canada*: (2018).

14. W. An, H. Wang, Q. Sun, J. Xu, Q. Dai, and L. Zhang.A PID controller approach for stochastic optimization of deep neural networks. *IEEE / CVF Conference on Computer Vision Pattern Recognition:* (2018).

15. H. Wang, Y. Luo, W. An, Q. Sun, J. Xu, and L. Zhang.PID controller-based stochastic optimization acceleration for deep neural networks. *IEEE Transactions on Neural Networks and Learning Systems* 31 (12): 1-10 (2020).

16. J. H. Horng. Hybrid MATLAB and LabVIEW with neural network to implement a SCADA system of AC servo motor. *Advances in Engineering Software* 39: 149-155 (2008).

Pakistan Academy of Sciences

Research Article

Mathematical Analysis on Conducting Sphere Embedded in Non Integer Dimensional Space

M Imran Shahzad[1], M Akbar[2], and Saeed Ahmed[3*]

[1]Department of Applied Physics, Federal Urdu University of Arts, Science and Technology, Islamabad, Pakistan
[2]Department of Electronics, Quaid-i-Azam University, Islamabad, Pakistan
[3]Department of Earth Sciences, Quaid-i-Azam University, Islamabad, Pakistan

Abstract: We have derived an analytical solution in low frequency using the idea of a fractional Laplacian equation. Fractional dimensional (FD) space has importance in describing the complex physics phenomena. Here, the Laplacian equation in spherical coordinated $(r,\theta,0)$ is expressed in fractional dimensional space using Gegenbauer polynomials. The analytical solution is obtained by the separation variable method. The general solution is a product of angular and radial solutions and is independent of ϕ due to azimuthal symmetry. The classical solution is retained by setting fractional parameter $\alpha=3$. Further, numerical results are discussed for different values of α and compared with available literature.

1. INTRODUCTION

The non integer dimensional (NID)- space is applied to various areas of physics discussed by many researchers [1-20]. They have applied it accordingly, like Wilson [3] has already mentioned quantum field theory (QFT) in FD space. In addition, the FD space can be used as a parameter in the Ising limit of QFT [6]. [4] Stillinger has defined axiomatics basis for concept in modelling Schrodiner and Gibbsian's theory related to Wave and Statisitcs Mechanics in the non integer dimensional space. Svozil and Zellinger [10] have shown the basic concept of time dimension space, which provides a possible way to experimentally predict the time dimension space. It has already mentioned been that the fractional dimension space if the space time is less than 4 slightly. In the new era, Gauss Law {11} has introduced the fractional dimensional space. The solution to the electrostatic problems [13-18] have also been formulated in NID space.

In this article, we have solved a problem from [20]. The main focus is to apply the Laplacian equation to find electric potential and electric field induced due to a conducting sphere in FD Space. In this paper, we analyze the model of the problem and then solve the Laplacian equation for non integer dimensional space by the method of separation variable using low frequency. We find here two kinds of second order differential equations, one deals with radial part and other with angular part. Further, we investigate a general solution in FD space. Next, we construct a solution for the outside and inside the sphere and impose boundary conditions for the proposed regions. After solving the boundary value problem (BVP), we calculate the unknown coefficients, which leads us to find the electric potential and electric field by substituting known coefficients in FD Space. On the last we discuss numerical results and concluding remarks.

2. MATHEMATICAL MODEL

We find here the Scalar Potential Ψ of a conducting sphere in a uniform external field shown in Fig1., of conductivity σ_2 and is buried in a host medium of conductivity σ_1. Since no time dependency is involved, therefore, the electric field is

$$E = -\nabla\Psi \quad (1)$$

we can determine the magnetic field from the Second Maxwell's equation

$$\nabla \times H = J \quad (2)$$

Let E_0 be the strength of the external field along x-axis.

$$E_0 = -\frac{\partial\Psi_0}{\partial x} \quad (3)$$

Negletting the constant of integration, we get

$$\Psi_0 = -E_0 x \quad (4)$$

To solve this problem for fractional dimensional space, we use the laplacian equation in non integer dimensional space [16] and [17]:

$$\nabla^2\Psi(r,\theta) = \left(\frac{\partial^2}{\partial r^2} + \frac{\alpha-1}{r}\frac{\partial}{\partial r} + \frac{1}{r^2\sin^{\alpha-2}\theta}\frac{\partial}{\partial\theta}\sin^{\alpha-2}\theta\frac{\partial}{\partial\theta}\right)\Psi(r,\theta) = 0 \quad (5)$$

Eq(5) is separable and suppose

$$\Psi(r,\theta) = R(r)\Theta(\theta) \quad (6)$$

The obtained angular and radial differential equations [18] are

$$\left[\frac{d^2}{d\theta^2} + (\alpha-2)\cot\theta\frac{d}{d\theta} + l(l+\alpha-2)\right]\Theta(\theta) = 0 \quad (7)$$

$$\left[\frac{d^2}{dr^2} + \frac{\alpha-1}{r}\frac{d}{dr} + \frac{l(l+\alpha-2)}{r^2}\right]R(r) = 0 \quad (8)$$

The solution of the angular equation (7) is Gegenbauer polynomials in $\cos\theta$ as explained in [16], namely

$$\Theta(\theta) = P_l^{\alpha/2-1}(\cos\theta), \quad l = 0,1,2... \quad (9)$$

which obeys the orthogonality relation:

$$\int_0^\pi P_l^{\alpha/2-1}(\cos\theta)P_{l'}^{\alpha/2-1}(\cos\theta)\sin^{\alpha-2}\theta d\theta = N(l)\delta_{l,l'} \quad (10)$$

$$N(l) = \frac{2^{(3-\alpha)}\pi\Gamma(l+\alpha-2)}{l!(l+\alpha/2-1)[\Gamma(l+\alpha/2-1)]^2} \quad (11)$$

The forms of first few Gegenbauer polynomials are

$$P_0^{\alpha/2-1}(z) = 1 \quad (12)$$

$$P_1^{\alpha/2-1}(z) = (\alpha-2)z \quad (13)$$

$$P_2^{\alpha/2-1}(z) = (\alpha/2-1)(\alpha z^2-1) \quad (14)$$

From Eq(6), the radial differential equation gives the first few solutions, such as

$$R_1(r) = r^l \quad (15)$$

$$R_2(r) = \frac{2}{r^{l+\alpha-2}} \quad (16)$$

The general solution of the Laplacian equation in Spherical Coordinates independent of ϕ can be written as

$$\Psi(r,\theta) = \sum_{l=0}^\infty \left(A_l r^l + \frac{B_l}{r^{l+\alpha-2}}\right)P_l^{\alpha/2-1}(\cos\theta), \quad 2 < \alpha \leq 3 \quad (17)$$

$$\sum_{l=0}^\infty A_l r^l P_l^{\alpha/2-1}(\cos\theta) = \left[-E_0 r + \frac{B_1}{r^{\alpha-1}}\right]P_1^{\alpha/2-1}(\cos\theta), \quad for \ r = R$$
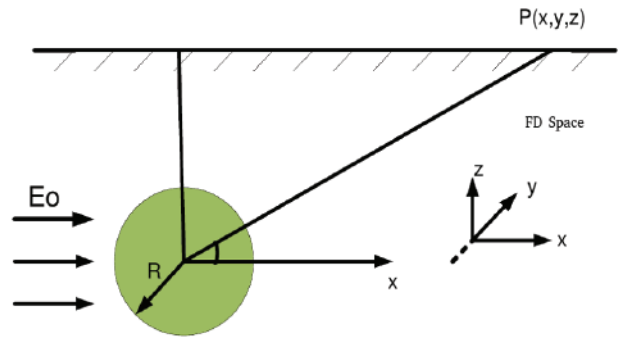

Fig. 1: Conducting Sphere Placed in Fraction Space

The external potential due to the sphere should be convergent at infinity. Inside the sphere, the solution must be bounded at origin. Hence the general solution reduces to following equations.

$\Psi_e^a(r,\theta) = \sum_{l=0}^{\infty} \frac{B_l}{r^{l+\alpha-2}} P_l^{\frac{\alpha}{2}-1}(\cos\theta), \; for \; r > 0 \; (18)$

$\Psi_i^a(r,\theta) = \sum_{l=0}^{\infty} A_l r^l P_l^{\alpha/2-1}(\cos\theta), \; for \; r < 0 \; (19)$

These are known as the anomalous potentials. The physically the solution must be finite at the origin, it means $B_l = 0$ inside the sphere and out side the sphere at infinity it means $a_l = 0$.

At infinity, the normal potential can be expressed as

$-E_0 x = -E_0 r(\alpha - 2)\cos\theta = -E_0 r P_1^{\alpha/2-1}(\cos\theta) \; (20)$

Now, that external potential can be expressed as

$\Psi_e(r,\theta) = \left[-E_0 r + \frac{B_1}{r^{\alpha-1}}\right] P_1^{\alpha/2-1}(\cos\theta),$
$for \; r > 0 \qquad\qquad (21)$

where $P_1^{\alpha/2-1}(\cos\theta) = (\alpha - 2)\cos\theta,$ while $-E_0 r P_1^{\alpha/2-1}(\cos\theta)$ and $B_1/r^{\alpha-1}$ shows the potential of the induced field respectively. At the surface of the sphere, both the potential and the normal component of the current density $n.J = \sigma E$ should be continous. So the potentials must be continuous at $r = R$.

$$\Psi_i^a = \Psi_e^a \qquad\qquad (22)$$

$\sum_{l=0}^{\infty} A_l r^l P_l^{\alpha/2-1}(\cos\theta) = \left[-E_0 r +\right.$
$\left.\frac{B_1}{r^{\alpha-1}}\right] P_1^{\alpha/2-1}(\cos\theta), \; for \; r = R \qquad (23)$

Therefore, $A_l = 0,$ all l except $l = 1$, we find

$A_1 r P_1^{\frac{\alpha}{2}-1}(\cos\theta) = \left[-E_0 r + \frac{B_1}{r^{\alpha-1}}\right] C_1^{\frac{\alpha}{2}-1}$

$(\cos\theta), \; for \; r = R \qquad\qquad (24)$

$A_1 R(\alpha - 2)\cos\theta = \left[-E_0 R + \frac{B_1}{R^{\alpha-1}}\right](\alpha - 2)\cos\theta \quad (25)$

By comparing the above equation

$$A_1 = -E_0 + \frac{B_1}{R^\alpha} \qquad\qquad (26)$$

Now the internal field becomes as

$\Psi_i^a = \left(-E_0 + \frac{B_1}{R^\alpha}\right) r(\alpha - 2)\cos\theta, \; for \; r < 0 \; (27)$

Simply the obtained expression is

$$\Psi_i^a = \left(-E_0 + \frac{B_1}{R^\alpha}\right)x, \; r < 0 \qquad (28)$$

The strength of the electric field within the sphere is

$$E_i^a = \left(E_0 - \frac{B_1}{R^\alpha}\right), \; r < 0 \qquad (29)$$

Next, we introduce the conductivities of the medium by using boundary conditions for the continuity of the normal component of the current density J on the surface of the sphere, as

$$n.J_1 = n.J_2 \qquad\qquad (30)$$

$$-\sigma_2 \frac{\partial \Psi_i}{\partial r} = -\sigma_1 \frac{\partial \Psi_e}{\partial r}, \; r = R \qquad (31)$$

$$\sigma_2 \left(E_0 - \frac{B_1}{R^\alpha}\right)(\alpha - 2)\cos\theta = \sigma_1 \left(E_0 + \frac{(\alpha-1)B_1}{R^\alpha}\right)$$

$$(\alpha - 2)\cos\theta \qquad\qquad (32)$$

$$B_1 = \frac{\sigma_2 - \sigma_1}{\sigma_2 + (\alpha-1)\sigma_1} E_0 R^\alpha \qquad (33)$$

For the integer order case $\alpha = 3$, we find

$$B_1 = \frac{\sigma_2 - \sigma_1}{\sigma_2 + 2\sigma_1} E_0 R^3 \qquad (34)$$

Hence, the external postential is

$$\Psi_e(r,\theta) = \left[-E_0 r + \frac{\sigma_2 - \sigma_1}{\sigma_2 + (\alpha-1)\sigma_1} E_0 R^\alpha \frac{1}{r^{\alpha-1}}\right](\alpha -$$
$$2)\cos\theta \qquad\qquad (35)$$

For the integer order case $\alpha = 3$, we see

$$\Psi_e(r,\theta) = \left[-E_0 r + \frac{\sigma_2 - \sigma_1}{\sigma_2 + 2\sigma_1} E_0 R^3 \frac{1}{r^2}\right]\cos\theta \qquad (36)$$

Where E_0 is the applied field that leads to the normal potential $\Psi_e^n = -r(\alpha - 2)\cos\theta$ and the anomalous potential is

$$\phi_e(r,\theta) = \frac{\sigma_2 - \sigma_1}{\sigma_2 + 2\sigma_1} E_0 R^3 \frac{1}{r^{\alpha-1}}(\alpha - 2)\cos\theta \qquad (37)$$

In the geophysical perspective, it is important to consider the anomalous field only and to find the gradient of the potential such that

$$E = -\nabla\phi_e(r,\theta) = \frac{\sigma_2 - \sigma_1}{\sigma_2 + 2\sigma_1} E_0 R^3 \frac{1}{r^{\alpha-1}}(\alpha - 2)\cos\theta$$

$$(38)$$

$$E = -\nabla\phi_e(r,\theta) = \frac{\sigma_2 - \sigma_1}{\sigma_2 + 2\sigma_1} E_0 R^3 (\alpha - 2)$$

$$\left[\frac{(\alpha-1)x^2 - y^2 - z^2}{r^{\alpha+2}} i + \frac{\alpha xy}{r^{\alpha+2}} j + \frac{\alpha xz}{r^{\alpha+2}} k\right] \quad (39)$$

Normally we are bound to find the applied field, i.e. along the x- direction, we require only the quantity

$$P = \frac{\sigma_2 - \sigma_1}{\sigma_2 + (\alpha-1)\sigma_1} E_0 R^\alpha (\alpha - 2) \quad (40)$$

This is the electric dipole moment induced due to the sphere.

and

$$E = \frac{\sigma_2 - \sigma_1}{\sigma_2 + (\alpha-1)\sigma_1} E_0 R^\alpha (\alpha - 2) \left[\frac{(\alpha-1)x^2 - y^2 - z^2}{r^{\alpha+2}} u_x + \frac{\alpha xy}{r^{\alpha+2}} u_y + \frac{\alpha xz}{r^{\alpha+2}} u_z\right] \quad (41)$$

This is the secondary electric field intensity of the conducting sphere.
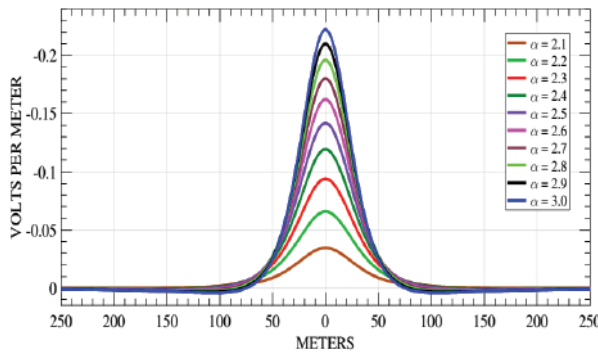
Fig.2: Graphical Representation of the Magnitude of the electric Field versus Distance x in Fractional Space electric field [20].

3 RESULTS AND DISCUSSION

The behaviour of the electric field E can be visualized by the variation in distance x (-250-250), from the figure 2. Through the graphical illustration, we observe that the field behaviour changes accordingly for the different values of FD space parameter ($\alpha = 2.1, 2.2, 2.3, 2.4, 2.5, 2.6, 2.7, 2.8, 2.9, 3.0$). However, the Field magnitude behaves like ordinary amplitude [20] at ($\alpha = 3$). It is clear that the electric field depends on the FD space

parameter. This behaviour predicts that the essentially the parameter α alters the material of the sphere due to which the different values of α cause the field amplitude variation, therefore, it affects the resonance conditions.

4. CONCLUSION

In the article, we have solved the Laplace equation for NID- space. The electric potential and electric field produced due to the conducting sphere are obtained in α -dimensional fractional space. We s

ee that the graphical behaviour of the curve shows that till $\alpha = 3$, the magnitude of the field increases by increasing the fractional parameter α between 2 and 3. From the results and discussion, we can say the field magnitude effects due to different FD space parameter values. Finally we can conclude that for all calculated results $\alpha = 3$, the classical results are retrieved.

5. ACKNOWLEDGEMENTS

6. REFERENCES

1. C.G. Bollini, J.J. Giambiagi, Dimensional renormalization: The number of dimensions as a regularizing parameter, Nuovo Cimento B 12 (1972) 2026.

2. J.F. Ashmore, On renormalization and complex space-time dimensions, Commun. Math. Phys. 29 (1973) 177-187.

3.   K.G. Wilson, Quantum field-theory models in less than 4 dimension, Phys. Rev. D 7 (10) (1973) 2911-2926.

4   F.H. Stillinger, Axiomatic basis for spaces with noninteger dimension, J. Math. Phys. 18 (6) (1977) 1224-1234.

5. X.F. He, Excitons in anisotropic solids: The model of fractional-dimensional space, Phys. Rev. B 43 (3) (1991) 2063-2069.

6. C.M. Bender, S. Boettcher, Dimensional expansion for the Ising limit of quantum field theory, Phy. Rev. D 48 (10) (1993) 4919-4923.

7. C.M. Bender, K.A. Milton, Scalar Casimir effect for a D-dimension sphere, Phys. Rev. D 50 (10) (1994) 6547-6555.

8. V.E. Tarasov, Fractional generalization of Liouville equations, Chaos 14 (2004) 123-127.

9. V.E. Tarasov, Electromagnetic fields on fractals, Modern Phys. Lett. A 21 (20) (2006) 1587-1600.

10. A. Zeilinger, K. Svozil, Measuring the dimension of space-time, Phys. Rev. Lett. 54 (1985) 2553-2555.

11. C. Palmer, P.N. Stavrinou, Equations of motion in a noninteger-dimensionspace, J. Phys. A 37 (2004) 6987-7003.

12. J.D. Jackson, Classical Electrodynamics, 3rd ed., John Wiley, New York, 1999.

13. Julius Adams Stratton, Electromagnetic Theory, 640 Pages, 1941, Wiley-IEEE Press.

14. T. Myint-U, L. Debnath, Linear Partial Differential Equations for Scientists and Engineers, 4th ed., 2007.

15. P. M. Morse and H. Feshbach, Methods of Theoretical Physics, Part II, pages 1184-1185, New York: McGraw-Hill, 1953.

16. S. Muslih, D. Baleanu, Fractional multipoles in fractional space, Nonlinear Anal. 8 (2007) 198-203.

17. Dumitru Baleanu, Alireza K. Golmankhaneh, Ali K. Golmankhaneh, On electromagnetic field in fractional space, Nonlinear Analysis: Real World Applications 11 (2010) 288-292.

18. V.E. Tarasov, Gravitational field of fractals distribution of particles, Celestial Mech. and Dynam. Astronom. 94 (2006) 1-15.

Instructions for Authors

Manuscript Format

The manuscript may contain Abstract, Keywords, INTRODUCTION, MATERIALS AND METHODS, RESULTS, DISCUSSION (or RESULTS AND DISCUSSION), CONCLUSIONS, ACKNOWLEDGEMENTS, CONFLICT OF INTEREST and REFERENCES, *and any other information that the author(s) may consider necessary*.

Abstract (font size 10; max 250 words)**:** Must be self-explanatory**,** stating the rationale, objective(s), methodology, main results, and conclusions of the study. Abbreviations, if used, must be defined on the first mention in the Abstract as well as in the main text. Abstract of review articles may have a variable format.

Keywords (font size 10)**:** Three to eight keywords**,** depicting the article.

INTRODUCTION: Provide a clear and concise statement of the problem, citing relevant recent literature, and objectives of the investigation.

MATERIALS AND METHODS: Provide an adequate account of the procedures or experimental details, including statistical tests (if any), concisely but sufficient enough to replicate the study.

RESULTS: Be clear and concise with the help of appropriate Tables, Figures, and other illustrations. Data should not be repeated in Tables and Figures, but must be supported with statistics.

DISCUSSION: Provide interpretation of the RESULTS in the light of previous relevant studies, citing published references.

ACKNOWLEDGEMENTS: (font size 10)**:** In a brief statement, acknowledge the financial support and other assistance.

CONFLICT OF INTEREST: State if there is any conflict of interest.

REFERENCES (font size 10)**:** Cite references in the text **by number only** in **square brackets**, e.g. "Brown et al [2] reported ..." or "... as previously described [3, 6–8]", and list them in the REFERENCES section, in the order of citation in the text, Tables and Figures (not alphabetically). Only published (and accepted for publication) journal articles, books, and book chapters qualify for REFERENCES.

Declaration: Provide a declaration that: (i) the results are original; (ii) the same material is neither published nor under consideration elsewhere; (iii) approval of all authors have been obtained; and (iv) in case the article is accepted for publication, its copyright will be assigned to *Pakistan Academy of Sciences*. Authors must obtain permission to reproduce, where needed, copyrighted material from other sources and ensure that no copyrights are infringed upon.

Manuscript Formatting

Manuscripts must be submitted in Microsoft Word (2007 Version .doc or .docx format); **pdf** files not acceptable. Figures can be submitted in Word format, TIFF, GIF, JPEG, EPS, PPT. Manuscripts, in *Times New Roman*, 1.15spaced (but use single-space for Tables, long headings, and long captions of tables & figures). The text must be typed in a double-column across the paper width. The Manuscript sections must be numbered, i.e., **1. INTRODUCTION, 2. MATERIALS AND METHODS,** and so on… (a) **Title** of the article **(**Capitalize initial letter of each main word; font-size 16; **bold**), max 160 characters (no abbreviations or acronyms), depicting article's contents; (b) Author' first name, middle initial, and last name (font size 12, **bold**), and professional affiliation (i.e., each author's Department, Institution, Mailing address and Email; but no position titles) (font size 12); (c) Indicate the corresponding author with *; (d) **Short running title**, max 50 characters (font size 10).

Headings and Subheadings (font size 11): All flush left

        LEVEL-1: **ALL CAPITAL LETTERS; Bold**

        Level-2: **Capitalize Each Main Word (**Except prepositions**); Bold**

        Level-3: Capitalize each main word (Except prepositions)*; **Bold, Italic***

        Level-4: *Run-in head*; *Italics, in the normal paragraph position. Capitalize the initial word only and end in a colon (i.e., **:**)*

List of REFERENCES must be prepared as under:

a. Journal Articles *(Name of journals must be stated in full)*

1. I. Golding, J. Paulsson, S.M. Zawilski, and E.C. Cox. Real time kinetics of gene activity in individual bacteria. *Cell* 123: 1025–1036 (2005).

2. W. Bialek, and S. Setayeshgar. Cooperative sensitivity and noise in biochemical signaling. *Physical Review Letters* 100: 258–263 (2008).

3. R.K. Robert, and C.R.L.Thompson. Forming patterns in development without morphogen gradients: differentiation and sorting. *Cold Spring Harbor Perspectives in Biology* 1(6) (2009).

4. D. Fravel. Commercialization and implementation of biocontrol. *Annual Reviews of Phytopathology* 43: 337359 (2005).

b. Books

5. W.R. Luellen. Fine-Tuning Your Writing. *Wise Owl Publishing Company, Madison, WI, USA* (2001).

6. U. Alon, and D.N. Wegner (Ed.). An Introduction to Systems Biology: Design Principles of Biological Circuits. *Chapman & Hall/CRC, Boca Raton, FL, USA* (2006).

c. Book Chapters

7. M.S. Sarnthein, and J.D. Stanford. Basal sauropodomorpha: historical and recent phylogenetic developments. In: The Northern North Atlantic: A Changing Environment. P.R. Schafer, & W. Schluter (Ed.), *Springer, Berlin, Germany*, pp. 365–410 (2000).

8. J.E. Smolen, and L.A. Boxer. Functions of Europhiles. In: Hematology, 4th ed. W.J. Williams., E. Butler and M.A. Litchman (Ed.), *McGraw Hill, New York, USA*, pp. 103–101 (1991).

d. Reports

9. M.D. Sobsey, and F.K. Pfaender. Evaluation of the H2S method for Detection of Fecal Contamination of Drinking Water, Report WHO/SDE/WSH/02.08, *Water Sanitation and Health Programme, WHO, Geneva, Switzerland* (2002).

e. Online references

These should specify the full URL for reference and give the date on which it was consulted. Please check again to confirm that the work you are citing is still accessible:

10. L. Branston. SENSPOL: Sensors for Monitoring Water Pollution from Contaminated Land, Landfills and Sediment (2000). http://www.cranfield.ac.uk/biotech/senspol/ (accessed 22 July 2005)

Tables and Figures

Insert all tables as editable text, not as images. Number tables consecutively following their appearance in the text, Figures should appear in numerical order, be described in the body of the text, and be positioned close to where they are first cited. Each figure should have a caption that describes the illustration, and that can be understood independently of the main text (Caption Table 1. and Fig 1. font size 10; Bold; Captions should be in sentence case; left-aligned). All Figures should have sufficiently high resolution (minimum 1000 pixels width/height, or a resolution of 300 dpi or higher) to enhance the readability. Figures may be printed in two sizes: column width of 8.0 cm or page width of 16.5 cm; number them as **Fig. 1**, **Fig. 2**, … in the order of citation in the text. Parts in a figure can be identified by A, B, C, D, ... and cited as Figure 2A, Figure 2B, Figure 2C. Captions to Figures must be concise but self-explanatory. Laser printed line drawings are acceptable. Do not use lettering smaller than 9 points or unnecessarily large. Photographs must be of high quality. A scale bar should be provided on all photomicrographs.

Tables: with concise but self-explanatory headings must be numbered according to the order of citation (like **Table 1.**, **Table 2.**). *Do not* abbreviate the word "Table" to "Tab.". Round off data to the nearest three significant digits. Provide essential explanatory footnotes, with superscript letters or symbols keyed to the data. Do not use vertical or horizontal lines, except for separating column heads from the data and at end of the Table.

Figures: Figures may be printed in two sizes: column width of 8.0 cm or page width of 16.5 cm; number them as **Fig. 1**, **Fig. 2**, … in the order of citation in the text. Captions to Figures must be concise but self-explanatory. Laser printed line drawings are acceptable. Do not use lettering smaller than 9 points or unnecessarily large. Photographs must be of high quality. A scale bar should be provided on all photomicrographs.

Note: The template of the manuscript is available at http://www.paspk.org/proceedings/; http://ppaspk.org/

Reviewers: Authors may suggest four relevant reviewers, two National and two International (with their **institutional E-mail** addresses).

SUBMISSION CHECKLIST

The following list will be useful during the final checking of an article before sending it to the journal for review.

Ensure that the following items are present:

One author has been designated as the corresponding author with contact details:

• E-mail address (Correct and valid)

• Full address of Institute/organization

• Keywords

• All figure captions

• All tables (including title, description, footnotes)

Further considerations

• Manuscript has been 'spell-checked' and 'grammar checked'

• References are in the correct format for this journal

• All references mentioned in the Reference list are cited in the text, and vice versa

• Permission has been obtained for the use of copyrighted material from other sources (including the Internet)

In case of any difficulty while submitting your manuscript, please get in touch with:

Editor
Pakistan Academy of Sciences
3-Constitution Avenue, Sector G-5/2
Islamabad, Pakistan
Email: editor@paspk.org
Tel: +92-51-920 7140
Websites: http://www.paspk.org/proceedings/; http://ppaspk.org/

CONTENTS

Volume 59, No. 1, March 2022   **Page**

Research Articles